Computational Design of the Basic Dynamical Processes of the UCLA General Circulation Model

AKIO ARAKAWA AND VIVIAN R. LAMB

DEPARTMENT OF ATMOSPHERIC SCIENCES
UNIVERSITY OF CALIFORNIA
LOS ANGELES, CALIFORNIA

I. Outline of the General Circulation Model

A NEW GENERAL CIRCULATION model, which has an improved finite-difference formulation, greater vertical resolution, and new parameterizations of the subgrid-scale processes, has been developed at UCLA to replace the earlier two- and three-level UCLA general circulation models.

The primary prognostic variables of the model are *horizontal velocity*, *temperature*, and *surface pressure*, governed by the horizontal momentum equation, the thermodynamic energy equation, and the surface pressure tendency equation, respectively. These governing equations, together with the hydrostatic equation, form the system of "quasi-static equations" or so-called "primitive equations."

A number of secondary prognostic variables, with corresponding governing equations, are added to the system to determine the heating and friction. The most important of the secondary prognostic variables is *water vapor*, which is governed by the water vapor continuity equation. *Ozone*, governed by an ozone continuity equation with parameterized sources and sinks, is added as a prognostic variable for use in the radiational heating calculation. The planetary *boundary layer depth* and the magnitudes of the *temperature discontinuity*, *moisture discontinuity*, and *momentum discontinuity* at the top of the boundary layer are made prognostic variables to determine the boundary layer structure. The *ground temperature*, *ground water storage*, and *mass of snow on the ground* are also taken as prognostic variables, governed by the energy and water budget equations of the ground.

The horizontal momentum equation includes the convergence of vertical flux of horizontal momentum due to the boundary layer turbulence and cumulus convection. The thermodynamic energy equation includes a heating term that consists of solar and infrared radiational heating, the convergence of vertical flux of sensible heat due to the boundary layer turbulence and cumulus convection, the release of latent heat due to cumulus-convective and large-scale condensation processes, and cooling due to evaporation of clouds and falling raindrops. The water vapor continuity equation includes the convergence of vertical flux of water vapor due to the boundary layer turbulence and cumulus convection, and both cumulus-convective and large-scale condensation and evaporation. The formulation of horizontal and vertical diffusion due to turbulence in the free atmosphere depends on the version of the model. We plan to introduce, in the near future, a formulation based on the quasi-geostrophic turbulence theory.

To use the general circulation model the following parameters must be prescribed for each grid point: surface characteristics (open ocean, ice-covered

ocean, bare land, and land covered by glacial ice); elevation of the land; surface roughness; thickness of the sea ice; and ocean surface temperature.

Figure 1 shows the vertical structure of the model. The lower boundary follows the earth's topography, where the surface pressure is defined. The upper boundary is the 1 mb pressure surface, which is approximately at the height of the stratopause. The atmosphere between the upper and lower boundaries is divided into twelve layers, and the boundaries of these layers follow the coordinate surfaces of a generalized σ coordinate (Section IV). From 100 mb upward these coordinate surfaces are also constant pressure surfaces. The lowest four layers have equal depth in pressure p, and the uppermost seven layers have equal depth in log p.

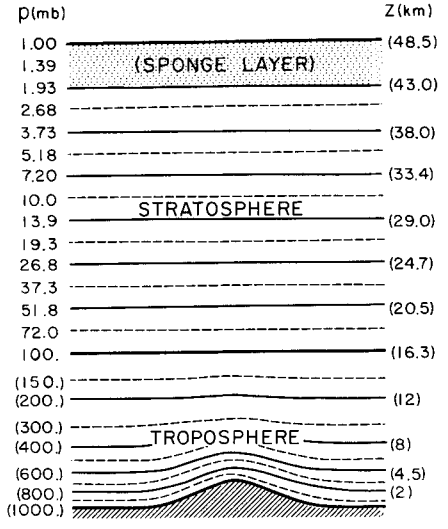

FIG. 1. The vertical structure of the 12-layer UCLA general circulation model. Solid lines define layers, broken lines indicate levels within layers at which prognostic variables are carried. Pressure levels and heights in parentheses are approximate, given for purposes of illustration.

The broken lines in Fig. 1 show the levels at which the prognostic variables of horizontal velocity, temperature, water vapor, and ozone are carried for each of the layers. These levels are approximately centered in p for the layers below 100 mb, and centered in log p for the layers above 100 mb.

The uppermost layer of the model, called the "sponge layer," has a damping term designed to absorb upward propagating wave energy and thus prevent a spurious reflection of wave energy at the upper boundary. The actual formulation of the damping term, however, is still in an experimental stage.

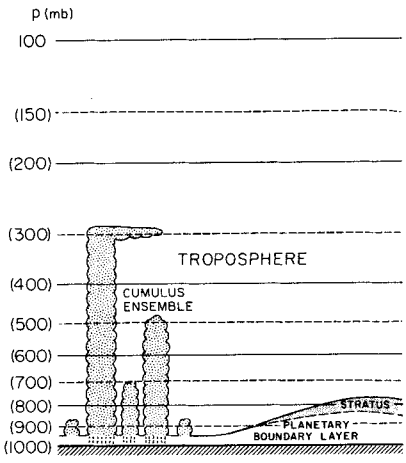

FIG. 2. The vertical structure of the tropospheric layers of the model showing the parameterized planetary boundary layer (light shaded area) and possible cloud types associated with the planetary boundary layer (stippled area).

Figure 2 shows the vertical structure of the lower layers of the model. The light shaded area represents the parameterized planetary boundary layer, which may or may not contain stratus cloud, and out of which there may or may not extend a cumulus cloud ensemble. The boundary layer depth may be less than, equal to, or greater than one or more of the model layers.

Although the model is designed and programmed to have as many as 12 layers, it can be used with fewer layers. A six-layer version of the model, with a vertical structure identical to the lower half of the 12 layer version, is also used at UCLA.

The horizontal coordinates are longitude and latitude; the current grid size is 5° of longitude and 4° of latitude. The convergence of the meridians toward the poles would normally necessitate the use of an extremely short time interval to maintain computational stability. To avoid this requirement, a longitudinal averaging is done of *selected terms* in the prognostic equations near the poles. At present, the finite-difference time step is 6 min, except for the heating, friction, and source and sink terms, for which the time step is 30 min.

II. Principles of Mathematical Modeling

The space finite difference scheme of the model is designed to maintain many of the important integral constraints of the continuous atmosphere, such as the conservation of total mass; the conservation of total kinetic

energy during inertial processes; the conservation of enstrophy (mean square vorticity) during vorticity advection by the nondivergent part of the horizontal velocity; the conservation of the integral constraint on the pressure gradient force; the conservation of total energy during adiabatic and nondissipative processes; and the conservation of total entropy and total potential enthalpy during adiabatic processes.

As the grid size approaches zero, the finite-difference solution obtained with any convergent scheme will approach the true solution and, therefore, in the limit will satisfy the integral constraints. The order of accuracy of a convergent scheme determines how rapidly its solution approaches the true solution as the grid size approaches zero. Although many schemes share the same order of accuracy, the solutions of such schemes generally approach the true solution along different paths in a function space, and with different statistics. One of the basic principles used in the design of the finite difference scheme for the model is the desirability of seeking that finite difference scheme in which the solutions approach the true solution along a path on which the statistics are analogous to those of the true solution. To this end, in the finite difference scheme used in the model, discretized analogs of the integral constraints are maintained, regardless of the grid size, which approach the true integral constraints as the grid size approaches zero.

Maintenance of the integral constraints by the finite difference scheme may not be a critical requirement for short-range numerical weather prediction (over a period of a day or two), because there the concern is with the local accuracy of the solution in space and time, and a formal maintenance of the integral constraints does not necessarily mean a greater accuracy of the solution at a particular place and time. In short-range predictions, the period of integration is usually not long enough for significant changes to occur in the integral properties. The local accuracy in short-range predictions is therefore more or less determined by the grid size and the order of accuracy of the scheme.

In numerical general circulation simulations, however, the governing equations are integrated beyond the physical limit of deterministic prediction, which is of the order of a few weeks. Because the atmosphere is turbulent, in a long-term integration there is no "true" solution in the deterministic sense, and such integrations (including long-range numerical weather prediction from an observed initial state) can only predict the statistical properties of the atmosphere. In a long-term integration, then, it is the accuracy of the statistical properties of the solution that concerns us.

It is shown in Section III that maintaining the conservation of enstrophy as well as of kinetic energy is of great advantage in the control of the statistical properties of nondivergent horizontal flow. It not only prevents nonlinear computational instability, but it also maintains the constraint on the kinetic

energy exchange between motions of different size. A false systematic computational cascade of kinetic energy into small-scale motions is prevented, and because there is then relatively little energy in the small-scale motions, the overall error is small. In this way, other statistical properties of the solution, such as conservation of the higher moments of the statistical distribution of vorticity, are approximately maintained.

If the energy in the shortest scale is the result of a spurious computational energy cascade, a decrease of the grid size does not help insofar as the long-term simulation of nonviscous flow is concerned. Such a result is completely different from that which might be expected from the usual analysis of truncation error, which is a measure of the formal difference of the finite-difference equation from the original differential equation. The paradox occurs because a decrease of the grid size allows a further computational cascade of energy into the added part of the spectral domain. After a sufficient period of integration, the cascading energy will again reach and accumulate in the shortest resolvable scale. The overall error will become large again and the prediction of some of the statistical properties will become even worse than with the coarser grid (Section III will show an example of this).

The existence of lateral viscosity can make a false computational cascade of energy less harmful. Since such viscosity is more effective for smaller scales, however, a spurious computational energy cascade into these scales falsely enhances the total amount of energy dissipation.

The second part of Section III describes a finite difference Jacobian that maintains the conservation of enstrophy and kinetic energy and that is suitable for the representation of advection of any quantity in two-dimensional, incompressible flow. The usefulness of this scheme as a guide in the formulation of a finite-difference scheme for the primitive equations rests on the fact that although the motions of the atmospheric general circulation are not exactly horizontal and nondivergent, they are to a good approximation quasi-geostrophic. This type of motion is quasi-nondivergent, as far as horizontal advection is concerned; divergence is important only in the linear, or approximately linear, terms. Thus as far as the consideration of the (nonlinear) advection terms is concerned, the finite-difference scheme for advection by the nondivergent part of the flow is crucial; indeed, a scheme that is inadequate for purely nondivergent motion is almost certainly inadequate for quasi-nondivergent motion.

The other integral constraints maintained by the finite-difference scheme of the UCLA model are not for the prevention of a computational cascade and, therefore, do not directly increase the overall accuracy of the statistics of the solution. The maintenance of these other integral constraints does help make the errors less systematic, however, in terms of the generation, destruction, and conversion of energy, entropy, and angular momentum or vorticity.

Therefore, in a statistical sense, they make the physics of the discrete model more analogous to the physics of the continuous atmosphere.

The following examples may serve to illustrate this point. A small error in the meridional velocity is tolerable if that error is random; but if the error is a systematic one resulting, say, from some latitudinal distribution of false mass sources and sinks, there will be a systematic false generation of the relative angular momentum of the global atmosphere. A small false residual of the line integral of the pressure gradient force, which is an irrotational vector, can drastically affect the angular momentum and vorticity budgets. A systematic small error in the vertical distribution of potential temperature in the troposphere can cause a significant error in the gross static stability, and thereby produce large errors in the motion field.

It is important to note that the integral constraints are maintained regardless of the initial condition, because their maintenance is guaranteed by the form of the finite-difference scheme. Difference schemes that do not have such a formal guarantee may approximately maintain the integral constraints with a particular set of initial conditions, but may not do so with another set of initial conditions. Because the governing equations are nonlinear, we have no way of knowing in advance the integral properties of the solutions obtained with such schemes.

In numerical models of the atmosphere, the energy propagation in physical space, as well as in spectral space, must be properly simulated. In particular, the energy propagation by small-scale dispersive inertia-gravity waves, excited by a local breakdown of the quasi-geostrophic balance, is important in restoring an approximately quasi-geostrophic flow by geostrophic adjustment. Unless the geostrophic adjustment process can operate properly, nothing is gained by maintaining integral constraints on quasi-geostrophic motion. The finite-difference scheme of the model is designed to control the small-scale inertia-gravity waves and the accompanying geostrophic adjustment process.

Computational problems also arise in the simulation of the vertical propagation of wave energy forced from below. The vertical differencing scheme and the location of the levels in the stratosphere are designed to eliminate any false computational internal reflections of the wave energy in a resting isothermal atmosphere.

III. Finite Difference Schemes for Homogeneous Incompressible Flow

Our governing equations are the primitive equations. Under typical conditions in the atmosphere (low Rossby and Froude numbers), these equations govern two well-separable types of motion. One type is the high-frequency

inertia-gravity wave, for which nonlinearity is usually small; the other is low-frequency, quasi-geostrophic motion, for which nonlinearity is usually dominant. It is known that the energy of locally excited inertia-gravity waves disperses away into a wider space, leaving the slowly changing quasi-geostrophic motion behind. This process is called "geostrophic adjustment."

Consequently, there are two main computational problems in the simulation of large-scale motions with the primitive equations. One computational problem is the proper simulation of the geostrophic adjustment. The other is the simulation of the slowly changing quasi-geostrophic (and, therefore, quasi-nondivergent) motion after it has been established by geostrophic adjustment.

This section discusses finite-difference schemes to deal with both of these computational problems for the case of homogeneous incompressible flow. The results of this section will be used in Section VI as a guide for the design of the horizontal finite-difference scheme for the model.

A. Distribution of Variables over the Grid Points

Winninghoff (1968) found that the simulation of the geostrophic adjustment process with a finite-difference scheme is highly dependent on the manner in which variables are distributed over the grid points. The following discussion is based on his work.

Consider the simplest fluid in which geostrophic adjustment can take place—namely, an incompressible, homogeneous, nonviscous, hydrostatic, rotating fluid with a flat bottom and a free top surface. The basic equations which govern such a fluid are the so-called shallow water equations, given by

$$du/dt - fv + g(\partial h/\partial x) = 0, \tag{1}$$

$$dv/dt + fu + g(\partial h/\partial y) = 0, \tag{2}$$

$$dh/dt + h(\partial u/\partial x + \partial v/\partial y) = 0, \tag{3}$$

where t is time, x and y are the horizontal cartesian coordinates, u and v are the velocity components in the x and y directions, respectively, h is the depth of the fluid, f is a constant coriolis parameter, and g is gravity. The individual time rate of change is defined by

$$\frac{d}{dt} \equiv \frac{\partial}{\partial t} + u\frac{\partial}{\partial x} + v\frac{\partial}{\partial y}. \tag{4}$$

In most of this study a linearized version of these equations is used, which is obtained by replacing d/dt by $\partial/\partial t$, and by replacing h as the factor on $(\partial u/\partial x + \partial v/\partial y)$ in Eq. (3) by H, the mean value of h. This procedure is justified when the Rossby number is small and the horizontal scale is of the order of the radius of deformation or less.

Consider the five distributions of the dependent variables h, u, and v, on a square grid illustrated in Fig. 3. Each of the following five space finite-difference schemes used with the linearized equations is the simplest second-order scheme for the correspondingly labeled distribution.

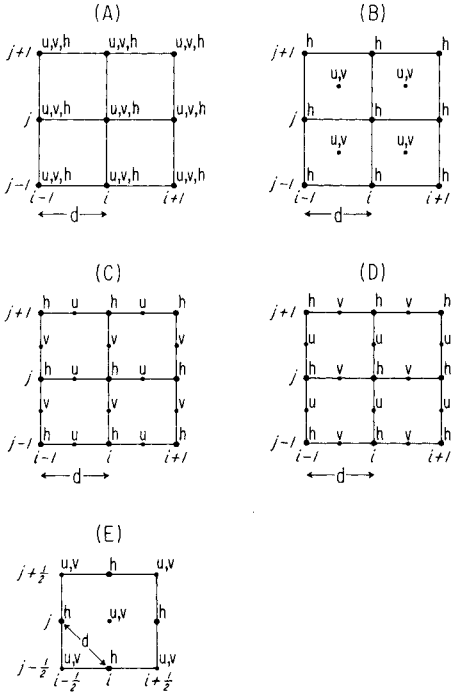

FIG. 3. Spatial distributions of the dependent variables on a square grid.

Scheme A:

$$\partial u/\partial t - fv + (g/d)(\overline{\delta_x h})^x = 0, \tag{5}$$

$$\partial v/\partial t + fu + (g/d)(\overline{\delta_y h})^y = 0, \tag{6}$$

$$\partial h/\partial t + (H/d)[(\overline{\delta_x u})^x + (\overline{\delta_y v})^y] = 0; \tag{7}$$

Scheme B:

$$\partial u/\partial t - fv + (g/d)(\overline{\delta_x h})^y = 0, \tag{8}$$

$$\partial v/\partial t + fu + (g/d)(\overline{\delta_y h})^x = 0, \tag{9}$$

$$\partial h/\partial t + (H/d)[(\overline{\delta_x u})^y + (\overline{\delta_y v})^x] = 0; \tag{10}$$

Scheme C:

$$\partial u/\partial t - f\bar{v}^{xy} + (g/d)(\delta_x h) = 0, \tag{11}$$

$$\partial v/\partial t + f\bar{u}^{xy} + (g/d)(\delta_y h) = 0, \tag{12}$$

$$\partial h/\partial t + (H/d)[(\delta_x u) + (\delta_y v)] = 0; \tag{13}$$

Scheme D:

$$\partial u/\partial t - f\bar{u}^{xy} + (g/d)(\overline{\delta_x h})^{xy} = 0, \tag{14}$$

$$\partial v/\partial t + f\bar{v}^{xy} + (g/d)(\overline{\delta_y h})^{xy} = 0; \tag{15}$$

$$\partial h/\partial t + (H/d)[(\overline{\delta_x u})^{xy} + (\overline{\delta_y v})^{xy}] = 0; \tag{16}$$

Scheme E:

$$\partial u/\partial t - fv + (g/d^*)(\delta_x h) = 0, \tag{17}$$

$$\partial v/\partial t + fu + (g/d^*)(\delta_y h) = 0, \tag{18}$$

$$\partial h/\partial t + (H/d^*)[(\delta_x u) + (\delta_y v)] = 0; \tag{19}$$

where we define

$$(\delta_x \alpha)_{ij} \equiv \alpha_{i+1/2,\,j} - \alpha_{i-1/2,\,j}, \tag{20}$$

$$(\bar{\alpha}^x)_{ij} \equiv \tfrac{1}{2}(\alpha_{i+1/2,\,j} + \alpha_{i-1/2,\,j}), \tag{21}$$

and where i and j are the indices of the grid points in the x and y directions, respectively. The symbols $(\delta_y \alpha)_{ij}$ and $(\bar{\alpha}^y)_{ij}$ are defined in a similar manner, but with respect to the y direction, and

$$(\bar{\alpha}^{xy})_{ij} \equiv (\bar{\bar{\alpha}}^{x}{}^{y})_{ij}. \tag{22}$$

For Schemes A through D, d is the grid size shown in Fig. 3. For Scheme E, d^* equals $\sqrt{2d}$; with this choice Scheme E will have the same number of grid points as the other schemes in a given two-dimensional domain.

In this study, all analyses with the linearized equations leave the time-change terms in differential form. If an explicit scheme is to be used for the time differencing, the time interval must be chosen to satisfy the Courant–Friedrich–Lewy type condition for linear computational stability of the wave with the largest possible phase speed, which for the primitive equations of atmospheric motion is the Lamb wave. A time interval so chosen is adequately small for all other waves, including internal gravity waves, and the time discretization error can be ignored in the first approximation.

Consider, first, the following one-dimensional linear equations:

$$\partial u/\partial t - fv + g(\partial h/\partial x) = 0, \tag{23}$$

$$\partial v/\partial t + fu = 0, \tag{24}$$

$$\partial h/\partial t + H(\partial u/\partial x) = 0. \tag{25}$$

Eliminating v and h yields

$$\partial^2 u/\partial t^2 + f^2 u - gH(\partial^2 u/\partial x^2) = 0. \tag{26}$$

If the solution is assumed proportional to $\exp[i(kx - \nu t)]$, then the angular frequency ν for the inertia-gravity waves is given by

$$(\nu/f)^2 = 1 + gH(k/f)^2, \tag{27}$$

where k is the wave number in the x direction. The frequency of inertia-gravity waves is a monotonically increasing function of the wave number k unless the radius of deformation λ defined by $\sqrt{gH}/f$, is zero. The group velocity $\partial\nu/\partial k$ is not zero unless $\lambda = 0$; this nonzero group velocity is very important for the geostrophic adjustment process.

The effect of the space discretization error on the frequency can now be examined. The space distributions of the dependent variables in this one-dimensional case for Schemes A through D are shown in Fig. 4; Scheme E is not shown, since it is equivalent to Scheme A, but with a smaller grid size. For Schemes A through D the following frequencies are obtained:

Scheme A:

$$(\nu/f)^2 = 1 + (\lambda/d)^2 \sin^2(kd), \tag{28}$$

Scheme B:

$$(\nu/f)^2 = 1 + 4(\lambda/d)^2 \sin^2(kd/2), \tag{29}$$

Scheme C:

$$(\nu/f)^2 = \cos^2(kd/2) + 4(\lambda/d)^2 \sin^2(kd/2), \tag{30}$$

Scheme D:

$$(\nu/f)^2 = \cos^2(kd/2) + (\lambda/d)^2 \sin^2(kd). \tag{31}$$

In all cases, the nondimensional frequency ν/f depends on the two parameters kd and λ/d.

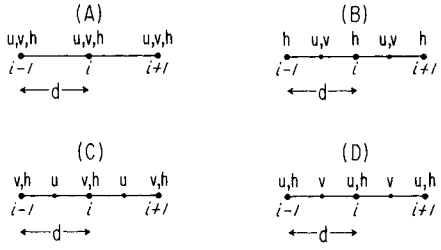

FIG. 4. Distributions of the dependent variables for a one-dimensional grid which correspond to those for a square grid shown in Fig. 3.

With these frequencies for the inertia-gravity waves, the dispersion properties of each scheme can be examined. The wavelength of the shortest resolvable wave is $2d$; the corresponding wave number $k_{\max}$ is π/d. Therefore, in examining Eqs. (28)–(31), it is sufficient to consider the range $0 < kd < \pi$.

Scheme A. The frequency reaches its maximum at $kd = \pi/2$, which means that the group velocity at $kd = \pi/2$ is zero. When inertia-gravity waves at about this wave number are excited somewhere in the domain (by nonlinearity, heating, etc.), the wave energy stays there. In this scheme, a wave with $kd = \pi$ behaves like a pure inertia oscillation.

Scheme B. For nonzero λ the frequency is monotonically increasing in the range $0 < kd < \pi$.

Scheme C. The frequency is monotonically increasing for $\lambda/d > \frac{1}{2}$ and monotonically decreasing for $\lambda/d < \frac{1}{2}$. For $\lambda/d = \frac{1}{2}$, $\nu^2 = f^2$ and the group velocity is zero for all k.

Scheme D. The frequency reaches a maximum at $(\lambda/d)^2 \cos(kd) = \frac{1}{4}$. Moreover, $kd = \pi$ is a stationary wave.

These results for the one-dimensional case show that Scheme B is the most satisfactory. However, when λ/d is sufficiently larger than 1/2, Scheme C is as good as Scheme B. To illustrate, Fig. 5 shows a comparison of the dependence of $|\nu|/f$ on kd/π for the case $\lambda/d = 2$.

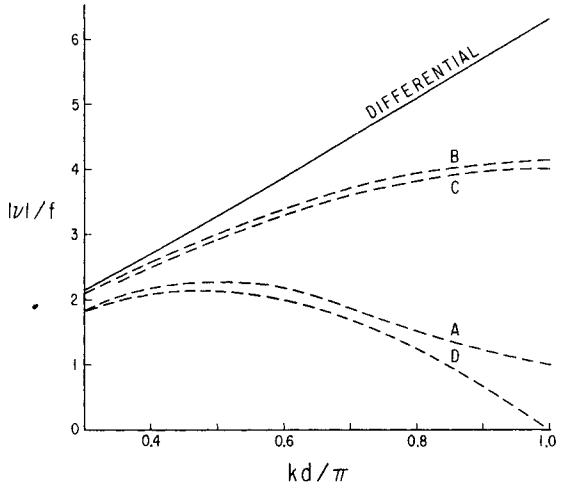

FIG. 5. The dependence of the (nondimensional) frequency on the (nondimensional) wave number for the shallow water equations for the case $\lambda/d = 2$. Solid line corresponds to the differential case, given by Eq. (27); dashed lines represent the difference Schemes A–D, given by Eqs. (28)–(31).

Cahn (1945) gave the solution of an initial value problem for which Eqs. (23)–(25) are the governing equations. At the initial time, he let $h =$ constant, $u = 0$, $v = V_0$ in the domain from $x = -a$ to $x = a$, and $v = 0$ outside of this domain.

A form of the solution $u(x, t)$ for these same initial conditions, suitable for use in a comparison of the differential and difference formulations, is obtained by first expressing $u(x, t)$ in Fourier integral form:

$$u(x, t) = \frac{1}{2\pi} \operatorname{Re} \int_{-\infty}^{\infty} e^{ikx} u^*(k, t)\, dk, \tag{32}$$

where

$$u^*(k, t) = \int_{-\infty}^{\infty} e^{-ikx} u(x, t)\, dx, \tag{33}$$

and k is the wave number in the x direction. The function $u^*(k, t)$ then satisfies the following equation

$$\frac{\partial^2 u^*(k, t)}{\partial t^2} + (f^2 + k^2 gH)u^*(k, t) = 0, \tag{34}$$

which has the general solution

$$u^*(k, t) = A(k) \cos(\nu t) + B(k) \sin(\nu t), \tag{35}$$

where

$$\nu^2 = f^2(1 + \lambda^2 k^2). \tag{36}$$

To determine $A(k)$, Eqs. (35) and (33) are applied at $t = 0$ to give

$$A(k) = u^*(k, 0) = \int_{-\infty}^{\infty} e^{-ikx} u(x, 0)\, dx = 0. \tag{37}$$

Moreover, Eqs. (35) and (33) give

$$\frac{\partial u^*(k, t)}{\partial t} = \nu[-A(k) \sin(\nu t) + B(k) \cos(\nu t)] \tag{38}$$

and

$$\frac{\partial u^*(k, t)}{\partial t} = \int_{-\infty}^{\infty} e^{-ikx} \frac{\partial u(x, t)}{\partial t}\, dx. \tag{39}$$

Applying Eqs. (38) and (39) at $t = 0$ gives an expression for $B(k)$,

$$B(k) = \frac{1}{\nu}\left(\frac{\partial u^*(k, t)}{\partial t}\right)_{t=0} = \frac{1}{\nu}\int_{-\infty}^{\infty} e^{-ikx}\left(\frac{\partial u(x, t)}{\partial t}\right)_{t=0} dx. \tag{40}$$

From the initial conditions and Eq. (23), we have

$$\left(\frac{\partial u(x, t)}{\partial t}\right)_{t=0} = \begin{cases} fV_0 & \text{for } |x| \leqslant a \\ 0 & \text{for } |x| > a. \end{cases} \tag{41}$$

Therefore, from Eq. (40),

$$B(k) = \frac{1}{v}\int_{-a}^{a} e^{-ikx} f V_0 \, dx = -\frac{f V_0 e^{-ikx}}{vik}\Bigg|_{x=-a}^{x=a} = \frac{2fV_0}{kv}\sin(ak). \quad (42)$$

Finally, Eq. (32) gives, with Eqs. (35) and (42), the desired solution

$$u(x, t) = \frac{faV_0}{\pi}\,\mathrm{Re}\int_{-\infty}^{\infty} \frac{\sin(ak)}{ak}\frac{\sin(vt)}{v} e^{ikx}\, dx, \quad (43)$$

or

$$u(x, t) = \frac{faV_0}{\pi}\int_{-\infty}^{\infty} \frac{\sin(ak)}{ak}\frac{\sin(vt)}{v}\cos kx\, dk. \quad (44)$$

Expressions for h were obtained using Eq. (44) with the equation of continuity (25) in the differential case and with the finite-difference analogs of the equation of continuity for each of the Schemes A–D. In the differential case, v was given by Eq. (36), while with finite-difference Schemes A–D the frequency v was given instead by Eqs. (28)–(31), respectively.* The integral in these expressions for h was evaluated numerically using Simpson's rule with 600 intervals in k from 0 to π/a. The solutions for h were calculated, with $f = 10^{-4}\ \mathrm{sec}^{-1}$, for constant x for values of t up to 40 hr at 15-min intervals, and for constant t over a range of x.

Some results of these calculations, with $a/d = 1$ and $\lambda/d = 2$, are shown in Figs. 6 and 7. Figure 6 shows the *time* variation of h at $x = a$ for the differential case, which approximates the solution obtained by Cahn, and for each of the difference schemes. Figure 7 gives the *space* variation of h in the differential case and for each of the schemes at $t = 80$ hr. As expected, Schemes B and C simulate the geostrophic adjustment better than the other schemes.

However, in the two-dimensional case there is a difficulty with Scheme B. Figure 8 shows $|v|/f$ for each of Schemes A through E, as a function of kd/π and ld/π, where k and l are the wave numbers in the x and y directions; again $\lambda/d = 2$. For comparison, $|v|/f$ for the differential case is shown in Fig. 9. The chain lines in Fig. 8 show the maximum $|v|/f$ for each of a range

*Note added in proof. Professor Arthur L. Schoenstadt, Department of Mathematics, United States Naval Postgraduate School, Monterey, has pointed out in a personal communication that f in Eq. (44) must also be modified for Schemes C and D. Figures 6 and 7 are based on his corrected expressions.

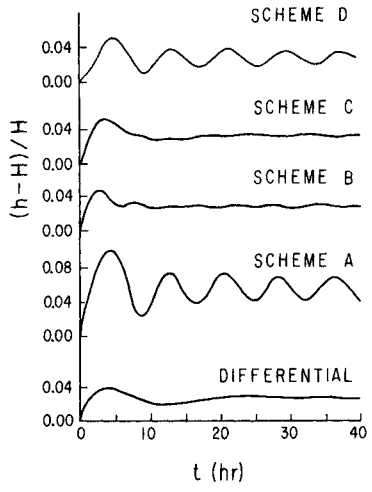

FIG. 6. Time variation of the (nondimensional) height perturbation at $x = a$ for the initial value problem posed by Cahn (1945): comparison of results for the differential case and for difference Schemes A–D.

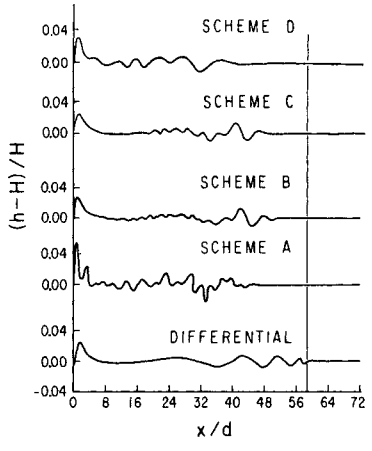

FIG. 7. The spatial variation of the (nondimensional) height perturbation at $t = 80$ hours for the same initial value problem: comparison of results for the differential case and for Schemes A–D. The thin vertical line at $x/d \doteqdot 59$ indicates the theoretical limit of influence.

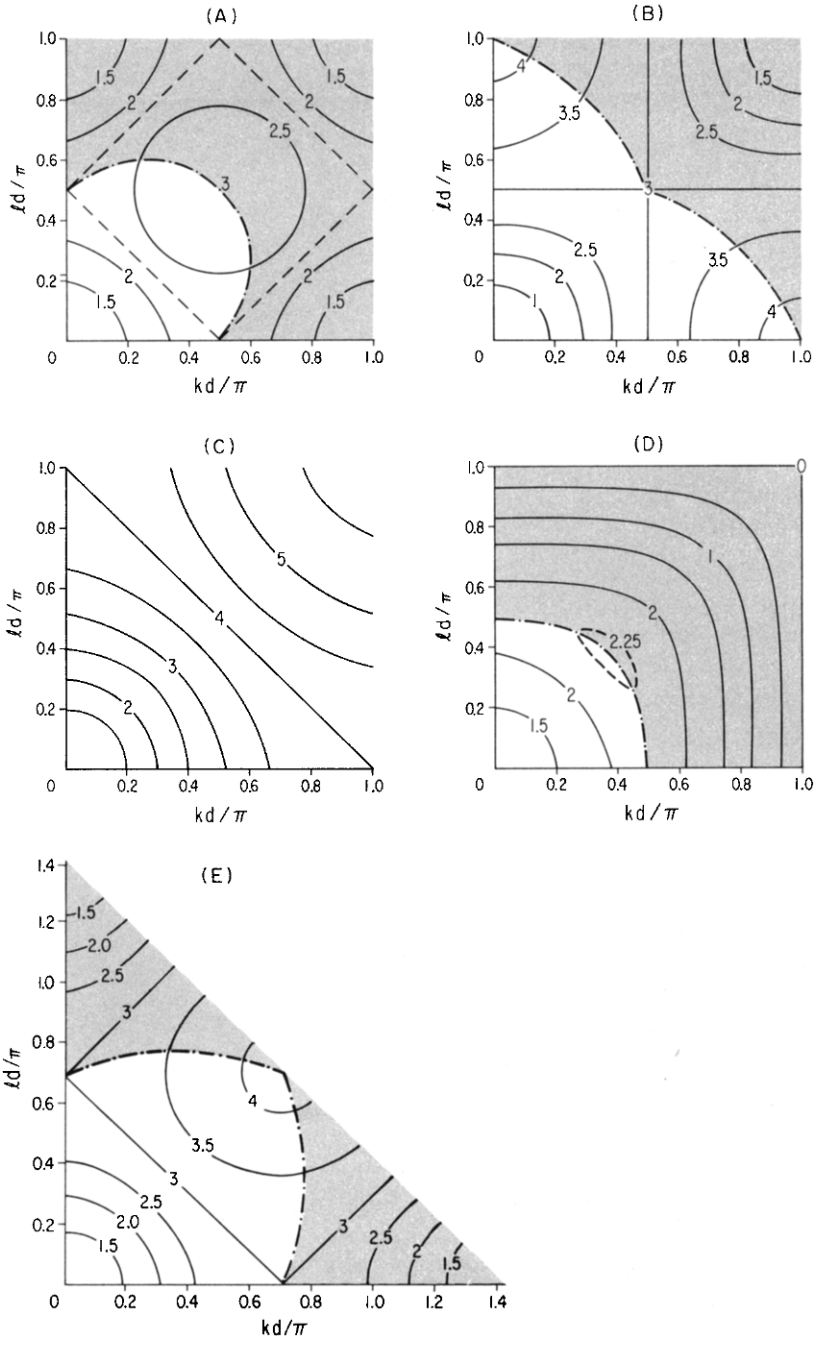

FIG. 8. Contours of the (nondimensional) frequency $|\nu|/f$ for Schemes A–E, as a function of the (nondimensional) horizontal wave numbers for the shallow water equations, for fixed $\lambda/d = 2$. Chain lines show the position of maximum values of the function for a range of the ratio l/k.

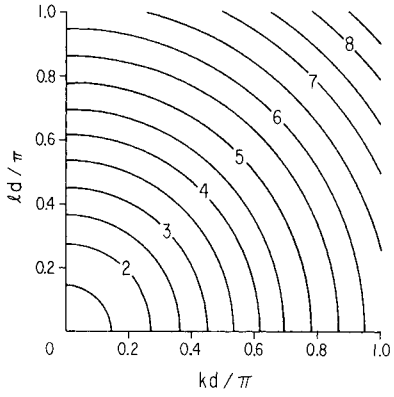

FIG. 9. Contours of the (nondimensional) frequency as a function of the (nondimensional) horizontal wave numbers for the differential shallow water equation for $\lambda/d = 2$, presented for comparison with Fig. 8.

of values of the ratio l/k. Note that there is no such maximum for Scheme C or the differential case.

In conclusion, the simulation of geostrophic adjustment is best with Scheme C, except for abnormal situations in which λ/d is less than or close to 1.

B. Two-Dimensional Nondivergent Flow

The next consideration must be the simulation of the slowly changing quasi-geostrophic (and, therefore, quasi-nondivergent) motion after it is established by the geostrophic adjustment process.

Consider, first, a flow which is purely horizontal and nondivergent, governed by the vorticity equation

$$\partial\zeta/\partial t + \mathbf{v} \cdot \nabla\zeta = 0, \tag{45}$$

where

$$\mathbf{v} = \mathbf{k} \times \nabla\psi, \qquad \zeta = \mathbf{k} \cdot \nabla \times \mathbf{v} = \nabla^2\psi, \tag{46}$$

and ψ is the stream function, ∇ is the two-dimensional del operator, and $\mathbf{k}$ is the unit vector normal to the plane of motion. Equation (45) can also be written as

$$\partial\zeta/\partial t = J(\zeta, \psi), \tag{47}$$

where J is the Jacobian operator, defined by

$$J(\zeta, \psi) = (\partial\zeta/\partial x)(\partial\psi/\partial y) - (\partial\zeta/\partial y)(\partial\psi/\partial x). \tag{48}$$

There are the following integral constraints, among others, on the Jacobian:

$$\overline{J(\zeta, \psi)} = 0, \tag{49}$$

$$\overline{\zeta J(\zeta, \psi)} = 0, \tag{50}$$

$$\overline{\psi J(\zeta, \psi)} = 0, \tag{51}$$

where the bar denotes the average over the domain, along the boundary of which ψ is constant. From these integral constraints it is seen that the mean vorticity $\overline{\zeta}$, the enstrophy (one half of the mean square vorticity) $\frac{1}{2}\overline{\zeta^2}$, and the mean kinetic energy $\frac{1}{2}\overline{(\nabla\psi)^2}$ are conserved with time. Conservation of these quantities during the advection process poses important constraints on the statistical properties of two-dimensional incompressible flow, as pointed out by Fjørtoft (1953). In particular, the average wave number k defined by

$$k^2 = \overline{(\nabla^2\psi)^2}/\overline{(\nabla\psi)^2}, \tag{52}$$

is conserved with time, so that no systematic cascade of energy into shorter waves can occur.

If the statistical properties are to be simulated numerically, a finite-difference scheme must be used that approximately conserves these quadratic quantities. Avoiding computational instability in the nonlinear sense is necessary but not sufficient for this purpose. Two examples of stable schemes that have a false energy cascade into shorter waves will be shown later.

It should be noted that if Eq. (47) is applied to a one-dimensional problem, the nonlinearity will be lost. Therefore, the tests of a finite-difference scheme for incompressible flow must be made with two-dimensional problems.

The finite-difference approximation for Eq. (47) may be written in a relatively general form as

$$\zeta_{ij}^{n+1} - \zeta_{ij}^{n} = \Delta t \mathbb{J}_{ij}(\zeta^*, \psi^*), \tag{53}$$

where $\zeta_{ij}^{n} = (\nabla_{ij}^2\psi)^n$ is a finite-difference approximation of $\zeta = \nabla^2\psi$ at the grid point $x = id$, $y = jd$, and at time $t = n\,\Delta t$. Here, d is the grid size, Δt is the time interval, and ∇_{ij}^2 and $\mathbb{J}_{ij}$ are finite difference approximations for the operators ∇^2 and J at the grid point $x = id$, $y = jd$. Hereafter, the subscripts i, j will be omitted unless they are necessary for clarity.

There are a number of time-difference schemes corresponding to different choices of ζ^* and ψ^*. For example, ζ^* may be equal to $\zeta^{n+1/2}$, as in the leapfrog scheme; or ζ^* may be a linear combination of ζ^n and ζ^{n+1} such as

$$\zeta^* = \tfrac{1}{2}(\zeta^n + \zeta^{n+1}), \tag{54}$$

which is an implicit scheme of the Crank–Nicholson type. As another example, ζ^* may be a provisional value of ζ, predicted by

$$\zeta^* = S\zeta^n + \alpha\, \Delta t \mathbb{J}^*(\zeta^n, \psi^n), \tag{55}$$

where S and α may be equal to 1, as in the Matsuno scheme, or S may be a smoothing operator and $\alpha = \frac{1}{2}$, as in the two-step Lax–Wendroff scheme. Here $\mathbb{J}^*$ is not necessarily the same as $\mathbb{J}$.

The change of enstrophy is obtained from Eq. (53), as

$$\tfrac{1}{2}[\overline{(\zeta^{n+1})^2} - \overline{(\zeta^n)^2}] = \Delta t \overline{[(\zeta^{n+1} + \zeta^n)/2]\mathbb{J}(\zeta^*, \psi^*)}, \tag{56}$$

where the bar denotes an average over all grid points in the domain considered. Equation (56) can be rewritten as

$$\begin{aligned}\tfrac{1}{2}[\overline{(\zeta^{n+1})^2} - \overline{(\zeta^n)^2}] = {} & \overline{\{[(\zeta^{n+1} + \zeta^n)/2] - \zeta^*\}(\zeta^{n+1} - \zeta^n)} \\ & + \overline{\Delta t \zeta^* \mathbb{J}(\zeta^*, \psi^*)}.\end{aligned} \tag{57}$$

To conserve enstrophy, ζ^* and the form of $\mathbb{J}$ must be chosen in such a way that the right-hand side of Eq. (57) vanishes. The first term on the right vanishes if ζ^* is chosen as $(\zeta^{n+1} + \zeta^n)/2$. The second term vanishes if the finite-difference Jacobian $\mathbb{J}$ maintains the integral constraint given by Eq. (50) for the differential Jacobian J. Similarly, it can be shown that a properly defined kinetic energy is conserved if ψ^* is chosen as $(\psi^{n+1} + \psi^n)/2$ and $\mathbb{J}$ maintains the integral constraint given by Eq. (51).

Consider the grid shown in Fig. 10. There are three basic second-order, finite-difference Jacobians:

$$\begin{aligned}\mathbb{J}_1 &= \Delta_x\zeta\, \Delta_y\psi - \Delta_y\zeta\, \Delta_x\psi, \\ \mathbb{J}_2 &= \Delta_y(\psi\, \Delta_x\zeta) - \Delta_x(\psi\, \Delta_y\zeta), \\ \mathbb{J}_3 &= \Delta_x(\zeta\, \Delta_y\psi) - \Delta_y(\zeta\, \Delta_x\psi),\end{aligned} \tag{58}$$

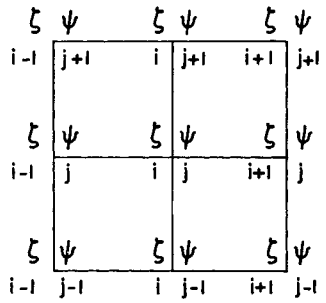

FIG. 10. Grid showing indexing for ζ, ψ points used in the finite-difference Jacobian schemes of Eq. (58).

where $(\Delta_x\alpha)$ is defined by $(\alpha_{i+1,j} - \alpha_{i-1,j})/2d$, and $\Delta_y\alpha$ is defined similarly with respect to y. It was shown by Arakawa (1966) that the Jacobian $\mathbb{J}$ given by

$$\mathbb{J} = \alpha\mathbb{J}_1 + \gamma\mathbb{J}_2 + \beta\mathbb{J}_3, \qquad \alpha + \gamma + \beta = 1, \tag{59}$$

conserves mean square vorticity if $\alpha = \beta$ and conserves energy if $\alpha = \gamma$. Examples of Jacobians which have the form of (59) are

$$\begin{aligned} \mathbb{J}_4 &= \tfrac{1}{2}(\mathbb{J}_1 + \mathbb{J}_2), \\ \mathbb{J}_5 &= \tfrac{1}{2}(\mathbb{J}_2 + \mathbb{J}_3), \\ \mathbb{J}_6 &= \tfrac{1}{2}(\mathbb{J}_3 + \mathbb{J}_1), \\ \mathbb{J}_7 &= \tfrac{1}{3}(\mathbb{J}_1 + \mathbb{J}_2 + \mathbb{J}_3). \end{aligned} \tag{60}$$

A schematic representation of the ζ and ψ points used in constructing the seven finite-difference Jacobians introduced above is given in Fig. 11.

$\mathbb{J}_7$ is the Jacobian proposed by Arakawa (1966) as conserving both enstrophy and energy. $\mathbb{J}_2$ and $\mathbb{J}_6$ conserve enstrophy, but not energy. $\mathbb{J}_3$ and $\mathbb{J}_4$ conserve energy, but not enstrophy. All five schemes mentioned thus far are stable. $\mathbb{J}_1$ does not conserve either quantity, and an analysis similar to that by Phillips (1959), but with the implicit scheme (54), shows that it is unstable. $\mathbb{J}_5$, also, does not conserve either quantity, but experience with numerical tests shows that the instability is very weak, if it exists at all. This is not surprising, since $2\mathbb{J}_5 = 3\mathbb{J}_7 - \mathbb{J}_1$; because $\mathbb{J}_7$ is a quadratic-conserving scheme the time rates of change of the mean quadratic quantities using $\mathbb{J}_5$, for given ζ and ψ, have opposite sign to the time rates of change of the mean quadratic quantities using $\mathbb{J}_1$.

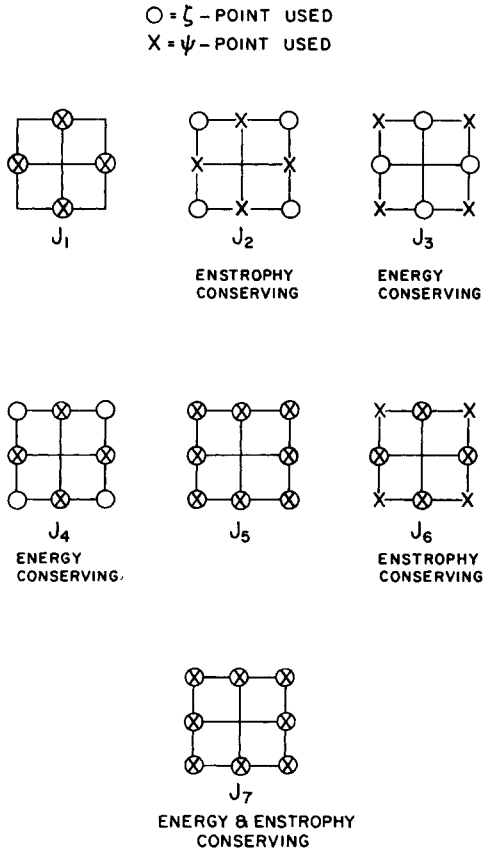

FIG. 11. Schematic representation of ζ and ψ points used in constructing the finite-difference Jacobians defined by Eqs. (58) and (60).

$\mathbb{J}_7$ is the best second-order scheme because of its formal guarantee for maintaining the integral constraints on the quadratic quantities. $\mathbb{J}_7$ is also just as accurate as any other second-order scheme. A further increase in accuracy can be obtained by going to higher order schemes. The more accurate fourth-order scheme that has the same integral constraints as $\mathbb{J}_7$ was also given by Arakawa (1966).

Numerical tests have been made with the above seven Jacobians. In these tests, the initial condition was given by

$$\psi = \Psi \sin(\pi i/8)[\cos(\pi j/8) + 0.1 \cos(\pi j/4)], \tag{61}$$

and Δt was chosen such that $\Delta t/d^2 = 0.7$. The leapfrog scheme was used instead of the implicit scheme. In order to eliminate the gradual separation of the solutions at even and odd time steps that occurs in the leapfrog scheme, a two-level scheme was inserted every 240 time steps. The simplest five-point Laplacian was used. Figures 12 and 13 show the time change of enstrophy and energy obtained with the seven Jacobians. The expected conservation properties are observed, even though the implicit scheme was not used. The energy conserving schemes $\mathbb{J}_3$ and $\mathbb{J}_4$ show considerable increase of enstrophy. On the other hand, the enstrophy conserving schemes $\mathbb{J}_2$ and $\mathbb{J}_6$ approximately conserve energy in spite of the lack of a formal guarantee. This is reasonable because the enstrophy is more sensitive to shorter waves for which the truncation errors are large. $\mathbb{J}_5$ approximately conserves both quantities, again in spite of the lack of formal guarantees.

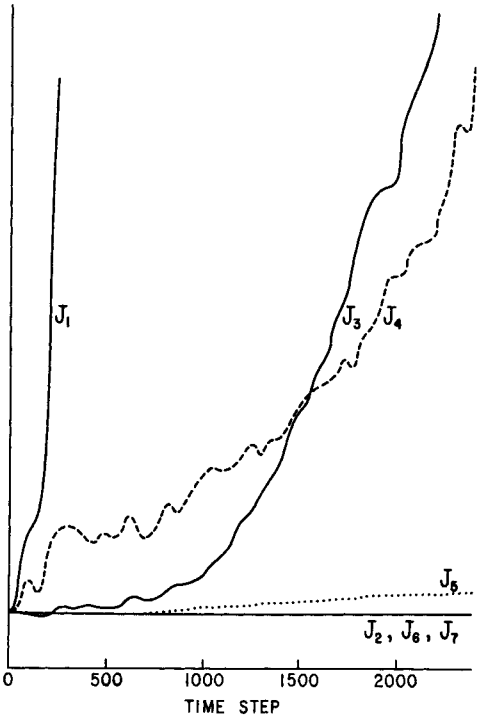

FIG. 12. Comparison of the time variation of the mean square vorticity (units arbitrary) during a numerical integration with the seven finite-difference Jacobians under consideration. (Arakawa, 1970). Reprinted with permission of the publisher American Mathematical Society from *SIAM-AMS Proceedings*. Copyright © 1970, Vol. 2, Fig. 5, p. 35.

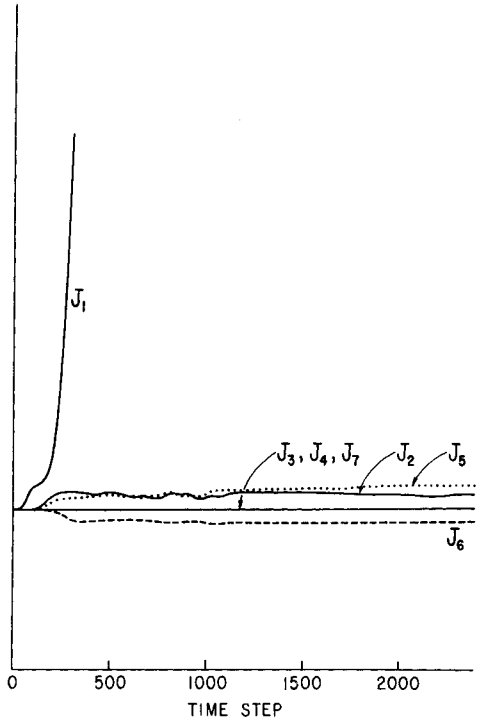

FIG. 13. Comparison of the time variation of the kinetic energy during a numerical integration with the seven finite-difference Jacobians under consideration (Arakawa, 1970). Reprinted with permission of the publisher American Mathematical Society from *SIAM-AMS Proceedings*. Copyright © 1970, Vol. 2, Fig. 6, p. 36.

$\mathbb{J}_7$ conserves both quantities, with only negligible errors arising from the leapfrog scheme. $\mathbb{J}_5$, like $\mathbb{J}_1$ and $\mathbb{J}_7$, maintains the property of the Jacobian $J(\zeta, \psi) = -J(\psi, \zeta)$.

Figure 14 shows the spectral distribution of kinetic energy obtained by the energy and enstrophy conserving scheme $\mathbb{J}_7$ and by the energy conserving scheme $\mathbb{J}_3$ at the end of the calculations. The small arrow shows the wave number for $\sin(\pi i/8) \cos(\pi j/8)$, which contained almost all of the energy at the initial time. Although the total energy was approximately conserved with $\mathbb{J}_3$ there was a considerable spurious energy cascade into the high wave numbers, whereas with $\mathbb{J}_7$ more energy went into a lower wave number than into the higher wave numbers, in agreement with the conservation of the average wave number as given by Eq. (52).

Whether the increase of the enstrophy is important in the simulation of large-scale atmospheric motion will depend on the viscosity used with the

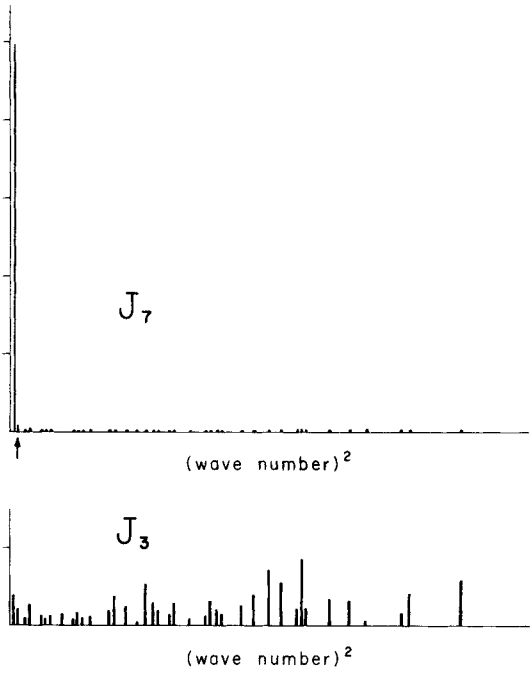

FIG. 14. A comparison of the spectral distribution of kinetic energy, obtained with $\mathbb{J}_3$ and $\mathbb{J}_7$, after a numerical integration of 2400 time steps. Arrow shows the wave number that contained most of the energy at the initial time.

complete equation. A relatively small amount of viscosity may be sufficient to keep the enstrophy quasi-constant in time. However, the viscosity will also remove energy, and as a result the average wave number, defined by Eq. (52), will falsely increase with time.

In Section II it was pointed out that when a scheme that produces a strong computational cascade is used, a decrease in grid size does not mean an increase in overall accuracy as far as long-term numerical integrations are concerned. Figure 15 shows such an example. With an identical initial condition, experiments have been made using $\mathbb{J}_3$ with three different grid sizes. The nondimensional parameter $\Psi\Delta t/d^2$ is kept the same for the three experiments. A two-level scheme was inserted every 120 time steps to suppress separation of the solution due to the leapfrog scheme. The figure shows a more rapid increase of enstrophy with the smaller grid sizes. Since the kinetic energy is practically conserved in all three experiments, a larger enstrophy means a smaller average scale of the motion. These results show that the convergence of the scheme, in the nonlinear sense, must be seriously questioned.

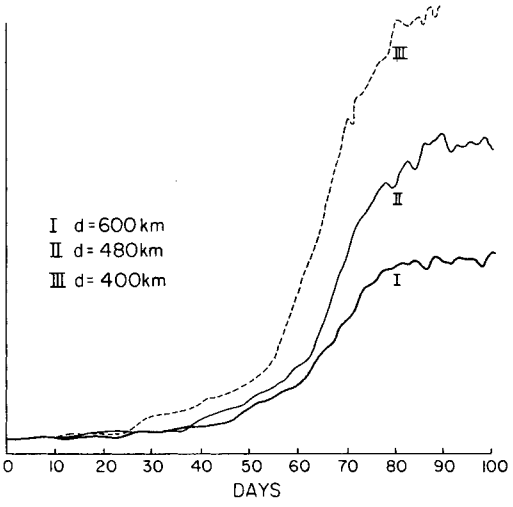

FIG. 15. A comparison of the time variation of mean square vorticity obtained by numerical integrations using $\mathbb{J}_3$ for three different grid sizes.

With the grid shown in Fig. 16, $\mathbb{J}_7$ may be written as

$$-\mathbb{J}_7(\zeta, \psi) = \frac{2}{3}\frac{1}{d^2}\{\delta_x(-\overline{\delta_y\psi}^{xy}\overline{\zeta}^x) + \delta_y(\overline{\delta_x\psi}^{xy}\overline{\zeta}^y)\}$$
$$+ \frac{1}{3}\frac{1}{2d^2}\{\delta_{x'}(-\delta_{y'}\psi\overline{\zeta}^{x'}) + \delta_{y'}(\delta_{x'}\psi\overline{\zeta}^{y'})\}, \tag{62}$$

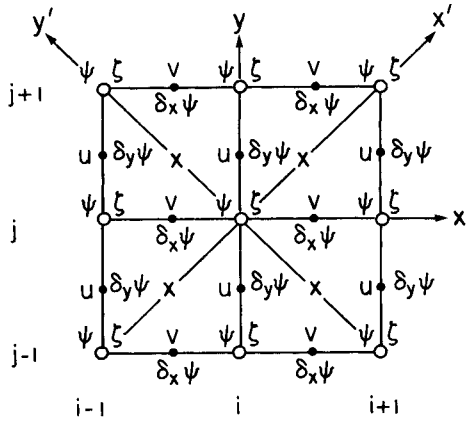

FIG. 16. Grid showing points of definition of the dependent variables and axes of definition for mean and difference operators used in the differencing of the momentum advection terms.

where $\delta_x\alpha$ and $\overline{\alpha}^x$ are defined as

$$(\delta_x\alpha)_{i+1/2,\,j} = \alpha_{i+1,\,j} - \alpha_{i,\,j} \tag{63}$$

and

$$(\overline{\alpha}^x)_{i+1/2,\,j} = \tfrac{1}{2}(\alpha_{i+1,\,j} + \alpha_{i,\,j}). \tag{64}$$

The symbols $\delta_y\alpha$ and $\overline{\alpha}^y$ are defined in a similar manner, but with respect to the y direction, and $\overline{\alpha}^{xy} = \overline{\overline{\alpha}^x}^y$. The symbols $\delta_{x'}$, $\delta_{y'}$, $\overline{\alpha}^{x'}$, and $\overline{\alpha}^{y'}$ follow the same definitions, but in the x' and y' directions and with the spacing $\sqrt{2}d$. It can easily be shown that

$$\delta_{x'}\psi = \overline{\delta_x\psi}^y + \overline{\delta_y\psi}^x, \qquad \delta_{y'}\psi = -\overline{\delta_x\psi}^y + \overline{\delta_y\psi}^x. \tag{65}$$

Since it is the momentum equation and not the vorticity equation that is used in the model, the next problem is to find a finite-difference scheme for the advection term in the momentum equation. The guiding assumption in our present approach is that a scheme that is inadequate for purely nondivergent motion is almost certainly also inadequate for the quasi-nondivergent motion typical of large-scale atmospheric motions. Thus the first constraint on a finite-difference scheme for the momentum equation is that it become equivalent to $\partial\zeta/\partial t = \mathbb{J}_7(\zeta, \psi)$ when the flow is horizontal and nondivergent.

The vorticity can be expressed as

$$\begin{aligned}\zeta_{ij} = (\nabla^2\psi)_{ij} &\equiv \frac{1}{d}\left(\frac{\psi_{i+1,\,j} - \psi_{ij}}{d} - \frac{\psi_{ij} - \psi_{i-1,\,j}}{d} + \frac{\psi_{i,\,j+1} - \psi_{ij}}{d} - \frac{\psi_{ij} - \psi_{i,\,j-1}}{d}\right) \\ &= \frac{1}{d^2}(\psi_{i+1,\,j} + \psi_{i-1,\,j} + \psi_{i,\,j+1} + \psi_{i,\,j-1} - 4\psi_{ij}).\end{aligned} \tag{66}$$

For the grid points shown in Fig. 16, u and v are defined by

$$u_{i,\,j+1/2} \equiv -\frac{(\delta_y\psi)_{i,\,j+1/2}}{d}, \qquad v_{i+1/2,\,j} \equiv \frac{(\delta_x\psi)_{i+1/2,\,j}}{d}. \tag{67}$$

Then the vorticity given by Eq. (66) is

$$\zeta_{ij} = (1/d)[(\delta_x v)_{ij} - (\delta_y u)_{ij}], \tag{68}$$

and the vorticity equation may be written as

$$(\partial/\partial t)[(\delta_x v)_{ij} - (\delta_y u)_{ij}] = \mathbb{J}_{ij}(\delta_x v - \delta_y u, \psi). \tag{69}$$

Here the symbol $\mathbb{J}$ is used for $\mathbb{J}_7$.

Consider $\mathbb{J}_{i,\,j+1/2}(u, \bar{\psi}^y)$. From a property of the Jacobian, which is maintained by $\mathbb{J}_7$,

$$\mathbb{J}_{i,\,j+1/2}(u, \bar{\psi}^y) = \mathbb{J}_{i,\,j+1/2}(u, \bar{\psi}^y + \tfrac{1}{2}ud), \tag{70}$$

and

$$\mathbb{J}_{i,\,j-1/2}(u, \bar{\psi}^y) = \mathbb{J}_{i,\,j-1/2}(u, \bar{\psi}^y - \tfrac{1}{2}ud). \tag{71}$$

Note that $(\bar{\psi}^y + \frac{1}{2}ud)_{i,\,j+1/2} = (\bar{\psi}^y - \frac{1}{2}ud)_{i,\,j-1/2} = \psi_{ij}$ for *arbitrary* i, j. Using (70) and (71),

$$\begin{aligned}[\delta_y \mathbb{J}(u, \bar{\psi}^y)]_{ij} &\equiv \mathbb{J}_{i,\,j+1/2}(u, \bar{\psi}^y) - \mathbb{J}_{i,\,j-1/2}(u, \bar{\psi}^y), \\ &= \mathbb{J}_{ij}(\delta_y u, \psi).\end{aligned} \tag{72}$$

Similarly,

$$[\delta_x \mathbb{J}(v, \bar{\psi}^x)]_{ij} = \mathbb{J}_{ij}(\delta_x v, \psi). \tag{73}$$

Equations (72) and (73) are analogs, respectively, of

$$(\partial/\partial y)J(u, \psi) = J(\partial u/\partial y, \psi), \qquad (\partial/\partial x)J(v, \psi) = J(\partial v/\partial x, \psi).$$

From Eqs. (72), (73), and (68),

$$\begin{aligned}[\delta_x \mathbb{J}(v, \bar{\psi}^x)]_{ij} - [\delta_y \mathbb{J}(u, \bar{\psi}^y)]_{ij} &= \mathbb{J}_{ij}(\delta_x v - \delta_y u, \psi) \\ &= d\mathbb{J}_{ij}(\zeta, \psi).\end{aligned} \tag{74}$$

The conclusion is that

$$\begin{aligned}&\mathbb{J}(u, \bar{\psi}^y) \quad \text{for} \quad -\mathbf{v} \cdot \nabla u \text{ at the } u \text{ points} \\ &\mathbb{J}(v, \bar{\psi}^x) \quad \text{for} \quad -\mathbf{v} \cdot \nabla v \text{ at the } v \text{ points}\end{aligned}$$

are consistent with

$$\mathbb{J}(\zeta, \psi) \quad \text{for} \quad -\mathbf{v} \cdot \nabla \zeta \text{ at the } \psi \text{ points.}$$

Equations (62) and (65), with ζ replaced by u and ψ by $\overline{\psi}^y$, give the form

$$-\mathcal{J}(u, \overline{\psi}^y) = \frac{2}{3d^2}\left[\delta_x(-\overline{\delta_y\overline{\psi}^{yxy}\overline{u}^x}) + \delta_y(\overline{\delta_x\overline{\psi}^{yxy}\overline{u}^y})\right]$$

$$+ \frac{1}{6d^2}\left[\delta_{x'}\{(\overline{\delta_x\overline{\psi}^{yy}} - \overline{\delta_y\overline{\psi}^{yx}})\overline{u}^{x'}\} + \delta_{y'}\{(\overline{\delta_x\overline{\psi}^{yy}} + \overline{\delta_y\overline{\psi}^{yx}})\overline{u}^{y'}\}\right]. \quad (75)$$

Define u^* and v^* by

$$u^* = -(1/d)\overline{\delta_y\overline{\psi}^x}, \qquad v^* = (1/d)\overline{\delta_x\overline{\psi}^y}. \quad (76)$$

Then (75), which is the divergence of u-momentum transport, becomes

$$\frac{2}{3d}\left[\delta_x(\overline{u^{*xy}\overline{u}^x}) + \delta_y(\overline{v^{*xy}\overline{u}^y})\right] + \frac{1}{6d}\left[\delta_{x'}(\overline{v^* + u^{*y}\overline{u}^{x'}}) + \delta_{y'}(\overline{v^* - u^{*y}\overline{u}^{y'}})\right]. \quad (77)$$

Similarly, the divergence of v-momentum transport becomes

$$\frac{2}{3d}\left[\delta_x(\overline{u^{*xy}\overline{v}^x}) + \delta_y(\overline{v^{*xx}\overline{v}^y})\right] + \frac{1}{6d}\left[\delta_{x'}(\overline{v^* + u^{*x}\overline{v}^{x'}}) + \delta_{y'}(\overline{v^* - u^{*x}\overline{v}^{y'}})\right]. \quad (78)$$

In Fig. 16, the distribution of u and v is staggered as in Schemes C and D of the last subsection. Results of the last subsection indicate, however, that Scheme C is definitely better than Scheme D in view of the geostrophic adjustment and therefore the x points rather than the ψ points in Fig. 16 carry pressure and temperature.

C. Finite Difference Scheme for the Nonlinear Shallow Water Equations

For use with the advection term of the momentum equations in the general circulation model, the finite-difference expressions (77) and (78) derived for the case of horizontal nondivergent flow must be generalized to the case of divergent flow. In this subsection, the principles guiding such a generalization will be illustrated through the derivation of a finite-difference scheme suitable for integration of the nonlinear shallow water equations on a square grid with the variables staggered as in the C scheme. The analogous development for the momentum equations governing three-dimensional motion in curvilinear coordinates is presented in Section VI.

The governing differential equations are Eqs. (1)–(3), restated below for convenience:

$$\frac{\partial u}{\partial t} + u\frac{\partial u}{\partial x} + v\frac{\partial u}{\partial y} - fv + g\frac{\partial h}{\partial x} = 0, \tag{79}$$

$$\frac{\partial v}{\partial t} + u\frac{\partial v}{\partial x} + v\frac{\partial v}{\partial y} + fu + g\frac{\partial h}{\partial y} = 0, \tag{80}$$

$$\frac{\partial h}{\partial t} + \frac{\partial (hu)}{\partial x} + \frac{\partial (hv)}{\partial y} = 0. \tag{81}$$

Combining Eq. (81) with Eqs. (79) and (80) gives another useful form of the momentum equations,

$$\frac{\partial (uh)}{\partial t} + \frac{\partial (huu)}{\partial x} + \frac{\partial (hvu)}{\partial y} - fhv + gh\frac{\partial h}{\partial x} = 0, \tag{82}$$

$$\frac{\partial (vh)}{\partial t} + \frac{\partial (huv)}{\partial x} + \frac{\partial (hvv)}{\partial y} + fhu + gh\frac{\partial h}{\partial y} = 0. \tag{83}$$

Multiplying Eq. (79) by u and Eq. (80) by v and combining the results with Eq. (81) yields the equations for the time change of kinetic energy,

$$\frac{\partial}{\partial t}(h\tfrac{1}{2}u^2) + \frac{\partial [hu\tfrac{1}{2}u^2]}{\partial x} + \frac{\partial [hv\tfrac{1}{2}u^2]}{\partial y} - fhuv + ghu\frac{\partial h}{\partial x} = 0, \tag{84}$$

$$\frac{\partial}{\partial t}(h\tfrac{1}{2}v^2) + \frac{\partial [hu\tfrac{1}{2}v^2]}{\partial x} + \frac{\partial [hv\tfrac{1}{2}v^2]}{\partial y} + fhuv + ghv\frac{\partial h}{\partial y} = 0. \tag{85}$$

Multiplying Eq. (81) by gh gives the equation for the change of potential energy,

$$\frac{\partial}{\partial t}\left(\frac{gh^2}{2}\right) + gh\left[\frac{\partial}{\partial x}(hu) + \frac{\partial}{\partial y}(hv)\right] = 0, \tag{86}$$

or

$$\frac{\partial}{\partial t}\left(\frac{gh^2}{2}\right) + \frac{\partial}{\partial x}(gh^2u) + \frac{\partial}{\partial y}(gh^2v) - gh\left[u\frac{\partial h}{\partial x} + v\frac{\partial h}{\partial y}\right] = 0. \tag{87}$$

The coriolis force of course makes no contribution to the change of total kinetic energy. Also, the summation of the last terms in Eqs. (84), (85), and (87) is zero. These points, which lead to conservation of the total energy, are utilized in the construction of the finite-difference scheme.

The differencing for the continuity equation is chosen on the basis of simplicity. At h points, Eq. (81) can be represented as

$$\frac{\partial}{\partial t} h_{i,j} + \frac{1}{d^2}\left[F_{i+1/2,j} - F_{i-1/2,j} + G_{i,j+1/2} - G_{i,j-1/2}\right] = 0, \quad (88)$$

where the mass fluxes

$$\begin{aligned} F_{i+1/2,j} &\equiv d[\overline{h}^x u]_{i+1/2,j} \\ G_{i,j+1/2} &\equiv d[\overline{h}^y v]_{i,j+1/2} \end{aligned} \quad (89)$$

are defined at u and v points, respectively. The time change terms are left in differential form throughout this section.

The first requirement on the finite-difference scheme is that it conserve total kinetic energy during inertial processes. To this end, considering first the u momentum equation (82), the terms

$$\frac{\partial}{\partial t}(uh) + \frac{\partial}{\partial x}(huu) + \frac{\partial}{\partial y}(hvu)$$

can be represented by the following form, which automatically guarantees proper conservation of integrated zonal momentum:

$$\begin{aligned} \frac{\partial}{\partial t}(H^{(u)}u)_{i,j} + \frac{1}{d^2}\left[\delta_x(\mathscr{F}^{(u)}\overline{u}^x) + \delta_y(\mathscr{G}^{(u)}\overline{u}^y)\right. \\ \left. + \delta_{x'}(\tilde{\mathscr{F}}^{(u)}\overline{u}^{x'}) + \delta_{y'}(\tilde{\mathscr{G}}^{(u)}\overline{u}^{y'})\right]_{i,j} \end{aligned} \quad (90)$$

where $H^{(u)}$ and $\mathscr{F}^{(u)}$, $\mathscr{G}^{(u)}$, $\tilde{\mathscr{F}}^{(u)}$, $\tilde{\mathscr{G}}^{(u)}$ are as yet undefined (see Fig. 17 for the points of definition of the new mass flux symbols). For simplicity, the convention of using the indices (i, j) for the variable whose prognostic equation is under consideration is followed. If these new terms are chosen in such a way that they satisfy

$$\frac{\partial}{\partial t} H^{(u)}_{i,j} + \frac{1}{d^2}\left[\delta_x\mathscr{F}^{(u)} + \delta_y\mathscr{G}^{(u)} + \delta_{x'}\tilde{\mathscr{F}}^{(u)} + \delta_{y'}\tilde{\mathscr{G}}^{(u)}\right]_{i,j} = 0, \quad (91)$$

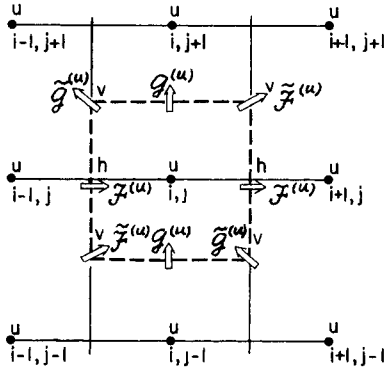

FIG. 17. Grid showing points of definition of fluxes introduced in Eq. (90) in the differencing of the advection terms of the u-momentum equation.

then by subtracting Eq. (91) multiplied by u_{ij}, (90) can be shown equivalent to

$$H^{(u)}_{i,j}\frac{\partial u_{i,j}}{\partial t} + \frac{1}{d^2}\left[\overline{\mathscr{F}^{(u)}\delta_x u}^{x} + \overline{\mathscr{G}^{(u)}\delta_y u}^{y} + \overline{\tilde{\mathscr{F}}^{(u)}\delta_{x'}u}^{x'} + \overline{\tilde{\mathscr{G}}^{(u)}\delta_{y'}u}^{y'}\right]_{i,j} \tag{92}$$

Multiplying (92) by u_{ij} and combining with Eq. (91) multiplied by $\frac{1}{2}u^2_{i,j}$, a finite-difference analog to the first three terms of Eq. (84) is obtained:

$$\begin{aligned}\frac{\partial}{\partial t}(H^{(u)}\tfrac{1}{2}u^2)_{ij} + \frac{1}{2d^2}\Big[&\mathscr{F}^{(u)}_{i+1/2,j}u_{i,j}u_{i+1,j} - \mathscr{F}^{(u)}_{i-1/2,j}u_{i-1,j}u_{i,j}\\ &+ \mathscr{G}^{(u)}_{i,j+1/2}u_{i,j}u_{i,j+1} - \mathscr{G}^{(u)}_{i,j-1/2}u_{i,j-1}u_{i,j}\\ &+ \tilde{\mathscr{F}}^{(u)}_{i+1/2,j+1/2}u_{i,j}u_{i+1,j+1} - \tilde{\mathscr{F}}^{(u)}_{i-1/2,j-1/2}u_{i-1,j-1}u_{i,j}\\ &+ \tilde{\mathscr{G}}^{(u)}_{i-1/2,j+1/2}u_{i,j}u_{i-1,j+1} - \tilde{\mathscr{G}}^{(u)}_{i+1/2,j-1/2}u_{i+1,j-1}u_{i,j}\Big].\end{aligned} \tag{93}$$

In (93), each of the kinetic energy flux terms reappears at a neighboring point but with the opposite sign. Thus, regardless of the subsequent definition of $H^{(u)}$, $\mathscr{F}^{(u)}$, $\mathscr{G}^{(u)}$, $\tilde{\mathscr{F}}^{(u)}$ and $\tilde{\mathscr{G}}^{(u)}$, the choice of form (90) and the constraint (91) together ensure that the total kinetic energy over the domain does not falsely increase or decrease.

The additional requirement on the difference scheme is that enstrophy be conserved during advection by the nondivergent part of the horizontal velocity. This will be guaranteed if the finite-difference scheme for the momentum advection terms reduces to (77) for the case of nondivergent flow.

If new symbols, based on Eq. (89), are defined at h points by

$$F^* \equiv \bar{F}^x \qquad G^* \equiv \bar{G}^y, \tag{94}$$

it is seen that in the case of nondivergent motion, F^* and G^* are equivalent, respectively, to (a constant) hd times u^* and v^* given by Eq. (76). The flux terms in (90) then reduce to (77) for this case if

$$\begin{aligned}
\mathscr{F}^{(u)}_{i+1/2,\,j} &= \tfrac{2}{3}(\overline{F^*}^{yy})_{i+1/2,\,j} \\
\mathscr{G}^{(u)}_{i,\,j+1/2} &= \tfrac{2}{3}(\overline{G^*}^{yx})_{i,\,j+1/2} \\
\tilde{\mathscr{F}}^{(u)}_{i+1/2,\,j+1/2} &= \tfrac{1}{6}(\overline{G^* + F^*}^{y})_{i+1/2,\,j+1/2} \\
\tilde{\mathscr{G}}^{(u)}_{i-1/2,\,j+1/2} &= \tfrac{1}{6}(\overline{G^* - F^*}^{y})_{i-1/2,\,j+1/2}.
\end{aligned} \tag{95}$$

It should be noted that this generalization of (77) is not unique.

The definition of $H^{(u)}$ is now determined by the requirement (91). Making use of Eqs. (95) and (94), Eq. (91) can be written in the form

$$\begin{aligned}
\frac{\partial}{\partial t} H^{(u)}_{i,j} + \frac{1}{d^2}\frac{1}{8}\big[&(\delta_x F + \delta_y G)_{i+1/2,\,j+1} + (\delta_x F + \delta_y G)_{i-1/2,\,j+1} \\
&+ (\delta_x F + \delta_y G)_{i+1/2,\,j-1} + (\delta_x F + \delta_y G)_{i-1/2,\,j-1} \\
&+ 2(\delta_x F + \delta_y G)_{i+1/2,\,j} + 2(\delta_x F + \delta_y G)_{i-1/2,\,j}\big] = 0.
\end{aligned} \tag{96}$$

From the continuity equation (88) it is then clear that Eq. (96) is satisfied only if

$$H^{(u)}_{i,j} = (\overline{h}^{xyy})_{i,\,j}. \tag{97}$$

An analogous development for the first terms of the v momentum equation (83) yields the form

$$\begin{aligned}
\frac{\partial}{\partial t}(H^{(v)}v)_{i,\,j} + \frac{1}{d^2}\big[&\delta_x(\mathscr{F}^{(v)}\overline{v}^x) + \delta_y(\mathscr{G}^{(v)}\overline{v}^y) \\
&+ \delta_{x'}(\tilde{\mathscr{F}}^{(v)}\overline{v}^{x'}) + \delta_{y'}(\tilde{\mathscr{G}}^{(v)}\overline{v}^{y'})\big]_{i,\,j},
\end{aligned} \tag{98}$$

which guarantees both conservation of kinetic energy, integrated over the domain, under inertial processes and conservation of enstrophy for the case

of nondivergent flow with the definitions

$$\begin{aligned}
\mathscr{F}^{(v)}_{i+1/2,\,j} &= \tfrac{2}{3}(\overline{F^*}^{xy})_{i+1/2,\,j} \\
\mathscr{G}^{(v)}_{i,\,j+1/2} &= \tfrac{2}{3}(\overline{G^*}^{xx})_{i,\,j+1/2} \\
\mathscr{F}^{(v)}_{i+1/2,\,j+1/2} &= \tfrac{1}{6}(\overline{G^* + F^*}^{x})_{i+1/2,\,j+1/2} \\
\mathscr{G}^{(v)}_{i-1/2,\,j+1/2} &= \tfrac{1}{6}(\overline{G^* - F^*}^{x})_{i-1/2,\,j+1/2}
\end{aligned} \tag{99}$$

and

$$H^{(v)}_{i,\,j} = (\overline{h}^{xxy})_{i,\,j}. \tag{100}$$

The coriolis term $-fhv$ in Eq. (82) is represented at the u point (i, j) by

$$-f_j(\overline{h\overline{v}^{y}}^{x})_{i,\,j}; \tag{101}$$

and the term $+fhu$ in Eq. (83) at the v point $(i + 1/2, j + 1/2)$ is represented by

$$(\overline{fh\overline{u}^{x}}^{y})_{i+1/2,\,j+1/2}. \tag{102}$$

Here the coriolis parameter f_j is defined at latitudes where h is carried.

The rate of increase in the kinetic energy of the u component at the point (i, j) due to the coriolis force is obtained by multiplying (101) by $u_{i,\,j}$. The contribution to this increase from the v point $(i + 1/2, j + 1/2)$ involves the portion

$$-\tfrac{1}{4}f_j h_{i+1/2,\,j} v_{i+1/2,\,j+1/2} u_{i,\,j}. \tag{103}$$

Similarly, the rate of increase in the kinetic energy of the v component at the point $(i + 1/2, j + 1/2)$ is given by (102) times $v_{i+1/2,\,j+1/2}$; and the fraction due to the u point (i, j) involves the term

$$+\tfrac{1}{4}f_j h_{i+1/2,\,j} u_{i,\,j} v_{i+1/2,\,j+1/2}. \tag{104}$$

Note that (103) and (104) exactly cancel so that total kinetic energy is not influenced by these terms.

Finally, the pressure gradient terms, which convert potential into kinetic energy, can be examined. At the u point (i, j), the term $gh(\partial h/\partial x)$ in Eq. (82) is represented as

$$g[\overline{h}^{x}\,\delta_x h]_{ij}; \tag{105}$$

and at the v point $(i + 1/2, j + 1/2)$, $gh(\partial h/\partial y)$ in Eq. (83) is represented as

$$g[\bar{h}^{y}\,\delta_{y}h]_{i+1/2,\,j+1/2}. \tag{106}$$

An argument completely analogous to that utilized in the discussion of the coriolis terms can be advanced to show that this finite-difference form of the pressure gradient terms does not cause any false production of total energy.

IV. Basic Governing Equations

A. The Vertical Coordinate

The vertical coordinate used in the model is a combination of the σ coordinate (Phillips, 1957) for the lower part of the atmosphere, and the pressure coordinate for the upper part of the atmosphere.

Let p be the pressure; p_T, the pressure at the top of the model atmosphere, taken as a constant; and p_S, the pressure at the earth's surface, which varies with the horizontal coordinates and time. A constant pressure p_I is chosen which lies between p_T and a lower bound of p_S, and the vertical coordinate σ is then defined by

$$\sigma \equiv \frac{p - p_I}{\pi}, \tag{107}$$

where

$$\pi = \begin{cases} \pi_U \equiv p_I - p_T & \text{for} \quad p_T \leqslant p < p_I, \\ \pi_L \equiv p_S - p_I & \text{for} \quad p_I < p \leqslant p_S. \end{cases} \tag{108}$$

Note that π_U is constant, whereas π_L is a function of the horizontal coordinates and time. It follows from Eqs. (107) and (108) that

$$\begin{aligned} \sigma &= -1 \quad && \text{for} \quad p = p_T, \\ \sigma &= 0 \quad && \text{for} \quad p = p_I, \\ \sigma &= 1 \quad && \text{for} \quad p = p_S. \end{aligned} \tag{109}$$

Figure 18 shows surfaces of constant σ in a vertical cross section. The lower boundary, which follows the earth's topography, is a coordinate surface; and the isobaric surfaces for $p_T \leqslant p \leqslant p_I$ are coordinate surfaces. When $p_I = p_T$, this vertical coordinate system reduces to the σ coordinate of earlier versions of the UCLA General Circulation Model (Mintz, 1965, 1968; Arakawa, 1972); and when $p_I = p_T = 0$, it reduces to the original σ coordinate of Phillips (1957).

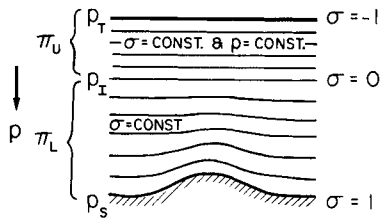

FIG. 18. Definition of the layers of the model in terms of the vertical σ coordinate.

Since π is either π_U, which is a constant, or π_L, which is a function only of the horizontal coordinates and time, (107) gives

$$\delta p = \pi \, \delta\sigma, \tag{110}$$

where δ denotes the differential under constant horizontal coordinates and time. $\pi \, \delta\sigma/g$ is the mass per unit horizontal area in a layer of depth $\delta\sigma$, where g is the acceleration of gravity.

From Eq. (107), the individual time derivative of pressure is given by

$$\omega \equiv dp/dt = \pi\dot{\sigma} + \sigma[(\partial\pi/\partial t) + \mathbf{v} \cdot \nabla\pi], \tag{111}$$

where $\dot{\sigma} \equiv d\sigma/dt$, $\mathbf{v}$ is the horizontal velocity, and ∇ is the horizontal gradient operator. Note that $\partial\pi/\partial t + \mathbf{v} \cdot \nabla\pi = 0$ for $\sigma < 0$ and, therefore,

$$\omega = \pi\dot{\sigma} \qquad \text{for} \quad \sigma \leqslant 0. \tag{112}$$

At the top of the model atmosphere, Eq. (112) gives $(\pi\dot{\sigma})_{\sigma=-1} = (\omega)_{p=p_T}$. It is assumed that $(\omega)_{p=p_T} = 0$, and thus

$$(\pi\dot{\sigma})_{\sigma=-1} = 0. \tag{113}$$

The earth's surface is a material surface as well as a coordinate surface. The kinematical boundary condition there is simply $\dot{\sigma} = 0$, so that

$$(\pi\dot{\sigma})_{\sigma=1} = 0. \tag{114}$$

Finally, the continuity of ω at $\sigma = 0$ requires

$$(\pi\dot{\sigma})_{\sigma=0-} = (\pi\dot{\sigma})_{\sigma=0+} = \omega_I, \tag{115}$$

where $\omega_I \equiv (\omega)_{p=p_I}$.

B. The Equation of State

The model atmosphere is assumed to be a perfect gas, so that

$$\alpha = RT/p, \tag{116}$$

where α is the specific volume, T is the temperature, and R is the gas constant. For simplicity, the difference of the gas constant from that of dry air (which determines the difference between the virtual temperature and the temperature) is neglected except in the parameterizations of subgrid scale turbulence and cumulus convection.

C. The Hydrostatic Equation

With Eq. (110), the hydrostatic equation $\delta\Phi = -\alpha\delta p$ becomes

$$\delta\Phi = -\pi\alpha\,\delta\sigma, \tag{117}$$

where Φ is the geopotential gz and z is height.

The following alternate forms of the hydrostatic equation can be derived from Eq. (117) and will be useful:

$$\delta(\Phi\sigma) = -(\pi\sigma\alpha - \Phi)\,\delta\sigma, \tag{118}$$

$$\delta\Phi = -RT\,\delta \ln p, \tag{119}$$

$$= -c_p\theta\,\delta(p/p_0)^\kappa \tag{120}$$

$$= c_p \frac{d \ln \theta}{d(1/\theta)}\,\delta\left(\frac{p}{p_0}\right)^\kappa, \tag{121}$$

$$\delta(c_pT + \Phi) = \left(\frac{p}{p_0}\right)^\kappa c_p\,\delta\theta, \tag{122}$$

where c_p is the specific heat at constant pressure, $\kappa \equiv R/c_p$, and θ is the potential temperature, $T(p_0/p)^\kappa$, where p_0 is a standard pressure.

D. The Equation of Continuity

In the pressure coordinate system, the equation of continuity takes the form

$$\nabla_p \cdot \mathbf{v} + (\partial\omega/\partial p) = 0. \tag{123}$$

Gradients in the pressure and σ-coordinate systems are related by

$$\nabla_p = \nabla_\sigma + (\nabla_p \sigma)(\partial/\partial\sigma), \tag{124}$$

Using the gradient ∇_p of Eq. (107), namely

$$\pi \nabla_p \sigma + \sigma \nabla \pi = 0,$$

Eq. (124) becomes

$$\nabla_p = \nabla_\sigma - \sigma/\pi \nabla\pi \, \partial/\partial\sigma. \tag{125}$$

Note that $\nabla_p = \nabla_\sigma$ for $\sigma \leqslant 0$, because π is constant for $\sigma \leqslant 0$.

Using Eq. (125) for $\nabla_p \cdot \mathbf{v}$ and using Eqs. (111) and (110) for $\partial\omega/\partial p$, Eq. (123) gives

$$\left[\nabla_\sigma \cdot \mathbf{v} - \frac{\sigma}{\pi} \nabla\pi \cdot \frac{\partial \mathbf{v}}{\partial\sigma}\right] + \frac{\partial}{\pi \, \partial\sigma}\left[\pi\dot{\sigma} + \sigma\left(\frac{\partial}{\partial t} + \mathbf{v} \cdot \nabla\right)\pi\right] = 0,$$

and finally

$$(\partial\pi/\partial t) + \nabla_\sigma \cdot (\pi\mathbf{v}) + (\partial/\partial\sigma)(\pi\dot{\sigma}) = 0. \tag{126}$$

The equation of continuity (126) is used to compute both $\pi\dot{\sigma}$ and $\partial\pi_L/\partial t = \partial p_S/\partial t$. Integrating Eq. (126) with respect to σ, from -1 to σ, and using Eq. (113) gives

$$\int_{-1}^{\sigma} \frac{\partial\pi}{\partial t} \, d\sigma + \pi\dot{\sigma} = -\int_{-1}^{\sigma} \nabla \cdot (\pi\mathbf{v}) \, d\sigma. \tag{127}$$

Since $\partial\pi/\partial t = \partial\pi_U/\partial t = 0$ for $\sigma < 0$ and $\partial\pi/\partial t = \partial\pi_L/\partial t$ for $\sigma > 0$, which is constant in σ,

$$\pi\dot{\sigma} = -\int_{-1}^{\sigma} \nabla \cdot (\pi\mathbf{v}) \, d\sigma \qquad \text{for} \quad \sigma < 0, \tag{128}$$

$$\sigma \frac{\partial\pi_L}{\partial t} + \pi\dot{\sigma} = -\int_{-1}^{\sigma} \nabla \cdot (\pi\mathbf{v}) \, d\sigma \qquad \text{for} \quad \sigma > 0. \tag{129}$$

From Eq. (129) applied at $\sigma = 1$, where $\pi\dot{\sigma} = 0$,

$$\frac{\partial\pi_L}{\partial t} = \frac{\partial p_S}{\partial t} = -\int_{-1}^{1} \nabla \cdot (\pi\mathbf{v}) \, d\sigma. \tag{130}$$

Substituting $\partial\pi_L/\partial t$ from Eq. (130) into Eq. (129) gives $\pi\dot{\sigma}$ for $\sigma > 0$.

E. The Individual Time Derivative and Its Flux Form

With the σ coordinate, the individual time derivative d/dt is expressed as

$$d/dt = (\partial/\partial t)_\sigma + \mathbf{v} \cdot \nabla_\sigma + \dot{\sigma}(\partial/\partial\sigma). \tag{131}$$

With A an arbitrary scalar, (131) gives

$$dA/dt = [(\partial/\partial t)_\sigma + \mathbf{v} \cdot \nabla_\sigma]A + \dot{\sigma}(\partial/\partial\sigma)A, \tag{132}$$

which is the advective form for dA/dt. Use of the continuity equation (126) then gives the flux form

$$\pi(dA/dt) = (\partial/\partial t)_\sigma(\pi A) + \nabla_\sigma \cdot (\pi \mathbf{v} A) + (\partial/\partial\sigma)(\pi\dot{\sigma}A). \tag{133}$$

F. The Momentum Equation

The pressure gradient force is given by $-\nabla_p\Phi$. Applying (125) to Φ gives

$$\nabla_p\Phi = \nabla_\sigma\Phi - (\sigma/\pi)\,\nabla\pi(\partial\Phi/\partial\sigma), \tag{134}$$

which with substitution from Eq. (117) becomes

$$\nabla_p\Phi = \nabla_\sigma\Phi + \sigma\alpha\,\nabla\pi. \tag{135}$$

For $\sigma < 0$, $\nabla_p\Phi = \nabla_\sigma\Phi$. For $\sigma > 0$, the pressure gradient force consists of two terms, as shown by Eq. (135). Where the slope of the earth's surface is steep, the individual terms are large but are approximately in opposite directions. In the particular case where $\nabla_p\Phi = 0$, complete compensation occurs.

The horizontal component of the equation of motion becomes

$$d\mathbf{v}/dt + f\mathbf{k} \times \mathbf{v} + \nabla_\sigma\Phi + \sigma\alpha\,\nabla\pi = \mathbf{F}, \tag{136}$$

where $\mathbf{F}$ is the horizontal frictional force and $d\mathbf{v}/dt$ is the horizontal acceleration. Note that

$$\pi(\nabla_\sigma\Phi + \sigma\alpha\,\nabla\pi) = \nabla_\sigma(\pi\Phi) + (\sigma\pi\alpha - \Phi)\,\nabla\pi, \tag{137}$$

which gives us another form of the equation of motion

$$\pi(d\mathbf{v}/dt + f\mathbf{k} \times \mathbf{v}) + \nabla_\sigma(\pi\Phi) + (\sigma\pi\alpha - \Phi)\,\nabla\pi = \pi\mathbf{F}, \tag{138}$$

or, using Eq. (118) in Eq. (138),

$$\pi(d\mathbf{v}/dt) + f\mathbf{k} \times \pi\mathbf{v} + \nabla_\sigma(\pi\Phi) - (\partial(\Phi\sigma)/\partial\sigma)\nabla\pi = \pi\mathbf{F}. \tag{139}$$

G. The Thermodynamic Energy Equation

The specific entropy is $c_p \ln \theta = \text{const}$, and the first law of thermodynamics is

$$d/dt\, c_p \ln \theta = Q/T, \tag{140}$$

where Q is the heating rate per unit mass. The flux form which corresponds to Eq. (140) is

$$\frac{\partial}{\partial t}(\pi c_p \ln \theta) + \nabla \cdot (\pi \mathbf{v} c_p \ln \theta) + \frac{\partial}{\partial \sigma}(\pi \dot{\sigma} c_p \ln \theta) = \pi \frac{Q}{T}. \tag{141}$$

The first law of thermodynamics can also be written as

$$c_p(dT/dt) = \omega\alpha + Q, \tag{142}$$

where $c_p T$ is the specific enthalpy and

$$\omega \equiv dp/dt = \pi\dot{\sigma} + \sigma(\partial/\partial t + \mathbf{v} \cdot \nabla)\pi,$$

as given by (111). The corresponding flux form is

$$\frac{\partial}{\partial t}(\pi c_p T) + \nabla_\sigma \cdot (\pi \mathbf{v} c_p T) + \frac{\partial}{\partial \sigma}(\pi \dot{\sigma} c_p T) = \pi(\omega\alpha + Q). \tag{143}$$

H. The Water Vapor and Ozone Continuity Equations

Let q be the mixing ratio of either water vapor or ozone. The continuity equation for either variable is expressed by

$$dq/dt = S, \tag{144}$$

where S is the source term. The corresponding flux form is

$$(\partial/\partial t)(\pi q) + \nabla_\sigma \cdot (\pi \mathbf{v} q) + (\partial/\partial\sigma)(\pi\dot{\sigma} q) = \pi S. \tag{145}$$

V. The Vertical Difference Scheme of the Model

A. Some Integral Properties of the Adiabatic Frictionless Atmosphere

The following integral properties of the governing equations, or of selected terms in these equations, are useful in designing the vertical finite difference scheme.

1. *Mass Conservatism*

Equation (130) gives

$$\frac{\partial p_S}{\partial t} = -\nabla \cdot \int_{-1}^{1} \pi \mathbf{v}\, d\sigma. \tag{146}$$

The area integral of Eq. (146) over the entire globe makes the divergence term vanish, which means that the total mass of the model atmosphere is conserved.

2. *Vertically Integrated Horizontal Pressure Gradient Force*

With the p coordinate, the horizontal pressure gradient force per unit mass is $-\nabla_p \Phi$. Vertical integration with respect to mass gives

$$\begin{aligned} -\frac{1}{g}\int_{p_T}^{p_S} \nabla_p \Phi\, dp &= -\frac{1}{g}\left[\nabla \int_{p_T}^{p_S} \Phi\, dp - \Phi_S \nabla p_S\right] \\ &= -\frac{1}{g}\left[\nabla \int_{p_T}^{p_S} (\Phi - \Phi_S)\, dp + (p_S - p_T)\nabla \Phi_S\right], \end{aligned} \tag{147}$$

where $\Phi_S \equiv g z_S$, and z_S is the height of the earth's surface. The first term in brackets in Eq. (147) is a gradient vector, and a line integral of its tangential component taken along an arbitrary closed curve on the sphere always vanishes. Only the second term contributes to such a line integral and therefore only when there is a nonhorizontal boundary surface can there be any acceleration of the circulation (any "spin-up" or "spin down" of the vertically integrated atmosphere) by the pressure gradient force.

With the σ coordinate, the horizontal pressure gradient force per unit $\delta\sigma$ is given by

$$-1/g\{\nabla_\sigma(\pi\Phi) - [\partial(\Phi\sigma)/\partial\sigma]\nabla\pi\} \tag{148}$$

[see Eq. (139)]. Vertical integration with respect to σ gives

$$-\frac{1}{g}\int_{-1}^{1}\left[\nabla_\sigma(\pi\Phi) - \frac{\partial(\Phi\sigma)}{\partial\sigma}\nabla\pi\right]d\sigma = -\frac{1}{g}\left[\nabla\int_{-1}^{1}\pi\Phi\,d\sigma - \Phi_S\nabla\pi\right], \quad (149)$$

where the fact that $\nabla\pi = 0$ for $\sigma < 0$ has been used. From Eqs. (110) and (108) it is easy to show that Eq. (149) is equivalent to Eq. (147).

3. *Conservation of Total Energy*

The equation of motion (136) readily gives the kinetic energy equation

$$\pi(d/dt)\tfrac{1}{2}\mathbf{v}^2 = -\pi\mathbf{v}\cdot(\nabla_\sigma\Phi + \sigma\alpha\nabla\pi) + \pi\mathbf{v}\cdot F. \quad (150)$$

The left-hand side of Eq. (150) can be written in the flux form given by Eq. (133) with $A = \frac{1}{2}\mathbf{v}^2$ as follows

$$\left(\frac{\partial}{\partial t}\right)_\sigma(\pi\tfrac{1}{2}\mathbf{v}^2) + \nabla_\sigma\cdot(\pi\mathbf{v}\tfrac{1}{2}\mathbf{v}^2) + \frac{\partial}{\partial\sigma}(\pi\dot\sigma\tfrac{1}{2}\mathbf{v}^2)$$
$$= -\pi\mathbf{v}\cdot[\nabla_\sigma\Phi + \sigma\alpha\nabla\pi] + \pi\mathbf{v}\cdot F. \quad (151)$$

The rate of kinetic energy generation by the pressure gradient force per unit $\delta\sigma/g$ is thus $-\pi\mathbf{v}\cdot[\nabla_\sigma\Phi + \sigma\alpha\nabla\pi]$. Using Eqs. (126), (117), (118), and (111), this becomes

$$\begin{aligned}
-\pi\mathbf{v}\cdot[\nabla_\sigma\Phi + \sigma\alpha\nabla\pi] &= -\nabla_\sigma\cdot(\pi\mathbf{v}\Phi) + \Phi\nabla_\sigma\cdot(\pi\mathbf{v}) - \sigma\pi\alpha\mathbf{v}\cdot\nabla\pi \\
&= -\nabla_\sigma\cdot(\pi\mathbf{v}\Phi) - \Phi\left[\frac{\partial}{\partial\sigma}(\pi\dot\sigma) + \frac{\partial\pi}{\partial t}\right] - \sigma\pi\alpha\mathbf{v}\cdot\nabla\pi \\
&= -\nabla_\sigma\cdot(\pi\mathbf{v}\Phi) - \frac{\partial}{\partial\sigma}(\pi\dot\sigma\Phi) + \pi\dot\sigma\frac{\partial\Phi}{\partial\sigma} - \Phi\frac{\partial\pi}{\partial t} - \sigma\pi\alpha\mathbf{v}\cdot\nabla\pi \\
&= -\nabla_\sigma\cdot(\pi\mathbf{v}\Phi) - \frac{\partial}{\partial\sigma}(\pi\dot\sigma\Phi) + (\sigma\pi\alpha - \Phi)\frac{\partial\pi}{\partial t} \\
&\quad - \pi\left[\sigma\left(\frac{\partial\pi}{\partial t} + \mathbf{v}\cdot\nabla\pi\right) + \pi\dot\sigma\right]\alpha \\
&= -\nabla_\sigma\cdot(\pi\mathbf{v}\Phi) - \frac{\partial}{\partial\sigma}\left(\pi\dot\sigma\Phi + \Phi\sigma\frac{\partial\pi}{\partial t}\right) - \pi\omega\alpha,
\end{aligned} \quad (152)$$

so that

$$\nabla_\sigma \cdot (\pi \mathbf{v}\Phi) + \frac{\partial}{\partial \sigma}\left[\left(\sigma \frac{\partial \pi}{\partial t} + \pi\dot{\sigma}\right)\Phi\right] = \pi \mathbf{v} \cdot [\nabla_\sigma \Phi + \sigma\alpha \nabla\pi] - \pi\omega\alpha. \tag{153}$$

The first law of thermodynamics as given by Eq. (143) is

$$\frac{\partial}{\partial t}(\pi c_p T) + \nabla_\sigma \cdot (\pi \mathbf{v} c_p T) + \frac{\partial}{\partial \sigma}(\pi\dot{\sigma} c_p T) = \pi Q + \pi\omega\alpha. \tag{154}$$

Taking the sum of Eqs. (151), (153), and (154), and integrating with respect to σ from -1 to 1 gives

$$\frac{\partial}{\partial t}\left[p_S\Phi_S + \int_{-1}^{1} \pi(\tfrac{1}{2}\mathbf{v}^2 + c_p T)\, d\sigma\right] + \nabla \cdot \int_{-1}^{1} \pi\mathbf{v}(\tfrac{1}{2}\mathbf{v}^2 + c_p T + \Phi)\, d\sigma$$
$$= \int_{-1}^{1} \pi(\mathbf{v} \cdot F + Q)\, d\sigma. \tag{155}$$

Here $\partial\pi/\partial t = 0$ at $\sigma = -1$, $\partial\pi/\partial t = \partial p_S/\partial t$ at $\sigma = 1$, $\partial\Phi_S/\partial t = 0$ and Eqs. (113) and (114) have been used. The area integral of Eq. (155) over the entire globe makes the contribution of the divergence term vanish, and total energy is thus conserved when $F = 0$ and $Q = 0$.

4. *Conservation of Total Potential Enthalpy and Total Entropy*

Under adiabatic processes the potential temperature θ and therefore any function of the potential temperature $f(\theta)$ are conserved with respect to an air parcel. The flux form which corresponds to $df(\theta)/dt = 0$ is given by Eq. (133), with A replaced by $f(\theta)$; that is,

$$(\partial/\partial t)_\sigma[\pi f(\theta)] + \nabla_\sigma \cdot [\pi \mathbf{v} f(\theta)] + (\partial/\partial\sigma)[\pi\dot{\sigma} f(\theta)] = 0. \tag{156}$$

Integrating Eq. (156) with respect to σ from -1 to 1 gives

$$\frac{\partial}{\partial t}\int_{-1}^{1} \pi f(\theta)\, d\sigma + \nabla \cdot \int_{-1}^{1} \pi\mathbf{v} f(\theta)\, d\sigma = 0, \tag{157}$$

where $f(\theta)$ can be any arbitrary function of θ whose global integral with respect to mass exists. Because the divergence term in Eq. (157) vanishes when the area integral is taken over the entire globe, the global integral

of $f(\theta)$ with respect to mass is conserved under adiabatic processes. Choosing $f(\theta) = c_p\theta$ gives conservation of the total potential enthalpy, and choosing $f(\theta) = c_p \ln \theta +$ const gives conservation of the total entropy.

The conservation of these quantities can be interpreted from a different point of view. For simplicity, consider motion in a stably stratified atmosphere. Under adiabatic processes, air parcels that carry potential temperatures larger than θ_0 stay above the isentropic surface $\theta = \theta_0$, and air parcels that carry potential temperatures smaller than θ_0 stay below the isentropic surface $\theta = \theta_0$; therefore the total mass of air above the isentropic surface is constant. This holds even when the isentropic surface intersects the ground, as does the surface $\theta = \theta_1$ in Fig. 19. In this respect, the earth's surface can be regarded as a continuation of the isentropic surface, as shown by the heavy line in the figure. Then, for quasi-static motion, the horizontal average of the pressure on each isentropic surface $\bar{p}(\theta)$ does not change with time. (This constraint was used by Lorenz (1955) in deriving an expression for available potential energy.) Because $(1/g)\, d\bar{p}\,(\theta)/d\theta$ is the mass of air per unit horizontal area and per unit increment of θ in the vertical, $d\bar{p}\,(\theta)/d\theta$ is termed the "mass density function in θ space." Since $\bar{p}(\theta)$ is constant in time, the mass density function is also constant in time. Figure 20 shows the shape of the function for a typical situation. The reciprocal of the density function is closely related to the static stability (but not exactly related, unless the isentropic surfaces coincide with the isobaric surfaces).

The global integral of $f(\theta)$ with respect to mass, where $f(\theta)$ is any function for which the integral exists, can be related to the mass density function

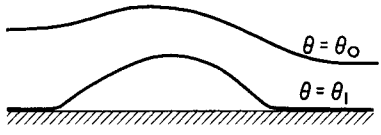

FIG. 19. Isentropic surfaces, one of which intersects the earth's surface.

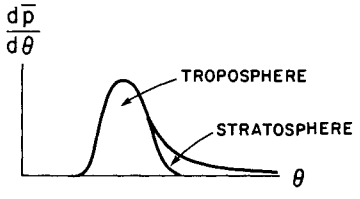

FIG. 20. Schematic representation of a typical distribution of the mass density function in θ space.

as follows

$$\overline{\int_0^{p_S} f(\theta)\, dp} = \overline{\int_{\theta_S}^{\infty} f(\theta) \frac{\partial p}{\partial \theta}\, d\theta}$$

$$= \overline{\int_{\theta_{min}}^{\infty} f(\theta) \frac{\partial p}{\partial \theta}\, d\theta}$$

$$= \int_{\theta_{min}}^{\infty} f(\theta) \frac{d\bar{p}}{d\theta}\, d\theta, \tag{158}$$

where for simplicity it has been assumed that $p_T = 0$ and therefore $\theta_T = \infty$. Here, the bar over the integral denotes the horizontal average; p_S and θ_S are, respectively, p and θ at the earth's surface, and $\theta_{min} = \min(\theta_S)$. In changing the lower limit of the integral from θ_S to θ_{min}, $\partial p/\partial\theta = 0$ for $\theta_S > \theta > \theta_{min}$ has been used. Thus conservation of the global integral of $f(\theta)$ with respect to mass is equivalent to a constraint on the density function. For example, when $f(\theta) = \theta^n$, the integral gives the nth moment of the density function.

In order to fully constrain the density function, it is generally necessary to specify an infinite sequence of moments or an integral transform such as the momentum generating function or the characteristic function. In a discrete system, however, such a full constraint on the density function is not possible unless the isentropic surfaces are taken as coordinate surfaces. In the next subsection it is shown that reasonably simple vertical difference schemes can exactly conserve global integrals with respect to mass of only two independent functions of θ, say $f(\theta)$ and $g(\theta)$; that is, only two independent constraints on the density function can be formally satisified. Consequently, some false distortion of the density function by discretization errors cannot be avoided in numerical simulation. It is to be expected, however, that certain features of the density function can be maintained by proper choice of $f(\theta)$ and $g(\theta)$.

The vertical difference scheme for the first law of thermodynamics in the current UCLA general circulation model has been derived with $f(\theta) = \theta$ and $g(\theta) = \ln \theta$ as the two functions. This choice is based on the following physical reasoning. Choosing $f(\theta) = \theta$ guarantees conservation of the first moment of the density function and, therefore, guarantees conservation of mean potential enthalpy, which is of physical importance. Lorenz (1960) showed that if we define a gross static stability S by

$$S = \left(\frac{\bar{p}_S}{p_0}\right)^{\kappa} \frac{E}{1 + \kappa} - (P + I), \tag{159}$$

where E and $(P + I)$ are, respectively, the potential enthalpy and the *total* potential energy of the whole atmosphere and $\bar{p}_S$ is the mean surface pressure, S becomes a weighted vertical integral of the static stability. Then, because $d(P + I)/dt = -dK/dt$, when $Q = 0$ and $F = 0$, where K is the kinetic energy of the whole atmosphere, $dE/dt = 0$ guarantees

$$dS/dt = dK/dt. \tag{160}$$

Thus when potential enthalpy is conserved, energy conversion from total potential energy to kinetic energy, which requires rising of warmer air and sinking of colder air, stabilizes the atmosphere.

The earlier UCLA general circulation models used $g(\theta) = \theta^2$. That choice, together with $f(\theta) = \theta$, guaranteed conservation of the second moment about the mean of the density function and, therefore, guaranteed conservation of the variance of the potential temperature. That was a reasonable choice for the earlier versions of the model, for they covered only the troposphere and the potential temperature distribution in the troposphere does not deviate greatly from a Gaussian distribution. That choice also guaranteed the approximate conservation of the total entropy because

$$(\ln \theta)_m \fallingdotseq \ln \theta_m + [(\theta'/\theta_m)^2]_m, \tag{161}$$

for small θ'/θ_m, where the subscript m denotes the mean and $\theta' \equiv \theta - \theta_m$.

However, the potential temperature distribution in the coupled troposphere-stratosphere system is highly skewed (see Fig. 20); and conservation of the second moment is not necessarily an effective constraint on the density function near its maximum, because the very large potential temperatures in the stratosphere make a dominant contribution to the second moment. With the present choice of $g(\theta) = \ln \theta$, instead of conservation of the variance, there is conservation of $(\ln \theta)_m - \theta_m$, which is a measure of the broadening of the density function near its maximum [see Eq. (161)]. In addition, $g(\theta) = \ln \theta$ guarantees the conservation of total entropy, which is a quantity of physical importance. Furthermore, as is shown in the next subsection, the finite-difference hydrostatic equation that is energetically consistent with this choice of $g(\theta)$ is very accurate for a wide range of vertical profiles of temperature.

B. A Vertical Difference Scheme Which Maintains Integral Properties

In this subsection the vertical differencing of all the basic equations except the water vapor and ozone continuity equations is presented. The

vertical differencing is designed to maintain finite-difference analogs of the integral constraints discussed in the last subsection.

1. *The Vertical Index*

The model atmosphere is divided into K layers by K-1 levels of constant σ. The layers are identified with odd k and carry the velocity $\mathbf{v}$, the temperature T, the water vapor mixing ratio q, and the ozone mixing ratio O_3. The levels which divide the layers are identified with even k and carry $\pi\dot{\sigma}$. The upper boundary $p = p_T$, the level $p = p_I$, and the lower boundary $p = p_S$ are identified with $k = 0$, $k = k_I$, and $k = K + 1$, respectively (see Fig. 21). Define, for odd k,

$$\Delta\sigma_k \equiv \sigma_{k+1} - \sigma_{k-1}; \tag{162}$$

then

$$\sum_{k=1}^{k_I-1}{}' \Delta\sigma_k = 1 \qquad \text{and} \qquad \sum_{k=k_I+1}^{K}{}' \Delta\sigma_k = 1, \tag{163}$$

where $\sum'$ represents a summation over odd k.

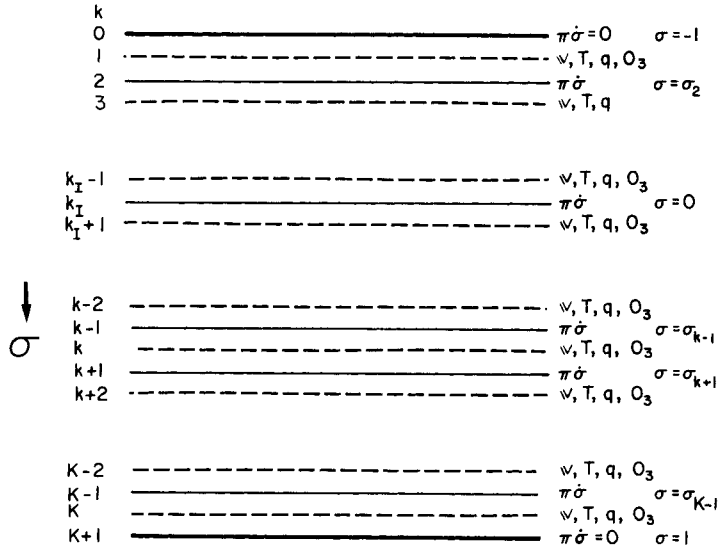

FIG. 21. The vertical structure of the model, showing distribution of the prognostic variables; solid lines (even k) indicate the levels dividing the layers; dashed lines (odd k) indicate levels within layers at which prognostic variables are carried (exact position discussed in Section V).

2. *The Equation of Continuity*

The continuity equation is written in the form

$$\frac{\partial \pi_k}{\partial t} + \nabla \cdot (\pi_k \mathbf{v}_k) + \frac{1}{\Delta\sigma_k}\left[(\pi\dot{\sigma})_{k+1} - (\pi\dot{\sigma})_{k-1}\right] = 0, \tag{164}$$

where k is odd. We have

$$\pi_k = \begin{cases} \pi_U & \text{for} \quad k < k_I \\ \pi_L & \text{for} \quad k > k_I. \end{cases} \tag{165}$$

With $\partial\pi_k/\partial t = 0$ for $k < k_I$, $\partial\pi_k/\partial t = \partial\pi_L/\partial t$ for $k > k_I$, and $(\pi\dot{\sigma})_0 = (\pi\dot{\sigma})_{K+1} = 0$, $\sum_{k=1}^{K}$ (164) $\Delta\sigma_k$ gives

$$\frac{\partial \pi_L}{\partial t} = -\sum_{k=1}^{K}{}' \nabla \cdot (\pi_k \mathbf{v}_k)\, \Delta\sigma_k, \tag{166}$$

which is an analog of Eq. (130). Because $\partial\pi_L/\partial t = \partial p_S/\partial t$, and the area integral of the right-hand side of Eq. (166) over the entire globe vanishes, total mass conservation is maintained with this vertical differencing for the continuity equation.

The quantity $(\pi\dot{\sigma})_{k+1}$ is given by

$$\begin{aligned} (\pi\dot{\sigma})_{k+1} &= -\sum_{k=1}^{k}{}' \nabla \cdot (\pi_k \mathbf{v}_k)\, \Delta\sigma_k && \text{for} \quad k < k_I, \\ (\pi\dot{\sigma})_{k+1} &= -\sum_{k=1}^{k}{}' \nabla \cdot (\pi_k \mathbf{v}_k)\, \Delta\sigma_k - \sigma_{k+1}\frac{\partial \pi_L}{\partial t} && \text{for} \quad k > k_I, \end{aligned} \tag{167}$$

which are analogs of Eqs. (128) and (129).

3. *Flux Forms*

For any variable A carried by the layers, the flux form analogous to Eq. (133) can be written as

$$\frac{\partial}{\partial t}(\pi_k A_k) + \nabla \cdot (\pi_k \mathbf{v}_k A_k) + \frac{1}{\Delta\sigma_k}\left[(\pi\dot{\sigma})_{k+1}\hat{A}_{k+1} - (\pi\dot{\sigma})_{k-1}\hat{A}_{k-1}\right]. \tag{168}$$

where the variable $\hat{A}$, defined at the levels between layers, is obtained by some manner of interpolation from A. Whatever the form of the interpolation, however, Eq. (168) guarantees that the analog of the global integral of A with respect to mass is conserved as far as advective processes are concerned, because $\sum'_{k=1}^{K}$ (168) $\Delta\sigma_k$ gives

$$\frac{\partial}{\partial t}\sum_{k=1}^{K}{}' \pi_k A_k \,\Delta\sigma_k + \sum_{k=1}^{K}{}' \nabla\cdot(\pi_k \mathbf{v}_k A_k)\,\Delta\sigma_k,$$

and the second term vanishes when the area integral over the entire globe is taken.

Equations (164) and (168) give the expression

$$\left(\pi\frac{dA}{dt}\right)_k = \pi_k\left(\frac{\partial}{\partial t} + \mathbf{v}_k\cdot\nabla\right)A_k + \frac{1}{\Delta\sigma_k}\left[(\pi\dot{\sigma})_{k+1}(\hat{A}_{k+1} - A_k) + (\pi\dot{\sigma})_{k-1}(A_k - \hat{A}_{k-1})\right], \quad (169)$$

which when divided by π_k gives the advective form for dA/dt which is consistent with the flux form in Eq. (168).

So far, the choice of $\hat{A}$ is completely arbitrary, provided that the choice does not violate the consistency of the scheme with the original differential equation. It is possible, then, to satisfy an additional requirement.

Let us require also that the finite-difference analog of the global integral of $F(A)$ with respect to mass be conserved. Let $F_k \equiv F(A_k)$ and $F'_k \equiv dF(A_k)/dA_k$. Then (169) multiplied by F'_k gives

$$\pi_k\left(\frac{\partial}{\partial t} + \mathbf{v}_k\cdot\nabla\right)F_k + \frac{1}{\Delta\sigma_k}\left[(\pi\dot{\sigma})_{k+1}F'_k(\hat{A}_{k+1} - A_k) + (\pi\dot{\sigma})_{k-1}F'_k(A_k - \hat{A}_{k-1})\right]. \quad (170)$$

Using the equation of continuity, (170) can be rewritten as

$$\frac{\partial}{\partial t}(\pi_k F_k) + \nabla\cdot(\pi_k\mathbf{v}_k F_k) + \frac{1}{\Delta\sigma_k}\left[(\pi\dot{\sigma})_{k+1}\{F'_k(\hat{A}_{k+1} - A_k) + F_k\} - (\pi\dot{\sigma})_{k-1}\{-F'_k(A_k - \hat{A}_{k-1}) + F_k\}\right]. \quad (171)$$

In order that (171) be in flux form, it is necessary that

$$\hat{F}_{k+1} = F'_k(\hat{A}_{k+1} - A_k) + F_k, \tag{172}$$

$$\hat{F}_{k-1} = -F'_k(A_k - \hat{A}_{k-1}) + F_k. \tag{173}$$

Replacing k in Eq. (173) by $k + 2$ and eliminating $\hat{F}_{k+1}$ with Eq. (172) gives

$$\hat{A}_{k+1} = \frac{(F'_{k+2}A_{k+2} - F_{k+2}) - (F'_kA_k - F_k)}{F'_{k+2} - F'_k}. \tag{174}$$

This may be interpreted as a finite-difference analog to the identity

$$A \equiv \frac{d(F'A - F)}{dF'}. \tag{175}$$

When $F(A) = A^2$, for example, Eq. (174) gives

$$\hat{A}_{k+1} = \tfrac{1}{2}(A_k + A_{k+2}). \tag{176}$$

That this constraint on $\hat{A}_{k+1}$ leads to conservation of the global integral of A^2 with respect to mass was first pointed out by Lorenz (1960).

4. *Vertically Integrated Horizontal Pressure Gradient Force*

In order to maintain the property of the vertically integrated horizontal pressure gradient force discussed in Section V, A, 2, it is convenient to start from the form given in Eq. (139). The terms $\nabla_\sigma(\pi\Phi) - \partial/\partial\sigma(\Phi\sigma)\,\nabla\pi$ are written for odd k as

$$\nabla(\pi_k\Phi_k) - \frac{1}{\Delta\sigma_k}(\hat{\Phi}_{k+1}\sigma_{k+1} - \hat{\Phi}_{k-1}\sigma_{k-1})\,\nabla\pi_k. \tag{177}$$

Again, the caret is a reminder that a variable is evaluated at the levels, that is, at even k. The analog to Eq. (149) is

$$-\frac{1}{g}\sum_{k=1}^{K}{}' (180)\,\Delta\sigma_k = \frac{1}{g}\left[\nabla\left(\sum_{k=1}^{K}{}' \pi_k(\Phi_k - \hat{\Phi}_S)\,\Delta\sigma_k\right) + (p_S - p_T)\,\nabla\hat{\Phi}_S\right]. \tag{178}$$

In this way the integral property is maintained.

The terms in (177) are equivalent to

$$\pi_k \nabla\Phi_k + [\Phi_k - (1/\Delta\sigma_k)(\hat{\Phi}_{k+1}\sigma_{k+1} - \hat{\Phi}_{k-1}\sigma_{k-1})] \nabla\pi_k. \tag{179}$$

If we let

$$\pi_k(\sigma\alpha)_k \equiv \Phi_k - (1/\Delta\sigma_k)(\hat{\Phi}_{k+1}\sigma_{k+1} - \hat{\Phi}_{k-1}\sigma_{k-1}), \tag{180}$$

(179) can be written as

$$\pi_k[\nabla\Phi_k + (\sigma\alpha)_k \nabla\pi_k], \tag{181}$$

which is the analog to $\pi(\nabla\Phi + \sigma\alpha \nabla\pi)$, another form of the horizontal pressure gradient force. Equation (180) provides an analog to Eq. (118), one form of the hydrostatic equation. However, because $\hat{\Phi}$ is not yet specified, Eq. (180) must be considered at this stage only a definition of the symbol $(\sigma\alpha)_k$.

5. *The Kinetic Energy Equation*

Following (169), the acceleration term is written as

$$\left(\pi \frac{d\mathbf{v}}{dt}\right)_k = \pi_k \left[\frac{\partial}{\partial t} + (\mathbf{v}_k \cdot \nabla)\right] \mathbf{v}_k + \frac{1}{\Delta\sigma_k}[(\pi\dot{\sigma})_{k+1}(\hat{\mathbf{v}}_{k+1} - \mathbf{v}_k) + (\pi\dot{\sigma})_{k-1}(\mathbf{v}_k - \hat{\mathbf{v}}_{k-1})]. \tag{182}$$

To have a flux form for $\mathbf{v}_k \cdot (\pi\, d\mathbf{v}/dt)_k$, Eq. (176) is used with $A = \mathbf{v}$; that is

$$\hat{\mathbf{v}}_{k+1} = \tfrac{1}{2}(\mathbf{v}_k + \mathbf{v}_{k+2}). \tag{183}$$

This guarantees the conservation of total kinetic energy, insofar as vertical advection is concerned. The finite-difference expression for the kinetic energy in a vertical column per unit horizontal area is

$$\frac{1}{g} \sum_{k=1}^{K}{}' \tfrac{1}{2}\mathbf{v}_k{}^2(\pi\,\Delta\sigma)_k. \tag{184}$$

To obtain the kinetic energy generation in finite-difference form, the procedure used in deriving Eq. (152) is followed:

$$
\begin{aligned}
&-\pi_k \mathbf{v}_k \cdot [\nabla \Phi_k + (\sigma\alpha)_k \nabla \pi_k] \\
&\quad = -\nabla_k \cdot (\pi \mathbf{v}_k \Phi_k) - \Phi_k \left[\frac{1}{\Delta\sigma_k} \{(\pi\dot{\sigma})_{k+1} - (\pi\dot{\sigma})_{k-1}\} + \frac{\partial \pi_k}{\partial t} \right] \\
&\qquad - \pi_k (\sigma\alpha)_k \mathbf{v}_k \cdot \nabla \pi_k \\
&\quad = -\nabla \cdot (\pi_k \mathbf{v}_k \Phi_k) - \frac{1}{\Delta\sigma_k} \{(\pi\dot{\sigma})_{k+1} \hat{\Phi}_{k+1} - (\pi\dot{\sigma})_{k-1} \hat{\Phi}_{k-1}\} \\
&\qquad + \frac{1}{\Delta\sigma_k} [(\pi\dot{\sigma})_{k+1} (\hat{\Phi}_{k+1} - \Phi_k) + (\pi\dot{\sigma})_{k-1} (\Phi_k - \hat{\Phi}_{k-1})] \\
&\qquad - \Phi_k \frac{\partial \pi_k}{\partial t} - \pi_k (\sigma\alpha)_k \mathbf{v}_k \cdot \nabla \pi_k \\
&\quad = -\nabla \cdot (\pi_k \mathbf{v}_k \Phi_k) - \frac{1}{\Delta\sigma_k} \{(\pi\dot{\sigma})_{k+1} \hat{\Phi}_{k+1} - (\pi\dot{\sigma})_{k-1} \hat{\Phi}_{k-1}\} \\
&\qquad + \{\pi_k (\sigma\alpha)_k - \Phi_k\} \frac{\partial \pi_k}{\partial t} - \pi_k \left[(\sigma\alpha)_k \left(\frac{\partial}{\partial t} + \mathbf{v}_k \cdot \nabla \right) \pi_k - \frac{1}{\pi_k \Delta\sigma_k} \right. \\
&\qquad \left. \times \{(\pi\dot{\sigma})_{k+1} (\hat{\Phi}_{k+1} - \Phi_k) + (\pi\dot{\sigma})_{k-1} (\Phi_k - \hat{\Phi}_{k-1})\} \right] \\
&\quad = -\nabla \cdot (\pi_k \mathbf{v}_k \Phi_k) - \frac{1}{\Delta\sigma_k} \left[\left\{ (\pi\dot{\sigma})_{k+1} + \sigma_{k+1} \frac{\partial \pi_k}{\partial t} \right\} \hat{\Phi}_{k+1} \right. \\
&\qquad \left. - \left\{ (\pi\dot{\sigma})_{k-1} + \sigma_{k-1} \frac{\partial \pi_k}{\partial t} \right\} \hat{\Phi}_{k-1} \right] - \pi_k (\omega\alpha)_k. \qquad (185)
\end{aligned}
$$

Here $(\omega\alpha)_k$ is defined by

$$
\begin{aligned}
(\omega\alpha)_k \equiv\ & (\sigma\alpha)_k \left(\frac{\partial}{\partial t} + \mathbf{v}_k \cdot \nabla \right) \pi_k \\
& - \frac{1}{\pi_k \Delta\sigma_k} \{(\pi\dot{\sigma})_{k+1} (\hat{\Phi}_{k+1} - \Phi_k) + (\pi\dot{\sigma})_{k-1} (\Phi_k - \hat{\Phi}_{k-1})\}. \qquad (186)
\end{aligned}
$$

At this stage, Eq. (186) is the definition of the symbol $(\omega\alpha)_k$.

From a finite-difference scheme for the first law of thermodynamics, another expression for $(\omega\alpha)_k$ will be derived. With Eq. (186), this will deter-

mine a form for $(\sigma\alpha)_k$ that, with (180), will fix the discrete form of the hydrostatic equation.

6. *Thermodynamic Energy Equation*

In this subsection, a vertical differencing of the thermodynamic energy equation is presented that maintains conservation of total potential enthalpy and total entropy under adiabatic processes.

To conserve an analog of the global integral of the potential temperature $\theta \equiv T(p_0/p)^\kappa$ with respect to mass, the form given by (168) is used with $A = \theta$. Then,

$$\frac{\partial}{\partial t}(\pi_k\theta_k) + \nabla\cdot(\pi_k\mathbf{v}_k\theta_k) + \frac{1}{\Delta\sigma_k}[(\pi\dot{\sigma})_{k+1}\hat{\theta}_{k+1} - (\pi\dot{\sigma})_{k-1}\hat{\theta}_{k-1}] = 0, \quad (187)$$

where the heating term is omitted for convenience. Here

$$\theta_k \equiv T_k/P_k \quad (188)$$

and P_k is an analog to $(p/p_0)^\kappa$ for the layer k. The actual form for P_k used in the model will be described later. Here it is sufficient to assume that P_k is a function of π_k, σ_{k-1}, and σ_{k+1} only.

The earlier versions of the UCLA general circulation model used $\hat{\theta}_{k+1} = \frac{1}{2}(\theta_k + \theta_{k+2})$ following Eq. (176). The present model, however, requires conservation of an analog of the global integral of $\ln\theta$ with respect to mass. Equation (174) with $A = \theta$ and $F(A) = \ln\theta$ gives

$$\hat{\theta}_{k+1} = \frac{\ln\theta_k - \ln\theta_{k+2}}{1/\theta_{k+2} - 1/\theta_k}. \quad (189)$$

The corresponding advective form is given by

$$\pi_k\left(\frac{\partial}{\partial t} + \mathbf{v}_k\cdot\nabla\right)\theta_k + \frac{1}{\Delta\sigma_k}[(\pi\dot{\sigma})_{k+1}(\hat{\theta}_{k+1} - \theta_k) + (\pi\dot{\sigma})_{k-1}(\theta_k - \hat{\theta}_{k-1})] = 0. \quad (190)$$

Substituting Eq. (188) into Eq. (190) gives

$$\pi_k\left(\frac{\partial}{\partial t} + \mathbf{v}_k\cdot\nabla\right)T_k - \pi_k\frac{T_k}{P_k}\frac{\partial P_k}{\partial\pi_k}\left(\frac{\partial}{\partial t} + \mathbf{v}_k\cdot\nabla\right)\pi_k + \frac{1}{\Delta\sigma_k}[(\pi\dot{\sigma})_{k+1}(P_k\hat{\theta}_{k+1} - T_k) + (\pi\dot{\sigma})_{k-1}(T_k - P_k\hat{\theta}_{k-1})] = 0, \quad (191)$$

or, introducing $\hat{T}$ to make the left-hand side an analog of $\pi d(c_p T)/dt$,

$$\pi_k\left(\frac{\partial}{\partial t}+\mathbf{v}_k\cdot\nabla\right)c_p T_k+\frac{1}{\Delta\sigma_k}[(\pi\dot{\sigma})_{k+1}c_p(\hat{T}_{k+1}-T_k)+(\pi\dot{\sigma})_{k-1}c_p(T_k-\hat{T}_{k-1})]$$
$$=\pi_k\frac{c_p T_k}{P_k}\frac{\partial P_k}{\partial\pi_k}\left(\frac{\partial}{\partial t}+\mathbf{v}_k\cdot\nabla\right)\pi_k+\frac{1}{\Delta\sigma_k}[(\pi\dot{\sigma})_{k+1}c_p(\hat{T}_{k+1}-P_k\theta_{k+1})$$
$$+(\pi\dot{\sigma})_{k-1}c_p(P_k\hat{\theta}_{k-1}-\hat{T}_{k-1})]. \tag{192}$$

The dependence of $\hat{T}$ on the odd index temperatures need not be specified at this point. The left-hand side of Eq. (192) may be written in flux form, as

$$\frac{\partial}{\partial t}(\pi c_p T_k)+\nabla\cdot(\pi\mathbf{v}_k c_p T_k)+\frac{c_p}{\Delta\sigma_k}(\pi\dot{\sigma}_{k+1}\hat{T}_{k+1}-\pi\dot{\sigma}_{k-1}\hat{T}_{k-1}). \tag{193}$$

7. *Total Energy Conservation and the Hydrostatic Equation*

In order that the total energy be conserved under an adiabatic, frictionless process, the right-hand side of Eq. (192) must agree with $\pi_k(\omega\alpha)_k$, where $(\omega\alpha)_k$ is defined by Eq. (186). For $k<k_I$, $\pi_k=\pi_U=$ const and therefore $(\partial/\partial t+\mathbf{v}_k\cdot\nabla)\pi_k=0$. For $k>k_I$, $(\partial/\partial t+\mathbf{v}_k\cdot\nabla)\pi_k$ is generally not zero, so that it is necessary to require

$$(\sigma\alpha)_k=\frac{c_p T_k}{P_k}\frac{\partial P_k}{\partial\pi_k}\quad\text{for}\quad k>k_I. \tag{194}$$

Comparison with Eq. (180) which also defines $(\sigma\alpha)_k$ gives

$$\Phi_k-\frac{1}{\Delta\sigma_k}(\hat{\Phi}_{k+1}\sigma_{k+1}-\hat{\Phi}_{k-1}\sigma_{k-1})=\pi_L\frac{c_p T_k}{P_k}\frac{\partial P_k}{\partial\pi_k}\quad\text{for}\quad k>k_I. \tag{195}$$

This is the form of the hydrostatic equation that corresponds to Eq. (118). It must also be required for all odd k that

$$c_p(\hat{T}_{k+1}-P_k\hat{\theta}_{k+1})=\Phi_k-\hat{\Phi}_{k+1} \tag{196}$$

and

$$c_p(P_k\hat{\theta}_{k-1}-\hat{T}_{k-1})=\hat{\Phi}_{k-1}-\Phi_k. \tag{197}$$

Rearranging the terms,

$$(c_p\hat{T}_{k+1} + \hat{\Phi}_{k+1}) - (c_pT_k + \Phi_k) = P_kc_p(\hat{\theta}_{k+1} - \theta_k), \tag{198}$$

and

$$(c_pT_k + \Phi_k) - (c_p\hat{T}_{k-1} + \hat{\Phi}_{k-1}) = P_kc_p(\theta_k - \hat{\theta}_{k-1}), \tag{199}$$

where $\hat{\theta}_{k+1}$ (and therefore $\hat{\theta}_{k-1}$) is given by Eq. (189). Equations (198) and (199) are analogs of the form of the hydrostatic equation given by Eq. (122).

Replacing k in Eq. (199) by $k + 2$ and adding it to Eq. (198) gives

$$\begin{aligned}(c_pT_{k+2} + \Phi_{k+2}) - (c_pT_k + \Phi_k) \\ = c_p[P_{k+2}(\theta_{k+2} - \hat{\theta}_{k+1}) + P_k(\hat{\theta}_{k+1} - \theta_k)],\end{aligned} \tag{200}$$

or, using Eq. (188),

$$\Phi_{k+2} - \Phi_k = -c_p(P_{k+2} - P_k)\hat{\theta}_{k+1}. \tag{201}$$

Equation (200) is an analog of Eq. (122) and Eq. (201) is an analog of Eq. (120). Using Eq. (189),

$$\Phi_{k+2} - \Phi_k = c_p\frac{\ln\theta_{k+2} - \ln\theta_k}{(1/\theta_{k+2}) - (1/\theta_k)}(P_{k+2} - P_k). \tag{202}$$

Equation (202) is a finite-difference approximation of Eq. (121):

$$\delta\Phi = c_p[d\ln\theta/d(1/\theta)]\delta(p/p_0)^\kappa$$

or of

$$\delta\Phi = c_p[\partial(p/p_0)^\kappa/\partial(1/\theta)]\delta\ln\theta.$$

Equation (202) is used to compute Φ_k for odd k. To do so, it is necessary to know Φ at a single odd k, say $k = K$; and Eq. (195) can be used for this purpose. From Eq. (195),

$$\sum_{k=k_I+1}^{K}{}' \Phi_k\,\Delta\sigma_k - \Phi_S = \sum_{k=k_I+1}^{K}{}' \pi_L\frac{c_pT_k}{P_k}\frac{\partial P_k}{\partial\pi_k}\Delta\sigma_k. \tag{203}$$

However, $\sum'^{K}_{k=k_I+1} \Phi_k \Delta\sigma_k$ can be written as

$$\sum_{k=k_I+1}^{K}{}' \Phi_k \Delta\sigma_k = \sum_{k=k_I+1}^{K}{}' \Phi_k(\sigma_{k+1} - \sigma_{k-1}) \tag{204}$$

$$= \Phi_K + \sum_{k=k_I+1}^{K-2}{}' \sigma_{k+1}(\Phi_k - \Phi_{k+2}).$$

Equations (204) and (203) then give

$$\Phi_K = \Phi_S + \sum_{k=k_I+1}^{K}{}' \pi \frac{c_p T_k}{P_k} \frac{\partial P_k}{\partial \pi_k} - \sum_{k=k_I+1}^{K-2}{}' \sigma_{k+1}(\Phi_k - \Phi_{k+2}) \tag{205}$$

8. *Summary of Subsections 5–8*

A vertical difference scheme has now been constructed that maintains the property of the vertically integrated horizontal pressure gradient force, total energy conservation under adiabatic and frictionless processes, and conservation of θ and $\ln \theta$, integrated over the entire mass under adiabatic processes. The function P_k, however, which is an analog to $(p/p_0)^\kappa$ for the layer k, remains to be determined.

a. Pressure Gradient Force. From Eqs. (180) and (194), expression (177) becomes

$$\nabla(\pi_k \Phi_k) + \left(\pi_k \frac{c_p T_k}{P_k} \frac{\partial P_k}{\partial \pi_k} - \Phi_k\right) \nabla \pi_k, \tag{206}$$

where

$$\pi_k = \begin{cases} \pi_U = p_I - p_T, & \text{for } k < k_I \\ \pi_L = p_S - p_I, & \text{for } k > k_I. \end{cases}$$

b. The Hydrostatic Equation. Equations (205) and (201) give

$$\Phi_K = \Phi_S + \sum_{k=k_I+1}^{K}{}' \pi_L \frac{c_p T_k}{P_k} \frac{\partial P_k}{\partial \pi_k} - \sum_{k=k_I+1}^{K-2}{}' \sigma_{k+1} c_p \hat{\theta}_{k+1}(P_{k+2} - P_k), \tag{207}$$

$$\Phi_k - \Phi_{k+2} = c_p(P_{k+2} - P_k)\hat{\theta}_{k+1}, \tag{207'}$$

where

$$\hat{\theta}_{k+1} = \frac{\ln \theta_k - \ln \theta_{k+2}}{(1/\theta_{k+2}) - (1/\theta_k)}. \tag{208}$$

c. The Thermodynamic Energy Equation. Using Eq. (193) for the left-hand side of Eq. (192), rearranging terms, dividing by c_p, and restoring the the heating term gives

$$\frac{\partial}{\partial t}(\pi_k T_k) + \nabla \cdot (\pi_k \mathbf{v}_k T_k) + \frac{1}{\Delta\sigma_k}\left[(\pi\dot{\sigma})_{k+1}(P_k\hat{\theta}_{k+1}) - (\pi\dot{\sigma})_{k-1}(P_k\hat{\theta}_{k-1})\right]$$
$$= \pi_k \frac{T_k}{P_k}\frac{\partial \pi_k}{\partial \pi_k}\left(\frac{\partial}{\partial t} + \mathbf{v}_k \cdot \nabla\right)\pi_k + \pi_k Q_k/c_p. \tag{209}$$

C. Vertical Propagation of Wave Energy in an Isothermal Atmosphere

In this subsection, the effect of the vertical differencing scheme in current use in the model on the vertical propagation of wave energy in an isothermal atmosphere is examined. The material presented here is based on part of a forthcoming paper by Tokioka. His study provided the foundation for our choice of the depth of the layers and the function P_k in the stratosphere.

1. *The Vertical Structure Equation—Continuous Case*

The quasi-static system of equations, linearized with respect to perturbations on a resting, isothermal basic state, may be written with the pressure coordinate as

$$\frac{\partial u}{\partial t} - (2\Omega \sin\varphi)v + \frac{1}{a\cos\varphi}\frac{\partial \phi}{\partial \lambda} = 0, \tag{210}$$

$$\frac{\partial v}{\partial t} + (2\Omega \sin\varphi)u + \frac{1}{a}\frac{\partial \phi}{\partial \varphi} = 0, \tag{211}$$

$$\frac{\partial T}{\partial t} - \omega \frac{1}{c_p}\frac{RT_0}{p} = 0, \tag{212}$$

$$\partial\phi/\partial p = -RT/p, \tag{213}$$

$$\frac{\partial u}{a\cos\varphi\,\partial\lambda} + \frac{\partial(v\cos\varphi)}{a\cos\varphi\,\partial\varphi} + \frac{\partial\omega}{\partial p} = 0, \tag{214}$$

where λ and φ are longitude and latitude, u and v are the eastward and northward components of the perturbation velocity, ϕ is the perturbation geopotential, ω is the perturbation p velocity, T is the perturbation temperature, a is the radius of the earth, Ω is the angular speed of rotation of the earth, and T_0 is the constant temperature of the basic state.

Let us consider a solution of the form

$$\begin{pmatrix} u \\ v \\ \phi \\ T \end{pmatrix} = \mathrm{Re}\begin{pmatrix} \hat{u} \\ \hat{v} \\ \hat{\phi} \\ \hat{T} \end{pmatrix} \exp[i(s\lambda + \sigma t)], \tag{215}$$

where s is the longitudinal wave number, assumed positive, and σ is the angular frequency. A positive σ then represents a westward-moving wave and a negative σ represents an eastward-moving wave. Using Eq. (215), Eqs. (210)–(214) become

$$i\sigma\hat{u} - (2\Omega \sin\varphi)\hat{v} + \frac{is}{a\cos\varphi}\hat{\phi} = 0 \tag{216}$$

$$i\sigma\hat{v} + (2\Omega \sin\varphi)\hat{u} + (1/a)(\partial\hat{\phi}/\partial\varphi) = 0, \tag{217}$$

$$i\sigma\hat{T} - (RT_0/c_p p)\hat{\omega} = 0 \tag{218}$$

$$\partial\hat{\phi}/\partial p = -(R/p)\hat{T}, \tag{219}$$

$$is\hat{u} + \frac{\partial(\hat{v}\cos\varphi)}{\partial\varphi} + a\cos\varphi\frac{\partial\hat{\omega}}{\partial p} = 0. \tag{220}$$

Following the theory of the atmospheric tides, $\hat{u}$ and $\hat{v}$ are eliminated from Eqs. (216), (217), and (220), giving

$$\mathscr{L}(i\sigma\hat{\phi}) = 4a^2\Omega^2(\partial\hat{\omega}/\partial p), \tag{221}$$

where the differential operator $\mathscr{L}$ is given by

$$\mathscr{L} \equiv -\frac{\partial}{\partial\mu}\left(\frac{1-\mu^2}{f^2-\mu^2}\frac{\partial}{\partial\mu}\right) + \frac{1}{f^2-\mu^2}\left(\frac{s}{\mu}\frac{f^2+\mu^2}{f^2-\mu^2} + \frac{s^2}{1-\mu^2}\right),$$

and

$$\mu \equiv \sin\varphi \qquad \text{and} \qquad f \equiv \sigma/2\Omega.$$

Equations (218) and (219), on the other hand, give

$$\partial/\partial p(i\sigma\hat{\phi}) = -(R^2T_0/c_p p^2)\hat{\omega}. \tag{222}$$

Eliminating $\hat{\phi}$ between Eqs. (221) and (222) gives a single equation for $\hat{\omega}$,

$$\mathscr{L}(\hat{\omega}) + (c_p p^2/R^2 T_0)4a^2\Omega^2(\partial^2\hat{\omega}/\partial p^2) = 0. \tag{223}$$

Let

$$\hat{\omega} = F(\mu)W(p). \tag{224}$$

Then Eq. (223) can be separated into horizontal and vertical structure equations, given respectively by

$$\mathscr{L}F = \varepsilon F \tag{225}$$

and

$$d^2W/dp^2 = -(\kappa H_0/h)(1/p^2)W, \tag{226}$$

where ε is the separation constant, h is the equivalent depth defined by $\varepsilon \equiv 4\Omega^2a^2/gh$, $H_0 \equiv RT_0/g$ is the scale height of the isothermal atmosphere, and $\kappa \equiv R/c_p$.

Transformation of the dependent variable in the vertical structure equation (226) from W to $\tilde{W} \equiv (p/p_0)^{-1/2}W$ gives

$$d^2\tilde{W}/d\zeta^2 = -n^2\tilde{W}, \tag{227}$$

where ζ is $-\ln(p/p_0)$, the height scaled by H_0; p_0 is a standard pressure; and n is defined by

$$n \equiv (\kappa(H_0/h) - \tfrac{1}{4})^{1/2}. \tag{228}$$

The quantity n gives the vertical wave number and therefore a measure of the index of refraction for vertical wave energy propagation. For a given equivalent depth, the vertical wave number n is constant in height. When n is real, the waves are oscillatory in height (internal waves), and transfer wave energy vertically; n is real for the range $0 < h < 4\kappa H_0$, that is, for $\varepsilon > (\Omega a)^2/g\kappa H_0$ (~ 10 for $T \sim 270$ °K).

The thin line in Fig. 22 shows n as a function of the parameter ε. Here $T_0 = 270$ °K and therefore $H_0 = 7.91$ km. The vertical wavelength is approximately $(49.7/n)$ km.

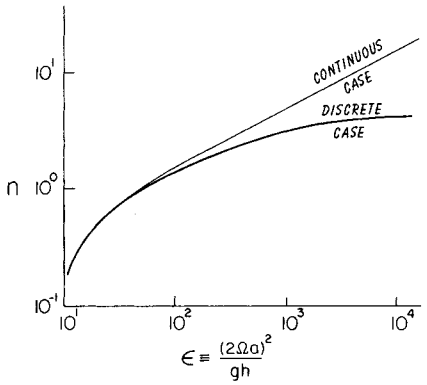

FIG. 22. Comparison between the vertical wave number n in the differential case, defined by Eq. (228), and that given by the vertical difference analog of the vertical structure equation (243).

2. *The Vertical Structure Equation—Discrete Case*

That the vertical wave number is constant in height for a given equivalent depth means that the index of refraction is constant in height, so that no internal reflection of wave energy takes place. This important property of an isothermal atmosphere is not necessarily maintained in a discrete model, where vertical differencing is employed. It will be shown here that the vertical differencing described in Section V, B maintains that property when the depths of the layers are equal in log p and

$$P_k = [(p_{k-1}p_{k+1})^{1/2}/p_0]^{\kappa}. \tag{229}$$

Using the vertical index k of Section V, B, the discrete versions of Eqs. (216)–(220) may be written as

$$i\sigma\hat{u}_k - 2\Omega \sin\varphi\hat{v}_k + \frac{is}{a\cos\varphi}\hat{\phi}_k = 0, \tag{230}$$

$$i\sigma\hat{v}_k + 2\Omega \sin\varphi\hat{u}_k + (1/a)(\partial\hat{\phi}_k/\partial\varphi) = 0, \tag{231}$$

$$i\sigma\hat{T}_k - (T_0/\Delta p_k)(Q_k{}^1\hat{\omega}_{k-1} + S_k{}^1\hat{\omega}_{k+1}) = 0, \tag{232}$$

$$\hat{\phi}_k - \hat{\phi}_{k+2} = c_p(S_k{}^2\hat{T}_k + Q_{k+2}^2\hat{T}_{k+2}), \tag{233}$$

$$\hat{u}_k + \frac{\partial(\hat{v}_k\cos\varphi)}{\partial\varphi} + a\cos\varphi\frac{(\hat{\omega}_{k+1} - \hat{\omega}_{k-1})}{\Delta p_k} = 0, \tag{234}$$

where $S_k{}^1$, $S_k{}^2$, $Q_k{}^1$, and $Q_k{}^2$ are coefficients which depend on the vertical

differencing of the thermodynamic energy equation and the hydrostatic equation.

With the vertical differencing given by Eqs. (209) and (201), the coefficients are defined as follows:

$$Q_k^{\,1} = (P_k/T_0)(\bar{\bar{\theta}}_{k-1} - \bar{\theta}_k), \tag{235}$$

$$S_k^{\,1} = (P_k/T_0)(\bar{\theta}_k - \bar{\bar{\theta}}_{k+1}), \tag{236}$$

$$S_k^{\,2} = (1/P_k)(P_{k+2} - P_k)(\partial\bar{\bar{\theta}}_{k+1}/\partial\bar{\theta}_k), \tag{237}$$

$$Q_{k+2}^{2} = (1/P_{k+2})(P_{k+2} - P_k)(\partial\bar{\bar{\theta}}_{k+1}/\partial\bar{\theta}_{k+2}), \tag{238}$$

where the overbar denotes the basic state. For an isothermal basic state, with the definition of $\hat{\theta}_{k+1}$ given by Eq. (208), these coefficients become

$$Q_k^{\,1} = Q_k^{\,2} = -\left[1 + \frac{\ln(P_{k-2}/P_k)}{1 - (P_{k-2}/P_k)}\right] \tag{239}$$

$$S_k^{\,1} = S_k^{\,2} = 1 + \frac{\ln(P_{k+2}/P_k)}{1 - (P_{k+2}/P_k)} \tag{240}$$

The equations corresponding to Eqs. (221) and (222) are then

$$\mathscr{L}(i\sigma\hat{\phi}_k) = 4a^2\Omega^2[(\hat{\omega}_{k+1} - \hat{\omega}_{k-1})/\Delta p_k], \tag{241}$$

$$\begin{aligned} i\sigma(\hat{\phi}_k - \hat{\phi}_{k+2}) = {} & C_p T_0[(S_k/\Delta p_k)(Q_k\omega_{k-1} + S_k\omega_{k+1}) \\ & + (Q_{k+2}/\Delta p_{k+2})(Q_{k+2}\omega_{k+1} + S_{k+2}\omega_{k+3})], \end{aligned} \tag{242}$$

where the superscripts of S and Q can now be omitted. Equations (224), (241), and (242) give a finite-difference analog of the vertical structure equation (226):

$$\begin{aligned} \frac{W_{k-1} - W_{k+1}}{\Delta p_k} - \frac{W_{k+1} - W_{k+3}}{\Delta p_{k+2}} = -\frac{C_p T_0}{gh}\Bigg[& \frac{S_k}{\Delta p_k}(Q_k W_{k-1} + S_k W_{k+1}) \\ & + \frac{Q_{k+2}}{\Delta p_{k+2}}(Q_{k+2} W_{k+1} + S_{k+2} W_{k+3})\Bigg]. \end{aligned} \tag{243}$$

When the even levels are chosen such that the intervals are equal in log p,

$$p_{k+1}/p_{k-1} \equiv e^d \tag{244}$$

for any odd k, where the constant d is the depth in ζ of each layer in the model. With the choice of P_k given by Eq. (229), P_{k-2}/P_k is then constant

and, therefore, the coefficients S_k and Q_k are constant. Equations (239), (240), (244), and (229) give

$$Q_k \equiv Q \equiv \frac{e^{-\kappa} - 1 - \kappa d}{1 - e^{-\kappa d}}, \tag{245}$$

and

$$S_k \equiv S \equiv \frac{e^{\kappa d} - 1 - \kappa d}{e^{\kappa d} - 1}. \tag{246}$$

In addition,

$$\frac{p_{k+1}}{\Delta p_k} = \frac{p_{k+1}}{p_{k+1} - p_{k-1}} = \frac{1}{1 - e^{-d}}, \tag{247}$$

and

$$\frac{p_{k+1}}{\Delta p_{k+2}} = \frac{p_{k+1}}{p_{k+3} - p_{k+1}} = \frac{1}{e^{d} - 1}, \tag{248}$$

which are also constant. Multiplication of Eq. (243) by p_{k+1} and use of Eqs. (247) and (248) gives a constant coefficient difference equation for W, whose solution is formally identical to the solution of Eq. (227). As a result, the vertical wave number n is constant in height for an isothermal atmosphere, just as it is in the continuous case. Spurious computational reflection of wave energy due to the discretization is thus prevented as far as a resting isothermal atmosphere is concerned. For these reasons, an equal interval in log p between even levels and the function P_k given by Eq. (229) have been chosen for the stratospheric part of the model (see Fig. 1). A value of $d = 0.657$ is used, that is, $e^d = 1.93$.

The heavy line in Fig. 22 shows the index of refraction obtained from the discrete model for the same isothermal atmosphere as in the continuous case. Although n is constant in height, there is some unavoidable error as n approaches π/d, the highest resolvable wave number.

D. Final Determination of the Vertical Difference Scheme

Thus far, each layer of the model and its corresponding representative temperature T_k, potential temperature θ_k, and geopotential ϕ_k, have been identified by an odd value of the index k. The variables θ_k, ϕ_k, and T_k are

uniquely related once the function P_k is defined. For a time integration, it is unnecessary to specify the particular *levels* within the layers at which these variables are carried. However, when it is necessary to compare the model results with observations or when it is necessary for the purpose of actual numerical weather predictions to initialize the model from observations, levels must be chosen, somewhere near the center of each layer, to which the values of T_k, θ_k, and ϕ_k can be assigned. The same odd index k will be used to identify such levels.

Once the function P_k is specified, it is logical to define p_k by

$$(p_k/p_0)^\kappa = P_k. \tag{249}$$

The odd levels $p = p_k$ determined by Eqs. (229) and (249) are constant pressure levels (and, therefore, constant σ levels) centered in log p. Then, with $\theta_k = T_k(p_0/p_k)^\kappa$, no discretization error exists in the definition of the potential temperature.

The discrete hydrostatic equation, however, given by Eqs. (207) and (207′), is generally subject to discretization errors. As Phillips (1974) pointed out, these errors can be intolerably large unless the function P_k is properly chosen. The function P_k has already been defined for the stratosphere ($k < k_1$) by Eq. (229), based on considerations of vertical energy propagation. This choice turns out to be satisfactory from the point of view of the accuracy of the discretized hydrostatic equation as well. The difference $\Phi_k - \Phi_{k+2}$ given by Eqs. (207′) and (208) is exact for an atmosphere that is isothermal between levels k and $k + 2$.

For the troposphere, however, the function P_k has not yet been defined. The earlier UCLA general circulation models, including the earlier version of the 12-level model, used Eq. (249) with $P_k = [\frac{1}{2}(p_{k-1} + p_{k+1})/p_0]^\kappa$. Phillips has pointed out that with such a choice, calculation of θ_k from given Φ_k (which is a necessary procedure for initialization of the model for numerical weather prediction from an observed initial geopotential field) shows a large amplitude oscillation in θ_k from level to level. Phillips showed that P_k given by

$$P_k = \frac{1}{p_0{}^\kappa} \frac{1}{1 + \kappa} \frac{p_{k+1}^{1+\kappa} - p_{k-1}^{1+\kappa}}{p_{k+1} - p_{k-1}} \tag{250}$$

drastically reduced this deficiency. Tokioka shows in a forthcoming paper that use of Eq. (250) does give the exact value of θ_k from Φ_k when the atmosphere is isentropic. He also showed that the optimum choice of P_k for a

polytropic atmosphere, for which $T_k(p_0/p_k)^a$ is constant in height, is

$$P_k = \frac{1}{p_0{}^\kappa}\left[\frac{1}{1+a}\frac{(p_{k+1}^{1+a} - p_{k-1}^{1+a})}{p_{k+1} - p_{k-1}}\right]^\kappa. \tag{251}$$

The current version of the model uses $a = 0.205$, which approximately gives the normally observed stratification.

VI. The Horizontal Difference Scheme of the Model

A. The Governing Equations in Orthogonal Curvilinear Coordinates

Let the orthogonal curvilinear coordinates be ξ and η. Let the actual distances corresponding to $d\xi$ and $d\eta$ be $(ds)_\xi$ and $(ds)_\eta$, respectively, and define the metric factors m, n such that

$$(ds)_\xi = (1/m)\, d\xi, \tag{252}$$

and

$$(ds)_\eta = (1/n)\, d\eta. \tag{253}$$

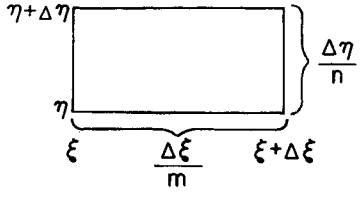

FIG. 23. A rectangular area element in the plane of the orthogonal curvilinear coordinates (ζ, η).

For the rectangular area element in the $\xi - \eta$ plane shown in Fig. 23, the actual lengths of the sides are $\Delta\xi/m$ and $\Delta\eta/n$, and the enclosed area is thus $\Delta\xi\,\Delta\eta/mn$. Let the component of $\mathbf{v}$ in ξ be u and the component of $\mathbf{v}$ in η be v.

1. *The Equation of Continuity*

The divergence is

$$\frac{\delta_\xi[u(\Delta\eta/n)] + \delta_\eta[v(\Delta\xi/m)]}{(\Delta\xi/m)(\Delta\eta/n)}, \tag{254}$$

where δ_ξ and δ_η are increments in the ξ and η directions, respectively. In the limit as $\Delta\xi, \Delta\eta \to 0$, the divergence can be written

$$\nabla_\sigma \cdot \mathbf{v} = mn\left[\frac{\partial}{\partial\xi}\left(\frac{u}{n}\right) + \frac{\partial}{\partial\eta}\left(\frac{v}{m}\right)\right]; \tag{255}$$

and the equation of continuity (126) thus becomes

$$\frac{\partial}{\partial t}\left(\frac{\pi}{mn}\right) + \frac{\partial}{\partial\xi}\left(\pi\frac{u}{n}\right) + \frac{\partial}{\partial\eta}\left(\pi\frac{v}{m}\right) + \frac{\partial}{\partial\sigma}\left(\frac{\pi\dot{\sigma}}{mn}\right) = 0. \tag{256}$$

2. *The Equation of Motion*

The equation of motion (136) may be written as

$$\frac{\partial\mathbf{v}}{\partial t} + \dot{\sigma}\frac{\partial\mathbf{v}}{\partial\sigma} + (f + \zeta)\mathbf{k} \times \mathbf{v} + \nabla(\tfrac{1}{2}\mathbf{v}^2 + \Phi) + \sigma\alpha\nabla\pi = \mathbf{F}, \tag{257}$$

where, by an argument similar to that for the divergence, the vorticity $\zeta = \mathbf{k} \cdot \nabla \times v$ can be expressed as

$$mn\left[\frac{\partial}{\partial\xi}\left(\frac{v}{n}\right) - \frac{\partial}{\partial\eta}\left(\frac{u}{m}\right)\right]. \tag{258}$$

The ξ component of (257) is then

$$\frac{\partial u}{\partial t} + \dot{\sigma}\frac{\partial u}{\partial\sigma} - \left[f + mn\left(\frac{\partial}{\partial\xi}\left(\frac{v}{n}\right) - \frac{\partial}{\partial\eta}\left(\frac{u}{m}\right)\right)\right]v + m\frac{\partial}{\partial\xi}(\tfrac{1}{2}u^2 + \tfrac{1}{2}v^2 + \Phi) + m\sigma\alpha\frac{\partial\pi}{\partial\xi} = F_\xi. \tag{259}$$

Rearranging the terms,

$$\frac{\partial u}{\partial t} + mu\frac{\partial u}{\partial\xi} + nv\frac{\partial u}{\partial\eta} + \dot{\sigma}\frac{\partial u}{\partial\sigma} - \left[f + mn\left(v\frac{\partial}{\partial\xi}\frac{1}{n} - u\frac{\partial}{\partial\eta}\frac{1}{m}\right)\right]v + m\left[\frac{\partial\Phi}{\partial\xi} + \sigma\alpha\frac{\partial\pi}{\partial\xi}\right] = F_\xi. \tag{260}$$

Similarly,

$$\frac{\partial v}{\partial t} + mu\frac{\partial v}{\partial \xi} + nv\frac{\partial v}{\partial \eta} + \dot{\sigma}\frac{\partial v}{\partial \sigma} + \left[f + mn\left(v\frac{\partial}{\partial \xi}\frac{1}{n} - u\frac{\partial}{\partial \eta}\frac{1}{m}\right)\right]u + n\left[\frac{\partial \Phi}{\partial \eta} + \sigma\alpha\frac{\partial \pi}{\partial \eta}\right] = F_\eta. \tag{261}$$

Combining (256) and (260) gives the flux form for the u momentum equation

$$\frac{\partial}{\partial t}\left(\frac{\pi}{mn}u\right) + \frac{\partial}{\partial \xi}\left(\frac{\pi u}{n}u\right) + \frac{\partial}{\partial \eta}\left(\frac{\pi v}{m}u\right) + \frac{\partial}{\partial \sigma}\left(\frac{\pi\dot{\sigma}}{mn}u\right) - \left[\frac{f}{mn} + \left(v\frac{\partial}{\partial \xi}\frac{1}{n} - u\frac{\partial}{\partial \eta}\frac{1}{m}\right)\right]\pi v + \frac{\pi}{n}\left[\frac{\partial \Phi}{\partial \xi} + \sigma\alpha\frac{\partial \pi}{\partial \xi}\right] = \frac{\pi}{mn}F_\xi; \tag{262}$$

and the flux form for v is similarly obtained,

$$\frac{\partial}{\partial t}\left(\frac{\pi}{mn}v\right) + \frac{\partial}{\partial \xi}\left(\frac{\pi u}{n}v\right) + \frac{\partial}{\partial \eta}\left(\frac{\pi v}{m}v\right) + \frac{\partial}{\partial \sigma}\left(\frac{\pi\dot{\sigma}}{mn}v\right) + \left[\frac{f}{mn} + \left(v\frac{\partial}{\partial \xi}\frac{1}{n} - u\frac{\partial}{\partial \eta}\frac{1}{m}\right)\right]\pi u + \frac{\pi}{m}\left[\frac{\partial \Phi}{\partial \eta} + \sigma\alpha\frac{\partial \pi}{\partial \eta}\right] = \frac{\pi}{mn}F_\eta. \tag{263}$$

The general circulation model uses the spherical coordinates $\xi = \lambda$ (longitude) and $\eta = \varphi$ (latitude) where $1/m = a\cos\varphi$ and $1/n = a$. Thus, from this point on, consideration will be restricted to those coordinate systems such as spherical (or cylindrical) in which m and n do not depend on ξ.

From (262) the (relative) angular momentum equation can be obtained,

$$\frac{\partial}{\partial t}\left(\frac{\pi}{mn}\frac{u}{m}\right) + \frac{\partial}{\partial \xi}\left(\frac{\pi u}{n}\frac{u}{m}\right) + \frac{\partial}{\partial \eta}\left(\frac{\pi v}{m}\frac{u}{m}\right) + \frac{\partial}{\partial \sigma}\left(\frac{\pi\dot{\sigma}}{mn}\frac{u}{m}\right) - \left[\frac{f}{mn}\frac{\pi v}{m}\right] + \pi\left[\frac{\partial}{\partial \xi}\frac{\Phi}{mn} + \sigma\alpha\frac{\partial}{\partial \xi}\frac{\pi}{mn}\right] = \frac{\pi}{mn}\frac{F_\xi}{m}. \tag{264}$$

3. *The Thermodynamic Energy Equation*

The thermodynamic energy equation (143) can be expressed in curvilinear coordinates as

$$\frac{\partial}{\partial t}\left(\frac{\pi}{mn}c_p T\right) + \frac{\partial}{\partial \xi}\left(\frac{\pi u}{n}c_p T\right) + \frac{\partial}{\partial \eta}\left(\frac{\pi v}{m}c_p T\right) + p^\kappa \frac{\partial}{\partial \sigma}\left(\frac{\pi \dot{\sigma}}{mn}c_p \theta\right)$$
$$= \pi\sigma\alpha\left(\frac{\partial}{\partial t}\left(\frac{\pi}{mn}\right) + \frac{u}{n}\frac{\partial \pi}{\partial \xi} + \frac{v}{m}\frac{\partial \pi}{\partial \eta}\right) + \frac{\pi}{mn}Q. \tag{265}$$

B. Horizontal Differencing of the Governing Equations

Despite the introduction here of the use of the σ coordinate and the presence of metric factors, the manner of derivation of a difference scheme for the continuity equation and for the advection and coriolis terms in the u and v momentum equations so closely parallels the methods presented in Section III, C that the representation chosen for these terms will be presented here without elaboration. The new considerations introduced by the requirement of total energy conservation in a three-dimensional domain will be explained more fully.

1. *The Continuity Equation*

For the continuity equation (256) multiplied by $\Delta\xi\Delta\eta$, the following form is chosen

$$\frac{\partial \prod_{i,j}}{\partial t} + (\delta_\xi F)^k_{i,j} + (\delta_\eta G)^k_{i,j} + \frac{1}{\Delta\sigma_k}(\delta_\sigma \dot{S})^k_{i,j} = 0, \tag{266}$$

where

$$\prod \equiv \pi(\Delta\xi\,\Delta\eta/mn), \qquad F \equiv \pi u(\Delta\eta/n),$$
$$G \equiv \pi v(\Delta\xi/m), \qquad \dot{S} \equiv \prod \dot{\sigma}. \tag{267}$$

The vertical index k now appears as a superscript on all variables except π and $\prod$. Although π and $\prod$ do have different definitions for $k < k_1$ and $k > k_1$, the superscript is dropped for simplicity.

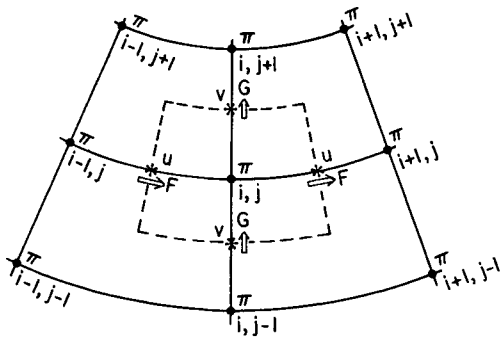

FIG. 24. A π-centered portion of the spherical grid showing points of definition of the fluxes introduced in Eq. (266).

For the mass fluxes F and G, shown in Fig. 24, the following forms are used:

$$F^k_{i+1/2,\,j} = \overline{\left(u\frac{\Delta\eta}{n}\right)^k}_{i+1/2,\,j}\,\bar{\pi}^{\xi}_{i+1/2,j}, \tag{268}$$

where

$$\left[u(\Delta\eta/n)\right]^k_{i+1/2,\,j} \equiv u^k_{i+1/2,\,j}(\Delta\eta/n)_j \tag{269}$$

and

$$G^k_{i,\,j+1/2} = \left[v(\Delta\xi/m)\right]^k_{i,\,j+1/2}\bar{\pi}^{\eta}_{i,\,j+1/2}, \tag{270}$$

where

$$\left[v(\Delta\xi/m)\right]^k_{i,\,j+1/2} \equiv v^k_{i,\,j+1/2}(\Delta\xi/m)_{j+1/2}. \tag{271}$$

The superior bar operator, which is a linear smoothing operator in ξ, should be ignored for the present. The form and role of this operator will be described in the next subsection.

2. *The Momentum Advection Terms*

The form chosen for the terms

$$\frac{\partial}{\partial t}\left(\pi\frac{\Delta\xi\,\Delta\eta}{mn}u\right) + \Delta\xi\frac{\partial}{\partial\xi}\left(\pi u\frac{\Delta\eta}{\eta}u\right)$$
$$+ \Delta\eta\frac{\partial}{\partial\eta}\left(\pi v\frac{\Delta\xi}{m}u\right) + \frac{\partial}{\partial t}\left(\pi\dot{\sigma}\frac{\Delta\xi\,\Delta\eta}{mn}u\right)$$

from Eq. (262) multiplied by $\Delta\xi\,\Delta\eta$ is

$$\frac{\partial}{\partial t}(\prod^{(u)}u^k)_{i,j} + \Big[\delta_\xi(\mathscr{F}^{(u)}\overline{u}^\xi) + \delta_\eta(\mathscr{G}^{(u)}\overline{u}^\eta) + \delta_{\xi'}(\tilde{\mathscr{F}}^{(u)}\overline{u}^{\xi'}) + \delta_{\eta'}(\tilde{\mathscr{G}}^{(u)}\overline{u}^{\eta'}) + \frac{1}{\Delta\sigma_k}\delta_\sigma(\dot{S}^{(u)}\overline{u}^\sigma)\Big]^k_{i,j}. \tag{272}$$

If the variables $\prod^{(u)}$ and $\dot{S}^{(u)}$ at u points and $\mathscr{F}^{(u)}$, $\mathscr{G}^{(u)}$, $\tilde{\mathscr{F}}^{(u)}$ and $\tilde{\mathscr{G}}^{(u)}$ shown in Fig. 25 satisfy the constraint

$$\frac{\partial}{\partial t}\prod^{(u)}_{i,j} + \Big[\delta_\xi\mathscr{F}^{(u)} + \delta_\eta\mathscr{G}^{(u)} + \delta_{\xi'}\tilde{\mathscr{F}}^{(u)} + \delta_{\eta'}\tilde{\mathscr{G}}^{(u)} + \frac{1}{\Delta\sigma_k}\delta_\sigma\dot{S}^{(u)}\Big]^k_{i,j} = 0, \tag{273}$$

then conservation of kinetic energy under a pure advective process is maintained.

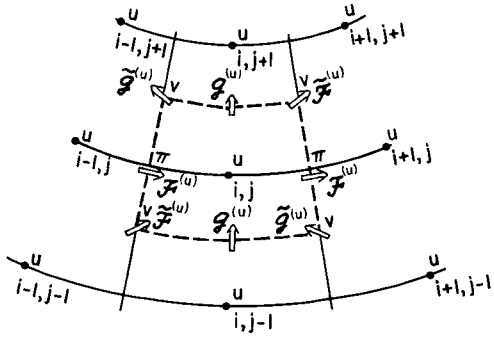

FIG. 25. A u-centered portion of the spherical grid showing points of definition of the flux terms introduced in Eq. (272).

With F^* and G^* defined by

$$F^*_{i,j} = (\overline{F}^\xi)_{i,j}, \qquad G^*_{i,j} = (\overline{G}^\eta)_{i,j}, \tag{274}$$

the following choice for the fluxes in Eq. (272) is guided by Eq. (95):

$$\begin{aligned}
\mathscr{F}^{(u)}_{i+1/2,j} &= \tfrac{2}{3}(\overline{F^{*\eta\eta}})_{i+1/2,j}\\
\mathscr{G}^{(u)}_{i,j+1/2} &= \tfrac{2}{3}(\overline{G^{*\eta\xi}})_{i,j+1/2}\\
\tilde{\mathscr{F}}^{(u)}_{i+1/2,j+1/2} &= \tfrac{1}{6}(\overline{G^{*\eta}} + \overline{F^{*\eta}})_{i+1/2,j+1/2}\\
\tilde{\mathscr{G}}^{(u)}_{i-1/2,j+1/2} &= \tfrac{1}{6}(\overline{G^{*\eta}} - \overline{F^{*\eta}})_{i-1/2,j+1/2}.
\end{aligned} \tag{275}$$

Then Eq. (273) is consistent with the continuity equation (266) if

$$\prod_{i,j}^{(u)} = (\overline{\prod}^{\xi\eta\eta})_{i,j} \tag{276}$$

and

$$\dot{S}_{i,j}^{(u)} = (\bar{S}^{\xi\xi\eta})_{i,j}. \tag{277}$$

For the v-momentum equation (263) multiplied by $\Delta\xi\,\Delta\eta$, a form identical to (272) is used, but with u replaced by v. The definitions corresponding to (275)–(277) are then

$$\begin{aligned}
\mathscr{F}_{i+1/2,j}^{(v)} &= \tfrac{2}{3}(\overline{F^{*\xi\eta}})_{i+1/2,j}, \\
\mathscr{G}_{i,j+1/2}^{(v)} &= \tfrac{2}{3}(\overline{G^{*\xi\xi}})_{i+1/2,j+1/2}, \\
\tilde{\mathscr{F}}_{i+1/2,j+1/2}^{(v)} &= \tfrac{1}{6}(\overline{G^{*\xi}} + \overline{F^{*\xi}})_{i+1/2,j+1/2}, \\
\tilde{\mathscr{G}}_{i-1/2,j+1/2}^{(v)} &= \tfrac{1}{6}(\overline{G^{*\xi}} - \overline{F^{*\xi}})_{i-1/2,j+1/2},
\end{aligned} \tag{278}$$

$$\prod_{i,j}^{(v)} = (\overline{\prod}^{\xi\xi\eta})_{i,j}, \tag{279}$$

and

$$\dot{S}_{i,j}^{(v)} = (\bar{S}^{\xi\eta\eta})_{i,j}. \tag{280}$$

3. *The Coriolis Terms*

From Eq. (262) the contribution from the coriolis force plus the metric term to $\partial(\prod u)/\partial t$ is

$$\left[f\frac{\Delta\xi\,\Delta\eta}{mn} - u\,\Delta\xi\,\Delta\eta\,\frac{\partial}{\partial\eta}\frac{1}{m}\right]\pi v \tag{281}$$

and the corresponding contribution to $\partial(\prod v)/\partial t$ is

$$-\left[f\frac{\Delta\xi\,\Delta\eta}{mn} - u\,\Delta\xi\,\Delta\eta\,\frac{\partial}{\partial\eta}\frac{1}{m}\right]\pi u. \tag{282}$$

A variable C_{ij}^{k} is defined at π points by

$$C_{i,j}^{k} = f_j\left(\frac{\Delta\xi\,\Delta\eta}{mn}\right) - (\bar{u}^{\xi})_{i,j}^{k}\,\delta_{\eta}\left(\frac{\Delta\xi}{m}\right)_j \tag{283}$$

Then, the following form is used for (281) at a u point (i, j):

$$(\overline{\pi C \bar{v}^{\eta}}^{\xi})^{k}_{i,j}; \tag{284}$$

and for (282) at a v point $(i + 1/2, j + 1/2)$,

$$-(\overline{\pi C \bar{u}^{\xi}}^{\eta})^{k}_{i+1/2,\, j+1/2}. \tag{285}$$

This choice of differencing does not lead to any false generation of total kinetic energy.

4. *The Pressure Gradient Force*

As in Eq. (262), the pressure gradient force in the ξ direction can be written as

$$-\frac{\pi}{n}\left[\frac{\partial \Phi}{\partial \xi} + \sigma\alpha \frac{\partial \pi}{\partial \xi}\right]. \tag{286}$$

The form chosen for the first term is

$$-\left(\frac{\pi}{n}\frac{\partial \Phi}{\partial \xi}\right)^{k}_{i+1/2,\, j} = -\frac{1}{\Delta\xi}\frac{\Delta\eta}{\Delta\eta}\frac{}{n_j}(\overline{\bar{\pi}^{\xi}\, \delta_{\xi}\Phi^{k}})_{i+1/2,\, j}. \tag{287}$$

Continue, for the time being, to ignore the bar operator.

Corresponding to the relation

$$-\frac{\pi}{n}\frac{\partial \Phi}{\partial \xi} = \frac{1}{n}\left[\frac{\partial}{\partial \xi}(\pi\Phi) - \Phi\frac{\partial \pi}{\partial \xi}\right],$$

Eq. (287) can be rewritten in the form

$$-\left(\frac{\pi}{n}\frac{\partial \Phi}{\partial \xi}\right)^{k}_{i+1/2,\, j} = -\frac{1}{\Delta\xi}\frac{\Delta\eta}{\Delta\eta}\frac{}{n_j}\overline{[\delta_{\xi}(\pi\Phi) - \bar{\Phi}^{\xi}\, \delta_{\xi}\pi]}^{k}_{i+1/2,\, j}. \tag{288}$$

To be consistent with Eq. (288), the following form is chosen for the second term in Eq. (286),

$$-\left(\frac{\pi}{n}\sigma\alpha\frac{\partial \pi}{\partial \xi}\right)^{k}_{i+1/2,\, j} = -\frac{1}{\Delta\xi}\frac{\Delta\eta}{\Delta\eta}\frac{}{n_j}\overline{[(\pi\sigma\alpha)^{\xi}\, \delta_{\xi}\pi]}^{k}_{i+1/2,\, j} \tag{289}$$

where, through the application of Eq. (194) at each grid point,

$$(\pi\sigma\alpha)_{ij}{}^{k} = \pi_{ij} c_{\mathrm{p}} \left[\frac{1}{P^k} \frac{\partial P^k}{\partial \pi} T^k \right]_{i,j}, \tag{290}$$

where $P^k_{i,j}$ is defined by Eq. (251).

Adding (289) to (288) gives a form that corresponds to

$$-\frac{1}{n}\left[\frac{\partial(\pi\Phi)}{\partial\xi} - \frac{\partial}{\partial\sigma}(\Phi\sigma)\frac{\partial\pi}{\partial\xi}\right],$$

from which it can readily be shown that the properties of the vertically integrated pressure gradient force discussed in Section V, A are maintained.

In summary, the pressure gradient force which contributes to $(\partial/\partial t) \times (\prod^{(u)} u)^k_{i+1/2,j}$ is

$$-\frac{\Delta\eta}{n_j}\overline{\left[\overline{\pi}^{\xi}\,\delta_\xi\Phi^k + \overline{(\pi\sigma\alpha)}^{\xi}\,\delta_\xi\pi\right]}^{k}_{i+1/2,j}. \tag{291}$$

Similarly, the pressure gradient force which contributes to $\partial/\partial t\,(\prod^{(v)} v)^k_{i,j+1/2}$ is

$$-\frac{\Delta\xi}{m_{j+1/2}}\left[\overline{\pi}^{\eta}\,\delta_\eta\Phi^k + \overline{(\pi\sigma\alpha)}^{\eta}\,\delta_\eta\pi\right]^k_{i,j+1/2}, \tag{292}$$

where $(\pi\sigma\alpha)^k_{i,j}$ is given by Eq. (290).

5. *Kinetic Energy Generation and the Thermodynamic Energy Equation*

The contribution of the pressure gradient force to the kinetic energy generation, $\partial/\partial t\,(\prod^{(u)}\frac{1}{2}u^2)^k_{i+1/2,j}$, is obtained by multiplying Eq. (291) by $u^k_{i+1/2,j}$. Then the kinetic energy generation is

$$-\left(u\frac{\Delta\eta}{n}\right)^{k}_{i+1/2,j}\overline{\left[\overline{\pi}^{\xi}\,\delta_\xi\Phi + \overline{(\pi\sigma\alpha)}^{\xi}\,\delta_\xi\pi\right]}^{k}_{i+1/2,j}. \tag{293}$$

From the form of the superior bar operator, it can be shown that Eq. (293) is equivalent to

$$\overline{\left(u\frac{\Delta\eta}{n}\right)}^{k}_{i+1/2,j}\left[\overline{\pi}^{\xi}\,\delta_\xi\Phi + \overline{(\pi\sigma\alpha)}^{\xi}\,\delta_\xi\pi\right]^k_{i+1/2,j}, \tag{294}$$

in the sense that the difference $R_{i+1/2}$ defined by

$$R_{i+1/2} \equiv (293) - (294)$$

vanishes when the summation over all i is taken; i.e.,

$$\sum_i R_{i+1/2} = 0.$$

Using the definition of F given by Eq. (268), Eq. (294) becomes

$$-[F\,\delta_\xi \Phi + u(\Delta\eta/n)\overline{(\pi\sigma\alpha)}^{\xi}\,\delta_\xi \pi]^k_{i+1/2,\,j}. \tag{295}$$

It can then be shown that

$$\sum_i (295) = \sum_i \left[\Phi \delta_\xi F - \overline{\overline{\left(u\frac{\Delta\eta}{n}\right)\overline{(\pi\sigma\alpha)}^{\xi}\,\delta_\xi \pi}^{\xi}}\right]^k_{i,\,j}. \tag{296}$$

Similarly, the contribution of the gradients of Φ and π to $\partial/\partial t$ $(\prod^{(v)}\frac{1}{2}v^2)^k_{i,\,j}$ is given by

$$\sum_j \left[\Phi \delta_\eta G - \overline{\left(v\frac{\Delta\xi}{m}\right)\overline{(\pi\sigma\alpha)}^{\eta}\,\delta_\eta \pi}^{\eta}\right]^k_{ij}. \tag{297}$$

Now $\sum_j (296) + \sum_i (297)$ give the discrete form of the total kinetic generation by the pressure gradient force, $-\pi\mathbf{v}\cdot[\nabla\sigma\Phi + \sigma\alpha\,\nabla\pi]$. It is useful to note that $\sum_i$ [first term of (296)] + $\sum_i$ [first term of (297)], which gives the contribution of $\Phi_{ij}{}^k$ to the kinetic energy generation, can be written using the equation of continuity (266) as

$$-\left[\frac{\partial \prod_{ij}}{\partial t} + \frac{1}{\Delta\sigma_k}(\dot{S}^{k+1}_{i,\,j} - \dot{S}^{k-1}_{i,\,j})\right]\Phi^k_{i,\,j}. \tag{298}$$

The derivation given in Eq. (185) leading to a finite-difference expression for $\omega\alpha$ can be followed exactly, but now with the horizontal differencing specified as well. Using such an expression in a manner completely analogous to the procedure in Section V, B, 8, allows us to write the thermodynamic energy equation given in Eq. (209), with the horizontal differencing

incorporated, as

$$\frac{\partial}{\partial t}(\prod T)^k_{i,j} + [\delta_\xi(F\overline{T}^\xi) + \delta_\eta(G\overline{T}^\eta)]^k_{i,j} + \frac{1}{\Delta\sigma_k} P^k_{i,j}\,\delta_\sigma(\dot{S}\hat{\theta})^k_{i,j}$$

$$= \frac{1}{c_p}\left[(\pi\sigma\alpha)\frac{\partial \prod}{\partial t} + u\frac{\overline{\Delta\eta}^{\xi}}{n}\overline{(\pi\sigma\alpha)}^{\xi}\delta_\xi\pi + v\frac{\overline{\Delta\xi}^{\eta}}{m}\overline{(\pi\sigma\alpha)}^{\eta}\sigma_\eta\pi + \prod Q\right]^k_{i,j}, \quad (299)$$

where $(\pi\sigma\alpha)^k_{i,j}$ is defined by Eq. (290).

C. Modification of the Horizontal Differencing Near the Poles

1. *Modification of the Difference Equations*

The poles are singular points of the spherical coordinates and the velocity components cannot be defined there; the poles are thus taken as π-points. The value of π at the poles must change as a result of the meridional mass flux G, defined by Eq. (270), at all the points on the nearest latitude circle where the meridional velocity component v is carried.

Consider the case of the North Pole, identified by $j = p$ in Fig. 26. To simplify the computation, the pole is treated as if it were a group of points. Each point has index i and represents the shaded area shown. Defining $\prod_{i,p}$ and $\dot{S}_{i,p}$ based on that area, the equation of continuity (266) is applied to $j = p$, omitting all horizontal mass flux terms except $G^k_{i,p-1/2}$. After computing $\partial\prod/\partial t$ and $\dot{S}$ for all i, the average is taken.

At the grid point $(i, p - 1/2, k)$, the form chosen for the first line of (263) multiplied by $\Delta\xi\,\Delta\eta$ is

$$\frac{\partial}{\partial t}(\prod{}^{(v)} v)^k_{i,p-1/2} + \delta_\xi(\mathscr{F}^{*(v)}\overline{v}^\xi)^k_{i,p-1/2} - (\mathscr{G}^{(v)}\overline{v}^\eta)^k_{i,p-1}$$

$$- (\mathscr{F}^{(v)}\overline{v}^{\xi'})^k_{i-1/2,p-1} - (\mathscr{G}^{(v)}\overline{v}^{\eta'})^k_{i+1/2,p-1} + \delta_\sigma(\dot{S}\overline{v}^\sigma)^k_{i,p-1/2}. \quad (300)$$

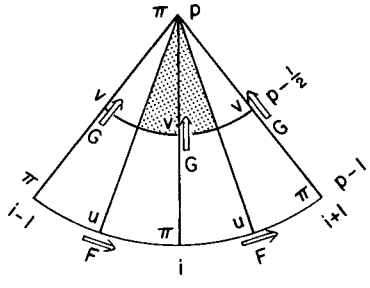

FIG. 26. A polar segment of the spherical grid showing mass fluxes.

Invoking the consistency requirement that the global sum of $\prod^{(v)}$ be equal to the global sum of $\prod$ gives

$$\prod^{(v)}_{i,\,p-1/2} \equiv \tfrac{1}{8}\{\prod_{i-1,\,p} + \prod_{i-1,\,p-1} + 2(\prod_{i,\,p} + \prod_{i,\,p-1}) + \prod_{i+1,\,p} + \prod_{i+1,\,p-1}\} + \tfrac{1}{2} \times \tfrac{1}{4}(\prod_{i-1,\,p} + 2\prod_{i,\,p} + \prod_{i+1,\,p}). \tag{301}$$

The definition of $\dot{S}^{(v)}$ is readily obtained by replacing $\prod$ everywhere in Eq. (301) by $\dot{S}$. The requirement for kinetic energy conservation during advective processes alone given in Section III, C can be shown equivalent to the requirement that the new variable $\mathscr{F}^*$ be chosen such that (300) vanish when v is replaced by a constant value, which can be taken as unity. The resulting equation can be shown consistent with the continuity equation (266) and $\partial/\partial t \prod^{i}_{i,\,p} = \bar{G}^{i}_{i,\,p-1/2}$ if

$$\mathscr{F}^{*(v)}_{i-1/2,\,p-1/2} \equiv \tfrac{1}{3}\overline{F^*}^{\xi}_{i-1/2,\,p-1}, \tag{302}$$

where F^* is defined by Eq. (274).

In a similar manner, at the grid point $(i,\ p-1,\ k)$, the form chosen for the first line of Eq. (262) multiplied by $\Delta\xi\,\Delta\eta$ is

$$\frac{\partial}{\partial t}(\prod^{(u)}u)^{k}_{i,\,p-1} + \delta_{\xi}(\mathscr{F}^{*(u)}\overline{u}^{\xi})^{k}_{i,\,p-1} - (\mathscr{G}^{(u)}\overline{u}^{\eta})^{k}_{i,\,p-3/2} - (\bar{\mathscr{F}}^{(u)}\overline{u}^{\xi'})^{k}_{i-1/2,\,p-3/2} - (\bar{\mathscr{G}}^{(u)}\overline{u}^{\eta'})^{k}_{i+1/2,\,p-3/2} + \frac{1}{\Delta\sigma_k}(\dot{S}\overline{u}^{\sigma})^{k}_{i,\,p-1}. \tag{303}$$

Again, it is required that the global sum of $\prod^{(u)}$ be equal to the global sum of $\prod$, which gives

$$\prod^{(u)}_{i,\,p-1} \equiv \tfrac{1}{8}\{\prod_{i-1/2,\,p} + \prod_{i+1/2,\,p} + 2(\prod_{i-1/2,\,p-1} + \prod_{i+1/2,\,p-1}) + \prod_{i-1/2,\,p-2} + \prod_{i+1/2,\,p-2}\} + \tfrac{1}{8}\{3(\prod_{i-1/2,\,p} + \prod_{i+1/2,\,p}) + \prod_{i-1/2,\,p-1} + \prod_{i+1/2,\,p-1}\}. \tag{304}$$

The definition of $\dot{S}^{(u)}$ is obtained by replacing $\prod$ everywhere in Eq. (304) by $\dot{S}$. For kinetic energy conservation during advective processes alone, it is necessary that (303) vanish when u is replaced by unity. The resulting equation is consistent with Eq. (266) and $(\partial/\partial t)\,\overline{\prod}^{i}_{i,\,p} = \bar{G}^{i}_{i,\,p-1/2}$ if

$$\mathscr{F}^{*}_{i-1/2,\,p-1} \equiv \tfrac{1}{6}(4F^{*}_{i-1/2,\,p-1} + F^{*}_{i-1/2,\,p-2}). \tag{305}$$

2. *Longitudinal Averaging of Selected Terms Near the Poles*

To avoid the use of the extremely short time interval necessary for computational stability due to the convergence of the meridians toward the poles, a longitudinal averaging is done of *selected terms* in the prognostic equations.

For the purpose of illustration, consider the simple system of linearized equations that governs a gravity wave on the spherical earth:

$$\frac{\partial u}{\partial t} + \frac{1}{a \cos \varphi} \frac{\partial \phi}{\partial \lambda} = 0, \tag{306}$$

$$\frac{\partial v}{\partial t} + \frac{1}{a} \frac{\partial \phi}{\partial \varphi} = 0, \tag{307}$$

$$\frac{\partial \phi}{\partial t} + \frac{gH}{a \cos \varphi} \left(\frac{\partial u}{\partial \lambda} + \frac{\partial (v \cos \varphi)}{\partial \varphi} \right) = 0, \tag{308}$$

where H is the equivalent depth. Other symbols are as defined in Section V, C. Because our concern here is only with waves that have frequencies sufficiently higher than the earth's rotation rate, the coriolis force has been omitted for simplicity.

With the grid shown in Fig. 26 and a space finite differencing consistent with that of the model, the discrete analogs of Eqs. (306)–(308) can be written as follows:

$$\frac{\partial u_{i+1/2,\,j}}{\partial t} + \frac{1}{a \cos \varphi} \frac{1}{\Delta \lambda} (\delta_\lambda \phi)_{i+1/2,\,j} = 0 \tag{309}$$

$$\frac{\partial v_{i,\,j+1/2}}{\partial t} + \frac{1}{a} \frac{1}{\Delta \varphi_j} (\delta_\varphi \phi)_{i,\,j+1/2} = 0, \tag{310}$$

$$\frac{\partial \phi_{i,\,j}}{\partial t} + \frac{gH}{a \cos \varphi} \left[\frac{1}{\Delta \lambda} (\delta_\lambda u) + \frac{1}{\Delta \varphi} \delta_\varphi (v \cos \varphi) \right]_{ij} = 0. \tag{311}$$

Let us consider a solution of the form

$$u_{i+1/2,\,j} = \mathrm{Re} \{ \hat{u}_j \exp [\bar{i}(s(i + 1/2)\, \Delta \lambda + \sigma t)] \} \tag{312}$$

$$v_{i,\,j+1/2} = \mathrm{Re} \{ \hat{v}_{j+1/2} \exp [\bar{i}(si\, \Delta \lambda + \sigma t)] \} \tag{313}$$

$$\phi_{i,\,j} = \mathrm{Re} \{ \hat{\phi}_j \exp [\bar{i}(si\, \Delta \lambda + \sigma t)] \} \tag{314}$$

where $\bar{\imath} \equiv \sqrt{-1}$. Substituting Eqs. (312), (313), and (314) into Eqs. (309), (310), and (311), we obtain

$$\bar{\imath}\sigma\hat{u}_j + \frac{\bar{\imath}s}{a\cos\varphi_j}\left(\frac{\sin(s\,\Delta\lambda/2)}{s\,\Delta\lambda/2}\right)S_j(s)\hat{\phi}_j = 0, \tag{315}$$

$$\bar{\imath}\sigma\hat{v}_{j+1/2} + (1/a\,\Delta\varphi)(\hat{\phi}_{j+1} - \hat{\phi}_j) = 0, \tag{316}$$

$$\bar{\imath}\sigma\hat{\phi}_j + \frac{gH}{a\cos\varphi_j}\left[\bar{\imath}s\left(\frac{\sin(s\,\Delta\lambda/2)}{s\,\Delta\lambda/2}\right)S_j(s)\hat{u}_j + \frac{1}{\Delta\varphi}\{(\hat{v}\cos\varphi)_{j+1/2} - (\hat{v}\cos\varphi)_{j-1/2}\}\right] = 0, \tag{317}$$

where $S_j(s) \equiv 1$ for present purposes. Eliminating $\hat{u}$ and $\hat{v}$ from Eqs. (315)–(317) gives

$$C^2\left[\frac{s}{a\cos\varphi_j}\frac{\sin(s\,\Delta\lambda/2)}{(s\,\Delta\lambda/2)}S_j(s)\right]^2\hat{\phi}_j + \frac{C^2}{(a\,\Delta\varphi)^2}\left[(\hat{\phi}_j - \hat{\phi}_{j-1})\frac{\cos\varphi_{j-1/2}}{\cos\varphi_j} - (\hat{\phi}_{j+1} - \hat{\phi}_j)\frac{\cos\varphi_{j+1/2}}{\cos\varphi_j}\right] = \sigma^2\hat{\phi}_j, \tag{318}$$

which is the discrete analog of the meridional structure equation for $\hat{\phi}$. Here $C^2 \equiv gH$.

For a given s, with the boundary condition $\hat{\phi} = 0$ at the poles, possible values of σ^2 are obtained as eigenvalues from the matrix equation represented by Eq. (318) applied to all j interior to the poles. When s is large, the matrix is very close to diagonal for j's near the poles and, therefore, the maximum eigenvalue can be only slightly larger than the maximum diagonal component, which is approximately the maximum value of the coefficient of the first term of Eq. (318). If $S_j(s) = 1$, this argument gives

$$|\sigma|_{\max} \doteq \frac{2|C|}{a\,\Delta\lambda}\frac{1}{(\cos\varphi_j)_{\min}}\sin\frac{s\,\Delta\lambda}{2}. \tag{319}$$

For most conditionally stable time difference schemes, the stability criterion is given by

$$|\sigma|\,\Delta t < \varepsilon, \tag{320}$$

where ε is a constant ($\varepsilon = 1$ for the leapfrog scheme). From Eq. (319), this stability criterion is approximately equivalent to

$$\frac{|C|\,\Delta t}{a\,\Delta\lambda} \sin\frac{s\,\Delta\lambda}{2} < \frac{\varepsilon}{2}(\cos\varphi_j)_{\min}. \tag{321}$$

To make the scheme stable for all resolvable waves, it is necessary to require

$$\frac{|C|\,\Delta t}{a\,\Delta\lambda} < \frac{\varepsilon}{2}(\cos\varphi_j)_{\min}. \tag{322}$$

Thus, since $(\cos\varphi_j)_{\min} \ll 1$, an extremely small Δt must be used to ensure stability.

The method devised to allow the use of a longer Δt in the model is to smooth the longitudinal pressure gradient in the momentum equation and the longitudinal divergence in the continuity equation with a longitudinal averaging operator. If the amplitude of the longitudinal pressure gradient and divergence are modified by the factor

$$S_j(s) = (a\,\Delta\lambda/d^*)[\cos\varphi_j/\sin(s\,\Delta\lambda/2)], \tag{323}$$

where d^* is a specified constant length, then Eq. (318) becomes

$$\frac{4C^2}{d^{*2}}\hat{\phi}_j + \frac{C^2}{(a\,\Delta\varphi)^2}\left[(\hat{\phi}_j - \hat{\phi}_{j-1})\frac{\cos\varphi_{j-1/2}}{\cos\varphi_j} - (\hat{\phi}_{j+1} - \hat{\phi}_j)\frac{\cos\varphi_{j+1/2}}{\cos\varphi_j}\right] = \sigma^2\hat{\phi}_{ij}, \tag{324}$$

for all j. Thus the first term now contributes to the eigenvalue σ^2 a constant amount $4C^2/d^{*2}$. The dependence of $|\sigma|_{\max}$ on $(\cos\varphi_j)_{\min}$ is eliminated, and a Δt satisfying the stability criterion depends now on the constant length d^*. In the model, d^* is taken as the latitudinal grid size, $a\,\Delta\varphi$.

In practice, it is sufficient to perform the smoothing only at higher latitudes. Then

$$S_j(s) = (\Delta\lambda/\Delta\varphi)[\cos\varphi_j/\sin(s\,\Delta\lambda/2)] \tag{325}$$

when the right-hand side is less than 1; $S_j(s) = 1$ otherwise.

To apply the operator, the zonal pressure gradient and the zonal mass flux are expanded into Fourier series and the amplitude of each wave component reduced by the factor $S_j(s)$. This is the bar operation shown in

Section VI, B. The form of the smoothing of the mass flux given by Eq. (268) is chosen to maintain the energy conservation.

It is important to note that this smoothing operation does not smooth or truncate the Fourier expansions of the fields of the variables. It is simply a generator of multiple point difference quotients in the space difference scheme. For the example given above, the solution of Eqs. (315), (316), and (317) is still a neutral oscillation.

VII. Vertical and Horizontal Differencing of the Water Vapor and Ozone Continuity Equations

A. Vertical Differencing

1. *ln q-Conserving Scheme*

Let q be the mixing ratio of water vapor or ozone. The corresponding continuity equation is given by Eq. (145). The vertical differencing given by

$$\frac{\partial}{\partial t}(\pi_k q_k) + \nabla \cdot (\pi_k \mathbf{v}_k q_k) + \frac{1}{\Delta\sigma_k}\left[(\pi\dot{\sigma})_{k+1}\hat{q}_{k+1} - (\pi\dot{\sigma})_{k-1}\hat{q}_{k-1}\right] = \pi_k S_k \quad (326)$$

guarantees the conservation of total water vapor or total ozone, when there are no sources and sinks, for any choice of $\hat{q}$.

The ozone mixing ratio varies in the vertical over a wide range of magnitudes and, as with potential temperature, shows a highly skewed "mass density function." Applying the considerations of Section V, B, 3 to the ozone mixing ratio, a $\hat{q}$ can be chosen that leads to conservation of a discrete analog of the global integral of ln q with respect to mass. From Eq. (189), such a $\hat{q}$ must be of the form

$$\hat{q}_{k+1} = \frac{\ln q_k - \ln q_{k+2}}{(1/q_{k+2}) - (1/q_k)}. \quad (327)$$

Further discussion of this scheme has been presented by Schlesinger (1976).

The same form for $\hat{q}_{k+1}$ could also be used for the water vapor mixing ratio. Release of heat of condensation, however, makes the choice of $\hat{q}$ for water vapor more difficult, as discussed below.

2. *Moist Adiabatic Process—Continuous Case*

Consider, first, a moist adiabatic process in the continuous atmosphere. Let the air be saturated and remain saturated, and let there be no heating other than the heat of condensation.

Let q be the mixing ratio and $q^*(T, p)$ be the saturation mixing ratio of water vapor. Then the water vapor continuity equation, when condensation is occurring, is

$$dq/dt = dq^*/dt = -C, \tag{328}$$

where C is the sink of water vapor per unit mass of dry air. This can also be written as

$$\left(\frac{\partial q^*}{\partial T}\right)_p \frac{dT}{dt} + \left(\frac{\partial q^*}{\partial p}\right)_T \omega = -C. \tag{329}$$

The thermodynamic energy equation is

$$(d/dt)c_p T = \omega\alpha + LC, \tag{330}$$

where L is the heat of condensation per unit mass. Then Eqs. (329) and (330) give

$$C = -\frac{\omega}{1 + [(L/c_p)(\partial q^*/\partial T)_p]}\left[\left(\frac{\partial q^*}{\partial p}\right)_T + \frac{\alpha}{c_p}\left(\frac{\partial q^*}{\partial T}\right)_p\right]. \tag{331}$$

Substituting Eq. (331) into Eq. (330) gives

$$dT/dt = \omega(\partial T/\partial p)_m, \tag{332}$$

or

$$[(\partial/\partial t) + \mathbf{v}\cdot\nabla]_p T = \omega[(\partial T/\partial p)_m - (\partial T/\partial p)]. \tag{333}$$

where

$$\left(\frac{\partial T}{\partial p}\right)_m \equiv \left[\frac{\alpha}{c_p} - \frac{L}{c_p}\left(\frac{\partial q^*}{\partial p}\right)_T\right] \Big/ \left[1 + \frac{L}{c_p}\left(\frac{\partial q^*}{\partial T}\right)_p\right], \tag{334}$$

Here $\partial/\partial p$ without a subscript is the derivative under constant horizontal coordinates and constant time.

The corresponding equation with the σ coordinate can be readily obtained by using the following relations:

$$\left(\frac{\partial}{\partial t} + \mathbf{v}\cdot\nabla\right)_p = \left(\frac{\partial}{\partial t} + \mathbf{v}\cdot\nabla\right)_\sigma - \frac{\sigma}{\pi}\left(\frac{\partial}{\partial t} + \mathbf{v}\cdot\nabla\right)\pi\frac{\partial}{\partial\sigma},$$

and

$$\omega = \sigma\left(\frac{\partial}{\partial t} + \mathbf{v}\cdot\nabla\right)\pi + \pi\dot{\sigma}.$$

With these, Eq. (333) becomes

$$\left(\frac{\partial}{\partial t} + \mathbf{v}\cdot\nabla\right)_\sigma T = \left(\frac{\partial T}{\partial p}\right)_m \sigma\left(\frac{\partial}{\partial t} + \mathbf{v}\cdot\nabla\right)\pi + \pi\dot{\sigma}\left[\left(\frac{\partial T}{\partial p}\right)_m - \frac{\partial T}{\partial p}\right], \quad (335)$$

where

$$\frac{\partial}{\partial p} = \frac{1}{\pi}\frac{\partial}{\partial \sigma}.$$

Now making use of the relation

$$\frac{\partial q^*}{\partial p} = \left(\frac{\partial q^*}{\partial p}\right)_T + \left(\frac{\partial q^*}{\partial T}\right)_p \frac{\partial T}{\partial p}, \quad (336)$$

the last term in Eq. (335) can be written as

$$\begin{aligned}\left(\frac{\partial T}{\partial p}\right)_m - \frac{\partial T}{\partial p} &= \frac{1}{1 + [(L/c_p)(\partial q^*/\partial T)_p]}\left[\frac{\alpha}{c_p} - \frac{\partial T}{\partial p} - \frac{L}{c_p}\frac{\partial q^*}{\partial p}\right] \\ &= \frac{1}{1 + [(L/c_p)(\partial q^*/\partial T)_p]}\left[-\left(\frac{p}{p_0}\right)^\kappa \frac{\partial \theta}{\partial p} - \frac{L}{c_p}\frac{\partial q^*}{\partial p}\right]. \quad (337)\end{aligned}$$

With this expression, Eq. (335) becomes

$$\begin{aligned}\left(\frac{\partial}{\partial t} + \mathbf{v}\cdot\nabla\right)_\sigma T = \left(\frac{\partial T}{\partial p}\right)_m &\sigma\left(\frac{\partial}{\partial t} + \mathbf{v}\cdot\nabla\right)\pi \\ &- \pi\dot{\sigma}\left[\left(\frac{p}{p_0}\right)^\kappa \frac{\partial \theta}{\partial p} + \frac{L}{c_p}\frac{\partial q^*}{\partial p}\right]\Bigg/\left[1 + \frac{L}{c_p}\left(\frac{\partial q^*}{\partial T}\right)_p\right]. \quad (338)\end{aligned}$$

From the form of the hydrostatic equation given by Eq. (122) the following equation can be derived

$$\left(\frac{p}{p_0}\right)^\kappa c_p\left(\frac{\partial \theta}{\partial p}\right) = \frac{\partial}{\partial p}(c_p T + \Phi). \quad (339)$$

If the moist static energy h and the saturation moist static energy h^* are defined by

$$h \equiv c_p T + \Phi + Lq, \qquad h^* \equiv c_p T + \Phi + Lq^*, \tag{340}$$

Eq. (339) can be written as

$$\left(\frac{p}{p_0}\right)^\kappa \frac{\partial \theta}{\partial p} + \frac{L}{c_p}\frac{\partial q^*}{\partial p} = \frac{1}{c_p}\frac{\partial h^*}{\partial p}. \tag{341}$$

Using this expression, Eq. (338) can be put in the final form

$$\left(\frac{\partial}{\partial t} + \mathbf{v}\cdot\nabla\right)_\sigma T = \left(\frac{\partial T}{\partial p}\right)_m \sigma\left(\frac{\partial}{\partial t} + \mathbf{v}\cdot\nabla\right)_\sigma \pi - \frac{\partial h^*/\partial p}{c_p + L(\partial q^*/\partial T)_p}\pi\dot{\sigma}, \tag{342}$$

where $\partial h^*/\partial p = 0$ when the lapse rate is moist adiabatic.

3. *Moist Adiabatic Process—Discrete Case*

The derivation of the vertically differenced form of the water vapor continuity equation is completely analogous to that for the continuous case presented in the previous subsection.

Let $q_k^* \equiv q^*(T_k, p_k)$. When level k is saturated and remains saturated, Eq. (326) may be rewritten as

$$\left(\frac{\partial}{\partial t} + \mathbf{v}_k\cdot\nabla\right) q_k^* + \frac{1}{(\pi\,\Delta\sigma)_k}\left[(\pi\dot{\sigma})_{k+1}(\hat{q}_{k+1} - q_k^*) + (\pi\dot{\sigma})_{k-1}(q_k^* - \hat{q}_{k-1})\right] = -C_k, \tag{343}$$

and then as

$$\left(\frac{\partial q^*}{\partial T}\right)_{pk}\left(\frac{\partial}{\partial t} + \mathbf{v}_k\cdot\nabla\right) T_k + \left(\frac{\partial q^*}{\partial p}\right)_{Tk}\sigma_k\left(\frac{\partial}{\partial t} + \mathbf{v}_k\cdot\nabla\right)\pi_k + \frac{1}{(\pi\,\Delta\sigma)_k}\left[(\pi\dot{\sigma})_{k+1}(\hat{q}_{k+1} - q_k^*) + (\pi\dot{\sigma})_{k-1}(q_k^* - \hat{q}_{k-1})\right] = -C_k, \tag{344}$$

where

$$\left(\frac{\partial q^*}{\partial T}\right)_{pk} \equiv \left(\frac{\partial q_k^*}{\partial T_k}\right)_{pk}, \qquad \left(\frac{\partial q^*}{\partial p}\right)_{Tk} \equiv \left(\frac{\partial q_k^*}{\partial p_k}\right)_{Tk}.$$

The thermodynamic energy equation is, from Eq. (209),

$$\left(\frac{\partial}{\partial t} + \mathbf{v}_k \cdot \nabla\right) T_k + \frac{1}{(\pi\,\Delta\sigma)_k}\left[(\pi\dot{\sigma})_{k+1}(P_k\hat{\theta}_{k+1} - T_k) + (\pi\dot{\sigma})_{k-1}(T_k - P_k\hat{\theta}_{k-1})\right]$$
$$= \frac{1}{c_p}\alpha_k\sigma_k\left(\frac{\partial}{\partial t} + \mathbf{v}_k \cdot \nabla\right)\pi_k + \frac{L}{c_p}C_k, \tag{345}$$

where $\alpha_k \equiv c_p\theta_k(\partial P_k/\partial\pi_k)/\sigma_k$ and $\sigma_k \equiv (p_k - p_I)/\pi_k$. Eqs. (344) and (345) give

$$C_k = -\frac{1}{1 + [(L/c_p)(\partial q^*/\partial T)_{pk}}\left[\left\{\left(\frac{\partial q^*}{\partial p}\right)_{Tk} + \frac{\alpha_k}{c_p}\left(\frac{\partial q^*}{\partial T}\right)_{pk}\right\}\sigma_k\left(\frac{\partial}{\partial t} + \mathbf{v}_k \cdot \nabla\right)\pi_k\right.$$
$$- \left(\frac{\partial q^*}{\partial T}\right)_{pk}\frac{P_k}{(\pi\,\Delta\sigma)_k}\{(\pi\dot{\sigma})_{k+1}(\hat{\theta}_{k+1} - \theta_k) + (\pi\dot{\sigma})_{k-1}(\theta_k - \hat{\theta}_{k-1})\}$$
$$\left. + \frac{1}{(\pi\,\Delta\sigma)_k}\{(\pi\dot{\sigma})_{k+1}(\hat{q}_{k+1} - q_k^*) + (\pi\dot{\sigma})_{k-1}(q_k^* - \hat{q}_{k-1})\}\right]. \tag{346}$$

Substituting Eq. (346) into Eq. (345) gives

$$\left(\frac{\partial}{\partial t} + \mathbf{v}_k \cdot \nabla\right) T_k = \left(\frac{\partial T}{\partial p}\right)_{mk}\sigma_k\left(\frac{\partial}{\partial t} + \mathbf{v}_k \cdot \nabla\right)\pi_k$$
$$- \frac{1}{1 + [(L/c_p)(\partial q^*/\partial T)_{pk}]}\frac{1}{(\pi\,\Delta\sigma)_k}\left[(\pi\dot{\sigma})_{k+1}\left(P_k\hat{\theta}_{k+1}\right.\right.$$
$$\left. + \frac{L}{c_p}\hat{q}_{k+1} - P_k\theta_k - \frac{L}{c_p}q_k^*\right) + (\pi\dot{\sigma})_{k-1}\left(P_k\theta_k + \frac{L}{c_p}q_k^*\right.$$
$$\left.\left. - P_k\hat{\theta}_{k-1} - \frac{L}{c_p}\hat{q}_{k-1}\right)\right], \tag{347}$$

where

$$\left(\frac{\partial T}{\partial p}\right)_{mk} \equiv \left[\frac{\alpha_k}{c_p} - \frac{L}{c_p}\left(\frac{\partial q^*}{\partial p}\right)_{Tk}\right]\Big/\left[1 + \frac{L}{c_p}\left(\frac{\partial q^*}{\partial T}\right)_{pk}\right]. \tag{348}$$

Equation (347) is an analog of Eq. (338).

The coefficient of $(\pi\dot{\sigma})_{k+1}$ in Eq. (347) is

$$P_k(\hat{\theta}_{k+1} - \hat{\theta}_k) + \frac{L}{c_p}(\hat{q}_{k+1} - q_k^*) = \frac{1}{c_p}[(c_p\hat{T}_{k+1} + \hat{\Phi}_{k+1} + L\hat{q}_{k+1}) - (c_pT_k + \Phi_k + Lq_k^*)]$$
$$\equiv \frac{1}{c_p}(\hat{h}_{k+1} - h_k^*),$$

where Eq. (199) has been used. Similarly, the coefficient of $(\pi\dot{\sigma})_{k-1}$ in Eq. (347) is

$$(1/c_p)(h_k^* - \hat{h}_{k-1}).$$

Thus Eq. (347) can be written as

$$\left(\frac{\partial}{\partial t} + \mathbf{v}_k \cdot \nabla\right) T_k = \left(\frac{\partial T}{\partial p}\right)_{mk} \sigma_k \left(\frac{\partial}{\partial t} + \mathbf{v}_k \cdot \nabla\right) \pi_k - \frac{1}{c_p + L(\partial q^*/\partial T)_{p_k}} \frac{1}{(\pi\,\Delta\sigma)_k}[(\pi\dot{\sigma})_{k+1}(\hat{h}_{k+1} - h_k^*) + (\pi\dot{\sigma})_{k-1}(h_k^* - \hat{h}_{k-1})]. \tag{349}$$

Equation (349) is an analog of Eq. (342), but the choice of $\hat{q}$ (or equivalently, $\hat{h}$) at the even levels remains to be specified.

4. *Choice of $\hat{q}$ for Water Vapor*

From Eq. (349) it is clear that a negative $(\pi\dot{\sigma})$ has a warming effect for $\hat{h}_{k+1} > h_k^*$. This may occur even when $h_{k+2}^* < h_k^*$, that is, when no conditional instability exists between the odd levels $k + 2$ and k, which carry the temperatures. (The same effect can similarly occur for a negative $(\pi\dot{\sigma})_{k-1}$ when $h_k^* > \hat{h}_{k-1}$, even when $h_k^* < h_{k-2}^*$.) Any moist convective instability produced by such a warming effect is the result merely of a poor choice of $\hat{q}_{k+1}$ and should be regarded as a kind of computational instability, which may be termed "conditional instability of a computational kind" (CICK).

The CICK phenomenon can be avoided if the choice of $\hat{q}_{k+1}$ and thus $\hat{h}_{k+1}$ satisfies the following requirements when $h_{k+2}^* < h_k^*$:

$$\hat{h}_{k+1} < h_k^* \qquad \text{when} \quad r_k = 1$$

and (350)

$$h_{k+2}^* < \hat{h}_{k+1} \qquad \text{when} \quad r_{k+2} = 1,$$

where r_k is the relative humidity of the level k, given by

$$r_k = q_k/q_k^*. \tag{351}$$

One definition of $\hat{h}_{k+1}$ that satisfies the above requirements is

$$\hat{h}_{k+1} = \hat{r}_{k+1}(\hat{h}_{k+1}^* - \hat{s}_{k+1}) + \hat{s}_{k+1}, \tag{352}$$

where

$$\hat{s}_{k+1} \equiv c_p \hat{T}_{k+1} + \hat{\Phi}_{k+1}, \tag{353}$$

$$\hat{r}_{k+1} = \frac{r_k + r_{k+2} - 2r_k r_{k+2}}{2 - r_k - r_{k+2}}; \tag{354}$$

and $\hat{h}_{k+1}^*$ is an interpolation of h^* from the levels k and $k+2$ to the level $k+1$ which guarantees $h_{k+2}^* < \hat{h}_{k+1}^* < h_k^*$ if $h_{k+2}^* < h_k^*$. Equation (354) gives $\hat{r}_{k+1} = 1$ (and, therefore, $\hat{h}_{k+1} = \hat{h}_{k+1}^*$) when either $r_k = 1$ or $r_{k+2} = 1$; then $h_{k+2}^* < \hat{h}_{k+1} < h_k^*$ is guaranteed regardless of the form of $\hat{h}^*$.

The form of the interpolation used to obtain $\hat{h}^*$ is important, however, in relation to that chosen for $\hat{s}_{k+1}$. Since

$$h_k^* = Lq_k^* + s_k,$$

an interpolation for $\hat{h}_{k+1}^*$ independent of that for $\hat{s}_{k+1}$ could in theory allow the implicit generation of a negative $\hat{q}_{k+1}^*$. To avoid this, the interpolation for $\hat{h}_{k+1}^*$ is chosen proportional to that for $\hat{s}_{k+1}$:

$$\begin{aligned} \hat{h}_{k+1}^* - h_k^* &= A(\hat{s}_{k+1} - s_k), \\ h_{k+2}^* - \hat{h}_{k+1}^* &= A(s_{k+2} - \hat{s}_{k+1}), \end{aligned} \tag{355}$$

and

$$A \equiv \frac{h_{k+2}^* - h_k^*}{s_{k+2} - s_k}. \tag{356}$$

Recall that Eqs. (198) and (199) give

$$\begin{aligned} \hat{s}_{k+1} - s_k &= P_k c_p(\hat{\theta}_{k+1} - \theta_k), \\ s_{k+2} - \hat{s}_{k+1} &= P_{k+2} c_p(\theta_{k+2} - \hat{\theta}_{k+1}), \end{aligned}$$

and thus

$$s_{k+2} - s_k = P_k c_p(\hat{\theta}_{k+1} - \theta_k) + P_{k+2} c_p(\theta_{k+2} - \hat{\theta}_{k+1}),$$

where

$$\hat{\theta} \equiv \frac{\ln \theta_k - \ln \theta_{k+2}}{(1/\theta_{k+2}) - (1/\theta_k)}.$$

Equation (352) gives

$$\hat{q}_{k+1} = (1/L)\hat{r}_{k+1}(\hat{h}^*_{k+1} - \hat{s}_{k+1}). \tag{357}$$

There is no reason to choose this $\hat{q}$, however, if the air is not near saturation. Presumably, the application of Eq. (327) to water vapor mixing ratio is a better choice for the relatively dry case. The final form chosen for use in the model is a weighted mean of Eqs. (357) and (327), given by

$$\hat{q}_{k+1} = \hat{r}_{k+1}\left[\frac{1}{L}(\hat{h}^*_{k+1} - \hat{s}_{k+1})\right] + (1 - \hat{r}_{k+1})\left[\frac{\ln q_k - \ln q_{k+2}}{(1/q_{k+2}) - (1/q_k)}\right]. \tag{358}$$

The CICK is still prevented because Eq. (358) becomes identical to Eq. (357) when $\hat{r}_{k+1} = 1$.

The use of Eq. (358) for $\hat{q}_{k+1}$, however, does not guarantee that q at odd levels remains positive or zero. For example, if $q_k = 0$, $\hat{q}_{k+1} > 0$ and $(\pi\dot{\sigma})_{k+1} > 0$, then the downward current removes a positive amount from zero. To avoid generation of a negative mixing ratio, $\hat{q}_{k+1}$ is replaced by zero when $(\pi\dot{\sigma})_{k+1} > 0$ and $q_k \leqslant 0$ [or when $(\pi\dot{\sigma})_{k+1} < 0$ and $q_{k+2} \leqslant 0$].

B. Horizontal Transport of Water Vapor and Ozone

The finite-difference scheme for the divergence of the horizontal transport of water vapor and ozone is similar to the corresponding scheme for temperature, given at the point (i, j) by the second term of Eq. (299), except that $\overline{q}^{\xi}$ and $\overline{q}^{\eta}$ are replaced by the harmonic mean when the corresponding mass flux, F or G, is outwardly directed from the grid point (i, j) under consideration. This guarantees zero transport out of the grid points where the mixing ratio is zero.

C. Large-Scale Condensation and Precipitation

In the model there is water vapor condensation and release of latent heat not only by the parameterized cumulus convection, which does not require that the air be saturated on the scale of the grid, but also when the air becomes super-saturated on the scale of the grid; the latter phenomenon is called "large-scale condensation." The excess water removed from an atmospheric layer in this way precipitates into the layer immediately below. The falling precipitation either evaporates completely in that layer or brings the layer to saturation and then passes to the next layer below, where the process is repeated. When the lowermost layer is saturated, the condensed water precipitates onto the ground as rain or snow.

Large-scale condensation occurs when ${q_{ij}}^k$ is greater than q_{ij}^{*k}, where ${q_{ij}}^k$ is the provisional value of the water vapor mixing ratio predicted by the advective process only, and q_{ij}^{*k} is the saturation mixing ratio at the temperature ${T_{ij}}^k$ and the pressure ${p_{ij}}^k$.

Let $C\,\Delta t$ denote the amount of condensation at level k per unit mass of dry air when ${q_{ij}}^k > q_{ij}^{*k}$. Then

$$({q_{ij}}^k)' = {q_{ij}}^k - C\,\Delta t, \tag{359}$$

$$({T_{ij}}^k)' = {T_{ij}}^k + \frac{L}{c_p} C\,\Delta t, \tag{360}$$

$$({q_{ij}}^k)' = q^*[({T_{ij}}^k)', {p_{ij}}^k], \tag{361}$$

where the primes denote values modified by condensation. Equation (361) describes the saturation condition for the modified moisture and temperature. From these three equations an equation for the modified temperature can be obtained

$${q_{ij}}^k - \frac{c_p}{L}[({T_{ij}}^k)' - {T_{ij}}^k] = q^*[({T_{ij}}^k)', {p_{ij}}^k]. \tag{362}$$

With ${q_{ij}}^k$, ${T_{ij}}^k$, ${p_{ij}}^k$ and the functional form of $q^*(T, p)$ given, the transcendental equation (362) can be solved iteratively for $({T_{ij}}^k)'$. After $({T_{ij}}^k)'$ is obtained, $C\,\Delta t$ and $({q_{ij}}^k)'$ may be computed from Eqs. (360) and (359).

Choosing

$$T_0 = {T_{ij}}^k \quad \text{and} \quad q_0 = {q_{ij}}^k, \tag{363}$$

$(T_{\nu+1}, q_{\nu+1})$ are determined recursively by

$$\begin{aligned} T_{\nu+1} &= T_\nu + (L/c_p)C_{\nu+1}\,\Delta t \\ q_{\nu+1} &= q_\nu - C_{\nu+1}\,\Delta t, \end{aligned} \tag{364}$$

where $\nu = 0, 1, 2, \ldots$, and

$$C_{\nu+1}\,\Delta t \equiv \frac{q_\nu - q^*(T_\nu)}{1 + (L/c_p)(\partial q^*/\partial T)_{T=T_\nu}}. \tag{365}$$

In summary,

$$(T_{ij}^{\,k})' = T_{ij}^{\,k} + \frac{L}{c_p}\sum_{\nu=1}^{\nu_{\max}} C_\nu\,\Delta t, \tag{366}$$

$$(q_{ij}^{\,k})' = q_{ij}^{\,k} - \sum_{\nu=1}^{\nu_{\max}} C_\nu\,\Delta t, \tag{367}$$

where $\nu_{\max}$ is the maximum number of iterations in the layer. A value of $\nu_{\max} = 3$ seems to give sufficient accuracy for present purposes.

The effect of evaporation of the falling precipitation on the layer immediately below is incorporated in the following expressions:

$$(T_{ij}^{k+2})' = T_{ij}^{k+2} - \frac{L}{c_p}\sum_{\nu=1}^{\nu_{\max}} C_\nu\,\Delta t\pi_k\,\Delta\sigma_k/(\pi_{k+2}\,\Delta\sigma_{k+2}), \tag{368}$$

$$(q_{ij}^{k+2})' = q_{ij}^{k+2} + \sum_{\nu=1}^{\nu_{\max}} C_\nu\,\Delta t\pi_k\,\Delta\sigma_k/(\pi_{k+2}\,\Delta\sigma_{k+2}). \tag{369}$$

If the layer becomes supersaturated due to the evaporation, the entire process is repeated for that layer.

VIII. Time Differencing

To explain the procedure, the equations can be written symbolically in the following form:

$$\frac{\partial}{\partial t}\pi = f(\pi, \mathbf{A}), \tag{370}$$

$$\frac{\partial}{\partial t}(\pi\mathbf{A}) = g(\pi, \mathbf{A}). \tag{371}$$

Equation (370) represents the continuity equation and Eq. (371) represents the prognostic equations for the other variables described in the previous sections.

The leapfrog scheme (L) is given by

$$\frac{\pi^{n+1} - \pi^{n-1}}{2\Delta t} = f(\pi^n, \mathbf{A}^n),$$

$$\frac{\pi^{n+1}\mathbf{A}^{n+1} - \pi^{n-1}\mathbf{A}^{n-1}}{2\Delta t} = g(\pi^n, \mathbf{A}^n),$$

where the superscript denotes a time level. The Matsuno scheme (M), which is sometimes called the Euler-backward scheme, is given by

$$\frac{\pi^{(n+1)*} - \pi^n}{\Delta t} = f(\pi^n, \mathbf{A}^n)$$

$$\frac{\pi^{(n+1)*}\mathbf{A}^{(n+1)*} - \pi^{(n)*}\mathbf{A}^{(n)*}}{\Delta t} = g(\pi^n, \mathbf{A}^n),$$

$$\frac{\pi^{n+1} - \pi^n}{\Delta t} = f(\pi^{(n+1)*}, \mathbf{A}^{(n+1)*})$$

$$\frac{\pi^{n+1}\mathbf{A}^{n+1} - \pi^n\mathbf{A}^n}{\Delta t} = g(\pi^{(n+1)*}, \mathbf{A}^{(n+1)*}).$$

The time differencing used in the model for the basic dynamical terms is essentially the leapfrog scheme, but with a periodic insertion of the Matsuno scheme, as shown in Fig. 27.

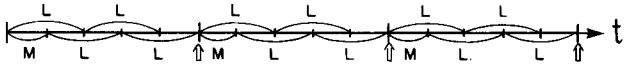

FIG. 27. Schematic representation of the time differencing of the model showing sequence of use of leapfrog (L) and Matsuno (M) schemes. Arrows indicate calculation of the heating and friction terms.

At present, the source and sink terms described in the Introduction and the vertical flux convergence term of the moisture equation are calculated every five time steps, as shown by the arrows in the figure. Those calculations are followed by a single step of the Matsuno scheme.

IX. Summary and Conclusions

In this chapter, only the computational design of the basic dynamical processes of the current UCLA general circulation model has been described. To determine the heating and friction, the model includes many important physical processes, such as those associated with radiation, photochemistry, the boundary layer, the thermodynamics and hydrology of the ground, as well as processes associated with grid- and subgrid-scale clouds. These physical processes could not be adequately described in a single chapter and, therefore, with the exception of the advective processes for water vapor and ozone and the large-scale condensation processes, were not included here.

Section I gives a brief outline of the model, whose 12 layers represent both troposphere and stratosphere. The prognostic variables of the model are the surface pressure, horizontal velocity, temperature, water vapor and ozone of each layer; the planetary boundary layer (PBL) depth and magnitudes of the temperature, moisture and momentum discontinuities at the PBL top; the ground temperature and water storage; and the mass of snow on the ground. It should be noted that the degree of freedom added by the PBL makes the model effectively equivalent to a 13-layer model.

Section II describes the principles of mathematical modeling that were followed in the computational design of the basic dynamical processes of the model. The basic principle employed in selecting a space finite-difference scheme from the many that share the same order of accuracy was a requirement that the scheme maintain discrete analogs of a number of physically important integral constraints of the continuous atmosphere. Energy propagation properties in physical space, as well as in spectral space, were also considered in the selection of a scheme.

Section III describes space finite-difference schemes for homogeneous incompressible flow, with and without a free surface. Section III, A shows that the dispersion properties of inertia-gravity waves are highly scheme-dependent and that from the point of view of geostrophic adjustment there is only one satisfactory distribution (staggering) of the dependent variables into grid points.

Section III, B discusses finite-difference schemes for nonlinear two-dimensional nondivergent flow and replaces Part II of the paper by Arakawa (1966), which was originally planned as a separate publication. A drastic difference in the energy cascade exists between solutions obtained by schemes that conserve enstrophy and by those that do not. Due to the relatively small amount of energy in the high wave number range with enstrophy-conserving schemes, the overall error is expected to be small. This subsection also derives, for the cartesian grid, the momentum advection

scheme consistent with the energy and enstrophy conserving vorticity advection scheme for two-dimensional nondivergent flow. The total momentum is also conserved with this scheme.

Section III, C generalizes the momentum advection scheme for nondivergent flow to a scheme that maintains conservation of total energy and momentum for divergent flow. It should be pointed out, however, that this generalization is not unique and is not necessarily the best choice from the standpoint of potential vorticity advection when the lower boundary has relatively steep topography. In general circulation models, horizontal discretization errors should be small for planetary-scale waves *after they are generated* because their horizontal scales are sufficiently large compared to the usual horizontal grid size. However, horizontal discretization errors can be very serious for the *generation* of planetary-scale waves by longitudinally narrow (but meridionally wide) mountain ridges. A search for a generalization to divergent flow that is better from this point of view is now in progress.

Section IV describes the vertical coordinate of the model. It is a version of the σ coordinate below 100 mb and the pressure coordinate above 100 mb. The basic governing equations in terms of that vertical coordinate are presented.

Section V describes the vertical difference scheme. Various integral properties are presented in Section V, A; Section V, B then discusses the logical procedure for deriving a scheme that maintains discrete analogs of these properties. Section V, C presents the final determination of the vertical difference scheme based on considerations of accuracy in both the vertical propagation of wave energy and the hydrostatic equation.

Section VI presents the horizontal difference scheme of the model. The scheme for three-dimensional motion on a sphere is a generalization, although not unique, of the scheme developed in Section III, C. With the current scheme, however, enstrophy is not conserved for two-dimensional incompressible flow on a sphere, and solutions from the model show some computational quasi-stationary noise near the poles that would seem to correspond to a false production of enstrophy. The new generalization now being sought should be better from this point of view also. Section VI, C, 2 describes the method devised to avoid the use of the extremely short time interval required for computational stability due to the convergence of meridians toward the poles. The method employs an operator to smooth, in a longitudinal sense, selected terms of the prognostic equations that involve longitudinal differences. The result is equivalent to the use of multipoint finite-difference quotients and the space finite-difference scheme remains energy conserving.

Section VII gives the space finite-difference schemes for the advection of water vapor and ozone. Special advection schemes are necessary both in

that the mixing ratios of these atmospheric constituents vary in space over a wide range of orders of magnitude, and also in that the release of latent heat through condensation of water vapor can cause a false moist convective instability. Our method for the calculation of the large-scale condensation is also described in this section.

In Section VIII is described the time differencing of the model. The heating and friction terms are calculated every fifth time step. For the basic dynamical processes, at the steps which immediately follow the calculations of heating and friction, the Matsuno scheme is inserted; for all other time steps, the leapfrog scheme is used.

Descriptions of physical and computational aspects of the model related to those physical processes that determine the heating and friction will be published separately elsewhere. The most complete documentation currently available for the radiation and photochemical processes is given in Schlesinger (1976) and for the boundary layer and stratus cloud processes in Randall (1976). The parameterization of cumulus convection is based on the theory proposed by Arakawa and Schubert (1974). Some computational problems associated with the application of the theory were discussed by Schubert (1973). A more complete description of this aspect of the model, including the more recent revisions, is now being prepared for publication.

Acknowledgments

The development of the UCLA atmospheric general circulation models has been carried out, over a number of years, with Professor Yale Mintz as the principal investigator. The authors also wish to acknowledge the considerable contributions of Drs. Akira Katayama, Jeong-Woo Kim, David Randall, Wayne Schubert, Michael Schlesinger, and Tatsushi Tokioka, and of Winston Chao and Stephen Lord to the development of the general circulation model.

We express our appreciation to Donna Hollingworth and Christopher Kurasch for their substantial assistance in programming the model. Appreciation is also due to Mrs. Grace McMurray for the typing and to Mrs. Beverly Gladstone for the drafting of the figures.

The research reported here was supported by the National Science Foundation under Grant GA-34306; the Department of Transportation Climatic Impact Assessment Program under Grant GA-34306X; and the National Aeronautics and Space Administration, Institute for Space Studies, Goddard Space Flight Center under Grant NGR 05-007-328.

Computing assistance was obtained from the UCLA Campus Computing Network.

References

Arakawa, A. (1966). *J. Comput. Phys.* **1**, 119–143.

Arakawa, A. (1970). *In* "SIAM-AMS Proceedings of the Symposium in Applied Mathematics" (G. Birkhoff and S. Varga, eds.), Vol. 2, pp. 24–40. American Mathematical Society, Providence, Rhode Island.

Arakawa, A. (1972). "Numerical Simulation of Weather and Climate," Tech. Rep. No. 7. Dept. Meteorol., University of California, Los Angeles.
Arakawa, A., and Schubert, W. H. (1974). *J. Atmos. Sci.* **31**, 674–701.
Cahn, A. (1945). *J. Meteorol.* **2**, 113–119.
Fjørtoft, R. (1953). *Tellus* **5**, 225–230.
Lorenz, E. N. (1955). *Tellus* **7**, 157–167.
Lorenz, E. N. (1960). *Tellus* **12**, 364–373.
Mintz, Y. (1965). *W.M.O. Tech. Notes* **66**, 141–167.
Mintz, Y. (1968). *Am. Meteorol. Soc., Monogr.* **8**, 20–36.
Phillips, N. A. (1957). *J. Meteorol.* **14**, 184–185.
Phillips, N. A. (1959). *In* "The Atmosphere and the Sea in Motion," (Bert Bolin, ed.) pp. 501–504. Rockefeller Inst. Press, New York.
Phillips, N. A. (1974). Natl. Meteorol. Cent. Off. Note 104. Natl. Weather Service, Washington, D.C.
Randall, D. A. (1976). "The Interaction of the Planetary Boundary Layer with Large-Scale Circulations." Ph.D. Thesis, Dept. Atmos. Sci., University of California, Los Angeles.
Schlesinger, M. E. (1976). "A Numerical Simulation of the General Circulation of Atmospheric Ozone." Ph.D. Thesis, Dept. Atmos. Sci., University of California, Los Angeles.
Schubert, W. H. (1973). "The Interaction of a Cumulus Cloud Ensemble with the Large-Scale Environment." Ph.D. Thesis, Dept. Meteorol., University of California, Los Angeles.
Winninghoff, F. J. (1968). "On the Adjustment toward a Geostrophic Balance in a Simple Primitive Equation Model with Application to the Problems of Initialization and Objective Analysis." Ph.D. Thesis, Dept. of Meteorol., University of California, Los Angeles.